

A Review of Water Treatment Membrane Nanotechnologies

Journal:	<i>Energy & Environmental Science</i>
Manuscript ID:	EE-REV-10-2010-000541.R1
Article Type:	Review Article
Date Submitted by the Author:	n/a
Complete List of Authors:	Pendergast, MaryTheresa; University of California, Los Angeles, Department of Civil and Environmental Engineering Hoek, Eric; University of California, Department of Civil and Environmental Engineering
Note: The following files were submitted by the author for peer review, but cannot be converted to PDF. You must view these files (e.g. movies) online.	
Figure.zip	

UCLA Engineering

HENRY SAMUELI SCHOOL OF ENGINEERING AND APPLIED SCIENCE

Civil & Environmental Engineering Department
and California NanoSystems InstituteEric M.V. Hoek, Associate Professor
5732-G Boelter Hall, Box 159310
Los Angeles, CA 90095-1593
TEL: (310) 206-3735
FAX: (310) 206-2222

January 28, 2011

Philip Earis, Editor *Energy & Environmental Science*
Royal Society of Chemistry, Thomas Graham House
Science Park, Cambridge, CB4 0WF, UK
Tel +44 (0)1223 432168, Mobile +44 7825 186310, Fax +44 (0)1223 420247RE: Revision to *Energy & Environmental Science* manuscript EE-REV-10-2010-000541

Dear Editor:

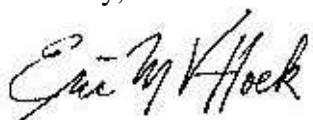
We thank the reviewers for their insightful comments and we have revised the above referenced manuscript in response. In addition, we addressed each reviewer comment in an itemized fashion in the attached "Response to Reviewer Comments."

We have uploaded high resolution (600 dpi minimum) TIF files for each image in the article. We have kept the images in color for the online version, but please convert these to grey-scale for the print version. We have ensured that no information is lost from the figure upon conversion.

We feel we have adequately addressed all reviewer comments and hope that you will accept our review paper for publication in *Energy & Environmental Science* without further revision.

Please let me know if you have any questions or require additional information.

Sincerely,



Dr. Eric M.V. Hoek, Ph.D.

SIGNIFICANT REVISIONS TO THE MANUSCRIPT

Figure 3. Thin Film Composite Cross-Section was removed because in grey-scale it seems redundant to Fig. 2 since the only visual difference between integrally-skinned and thin film composite is that one has thin film and support made of same material and the other has two separate materials.

Figure 4. Zeolite Cage Structures was removed because it seemed to accompany excessive and unnecessary detail, relative to the other materials discussed.

Figure 6. Percolation Threshold was removed because it also seemed to provide superfluous detail.

Section 3.2.1. Mixed Matrix Membranes

Selections have been deleted due to excessive explanation of mixed matrix theory; the detail of background theory here appeared to be out of proportion with that in other sections. The important points from the deleted paragraphs have, however, been shortened and inserted into the present introduction so that major points are not lost. Also, it was re-emphasized that details about gas separation membranes were included only to show the past application and strength of these materials now being re-engineered for water treatment purposes.

Section 3.3.3. Isoporous Block Copolymer Membranes

Selections have been deleted, again when out of proportion detail in background explanation was found. Within the particular works cited and described, some specific details have been removed or minimized in order to highlight the most important achievement of each work. Lengthy block copolymer names have also been removed in most cases, in lieu of the type (i.e., tri-block, homopolymer) so that the individual methods described can be seen in a more general system framework. Some of the extensive deleted sections have been shortened/rewritten and inserted in the section so that significant points are not lost, but only the excess detail.

Discussion

The discussion section has been significantly lengthened and clarified. Each technology is summarized to shed light upon the benefits and hurdles of each material that led to its individual ranking in our system. Each score is justified and explained within our metric.

Throughout the text, an effort was made to reduce excess detail and highlight the major hurdles achieved by each researcher cited. Primary accomplishments and future needs for each material were further emphasized throughout the body of this paper.

Specific responses to the referees follows.

RESPONSES TO REVIEWER COMMENTS

REFEREE 1

Within their extensive review the authors state that in their review "... the published literature describing ... membrane technologies (i.e. nanotechnologies) is critically reviewed and discussed within the context of conventional membrane materials used in the relevant water treatment applications" and "a ranking system was developed ..." (all citations from the Abstract) Yet, from my point of view these goals are not achieved on the light of the high standards of E&ES.

- **REFEREE COMMENT 1**

The authors provide an extensive, yet often bulky, listing of the paper dealing with membrane nanotechnologies. They cite numerous papers (>230), but do not discuss them critically and do not analyze the strengths and weaknesses of the respective materials.

Our Response: We thank the reviewer for their feedback. We have gone through the paper, particularly the lengthier sections (i.e., zeolite-coated ceramic membranes, mixed-matrix membranes, and block copolymer membranes) and trimmed the excess details. Instead, we focused on the primary strengths of each work cited and its merit as a new advanced material or process. We have not removed citations, but have rather made it clearer why each is being cited.

- **REFEREE COMMENT 2**

Furthermore, all water treatment technologies are summarized in one terminus. This is a further major drawback. The authors should rather list and introduce the different application possibilities (treatment of waste water, of grey-water, deionization of sea water etc.) and enlighten the respective prerequisites and thereby following desired membrane properties.

Our Response: We thank the reviewer for this insightful comment. During the initial stages of preparing this review, the authors went through multiple iterations of outlines, some presenting the technologies by application, others by material type. As we began compiling data, this final structure as presented seemed to be the most comprehensive and clear way to present this body of literature. Each of the material types detailed can be adapted to multiple applications and setting limitations on the purpose of each is not something the authors see as the purpose or right of this article. The most likely and currently evaluated applications for each material type have been highlighted in the revised introductions to each section. The goal of the article is not to review the current state of applications, but rather of the materials being developed in this field.

- **REFEREE COMMENT 3**

This leads clearly to the next major point – the ranking system. In principle, the development and application of such a ranking system should be favored. However, the authors provide only a very short snapshot (in the last two pages of their article) on this topic. Yet, they introduce some criteria/ properties but do not clearly discuss how they ranked the respective membrane materials. In the present stage the ranking might be

arbitrary to some point. Here again, the ranking should be / has to be based on the envisaged application.

Our Response: We have extended the discussion section to elucidate the way each technology ranking was determined. This can be found on pages 51-53 of the revised manuscript. For the purpose of performance enhancement, however, we did rate these materials against current industry standards as they have been tested in the literature. We do not, however, want to define the materials by these tested applications since multiple opportunities for their successful use are available and must only be determined.

- **REFEREE COMMENT 4**

In summary, when only these major points are considered, the review does provide critical and novel analyses suitable for wide readership. Up to now, it is rather a listing of the present literature of the topic. Thus, from point of view it does not meet the high standards of E&ES. Maybe, the work can be reconsidered after an extensive revision (that has to be almost a complete re-writing of the article).

Our Response: We hope that the current revised manuscript meets the reviewer's standards. At this point, the authors feel confident that the review article provides a thorough and educative snapshot of the current state of nanotechnology-enabled membrane materials being developed.

- **REFEREE COMMENT 5**

P.S. The authors should furthermore revise their Figures.

Our Response: We have updated the figures to have higher resolution (600 dpi) and clear contrast in grey-scale. We have also removed Figures 3, 4, and 6 from the original manuscript, after deeming them superfluous.

REFEREE 2

This manuscript reviews water treatment membrane nanotechnologies. It is a very good topic to summarize membrane nanotechnologies for water treatment, including conventional membrane materials, nano-structured ceramic membrane, inorganic-organic membrane (such as hybrid protein-polymer, biomimetic membranes, aligned nanotube membranes, and block copolymer membranes).

In particular, the vertically aligned carbon nanotube membranes imply significant advantages over conventional porous membrane through reduced driving pressure and lower energy cost.

Systematically, it presents almost membrane nanotechnologies in terms of merits and defects, which ideally provide clear knowledge to new readers to water treatment realm.

Therefore, it is a well organized and illustrated manuscript, and recommended to be published in ENERGY & ENVIRONMENTAL SCIENCE.

Our Response: We appreciate your comments and thank you for your positive recommendation.

REFEREE 3

This review manuscript illustrated a review study of water treatment membrane nanotechnologies (hybrid protein-polymer, biomimetic membranes, aligned nanotube membranes, and block copolymer membrane). The authors intensively reviewed the formation and performance of various nanotechnology-enabled membranes for water related applications or studies. It is a well-organized paper, but it lacks something important such as critical analyses and discussions that validate its value. For a paper to be published in E&ES, it should be educative instead of only listing what have been done.

However, this manuscript benefits from clear writing style and systematic discussion. In every section, the authors always started with an introduction on the importance of the technologies, followed by an enormous example of published literature in that specific area with the obtained performance and ended by the challenges that need to be overcome. The prospective research direction was also elaborated in some section. Another interesting point is comparison between the projected performance for thin films containing nanoparticles with the current polymeric seawater RO membranes revealing the potencies of membrane nanotechnologies to replace RO membrane in the This manuscript may be future considered for publication only after the major issues listed below can be clearly addressed.

- **REFEREE COMMENT 1**

We do agree with reviewer #1 that the weakness of this paper is: “The authors provide an extensive, yet often bulky, listing of the paper dealing with membrane nanotechnologies. They cite numerous papers (>230), but do not discuss them critically and do not analyze the strengths and weaknesses of the respective materials”. This manuscript is lacked of in depth discussion. So, the authors may comment summarize and report only the important finding for significant works in each area of research and this would greatly benefit the readers and membrane reaches in related field and strengthen this review paper.

Our Response: As stated in response to Referee 1, we thank the reviewers for their feedback. We have gone through the paper, particularly the lengthier sections (i.e., zeolite-coated ceramic membranes, mixed-matrix membranes, and block copolymer membranes) and trimmed the excess details. Instead, we focused on the primary strengths of each work cited and its merit as a new advanced material or process.

- **REFEREE COMMENT 2**

Another suggestion is discuss more about the technical hurdles of each technology and suggest more potential research directions. In my opinion, the review topic is too broad and it may over the authors' expertise to provide critical comments.

Our Response: Both in text and in the final Discussion section we have emphasized the future work that needs to be accomplished to bring these materials out of the laboratory and into commercial realization.

- **REFEREE COMMENT 3**

The conclusion part could be significantly improve via summarizing valuable research and work done in areas of water treatment membrane nanotechnologies. Besides what are the areas for future direction in term of hybrid protein-polymer, biomimetic membranes, aligned nanotube membranes, and block copolymer membrane from authors' point of view?

Our Response: We thank the reviewer for this insightful comment. We have extended the discussion to elucidate the way each technology ranking was arrived at. This can be found on pages 51-53 of the revised manuscript.

- **REFEREE COMMENT 4**

This manuscript is also compounded by the authors tendency to cite paper on membrane for other applications, such as pervaporation or membrane fuel cell.

Our Response: We have removed mention/citation of off-topic technologies where necessary. In some places the comments were kept (e.g., p. 15, line 22) if they were included to explain previous applications of materials and how they must be adapted for novel applications, such as zeolite films previously looked at only for gas separations now applied for desalination.

REVISED TEXT:

p. 16, line 23

Mention of results in pervaporation testing has been removed.

p. 37, line 15

Mention of aligned CNT membranes used in a fuel cell application has been removed.

- **REFEREE COMMENT 5**

The writing of this manuscript need to be polished, there are a lot of grammatical error, inconsistency of abbreviation... Similar mistaken can be easily found in the manuscript and should be revised accordingly

Our Response: We thank the reviewer for their close attention. The following mistakes have been corrected, along with several others. Abbreviations replaced written terms that had already been laid out when possible (e.g., PSf, PA, RO). Full terms were left, however, when they were found at the beginning of a sentence since it is not common practice to being sentences with abbreviations (e.g., p. 8, line 21, "Cellulose acetate...") in formal writing.

- Page 8, last 4-5th sentences: “Dense-skinned.... Desalination due their.... permeability” should be due to

REVISED TEXT:

p. 8, line 20

Dense-skinned CA membranes are particularly useful for desalination due to their high water permeability and low salt permeability.

- Page 8, last 3rd sentence: cellulose acetate should be CA
Did not correct this since “Cellulose acetate” appeared at the beginning of a sentence.

- Page 9, end paragraph, last 4th sentence, page 22 second paragraph, Page 12, 2nd paragraph and so on: polysulfone should be PSf
Did not correct p. 9 since “Polysulfone” appeared at the beginning of a sentence.

REVISED TEXT:

p. 24, line 15

One example of this is the Zirfon® UF membrane, composed of an asymmetric PSf membrane with zirconia (ZrO₂) particles.

p. 12, line 7

Recently, Kim et al. produced nano structured RO membranes through plasma induced graft polymerization, in which a PSf supported PA RO membrane is exposed ...

- Page 11, 2nd sentence, Page 12, 2nd paragraph and so on: polyamide should be PA
Similar mistaken can be easily found in the manuscript and should be revised accordingly

REVISED TEXT:

p. 11, line 15

...(e.g., PA monomer) ...

p. 11, line 20

The industry standard PA RO membrane is based on...

A REVIEW OF WATER TREATMENT MEMBRANE NANOTECHNOLOGIES

by

*MaryTheresa M. Pendergast, Eric M.V. Hoek**

Department Civil & Environmental Engineering and California NanoSystems
Institute, University of California, Los Angeles, California, USA

Submitted to

Energy and Environmental Science

January 28, 2011

* Corresponding author contact: University of California, Los Angeles; 5732-G Boelter Hall;
P.O. Box 951593; Los Angeles, California, 90095-1593, USA; Tel: (310) 206-3735; Fax: (310)
206-2222; E-mail: emvhoek@ucla.edu

ABSTRACT

Nanotechnology is being used to enhance conventional ceramic and polymeric water treatment membrane materials through various avenues. Among the numerous concepts proposed, the most promising to date include zeolitic and catalytic nanoparticle coated ceramic membranes, hybrid inorganic-organic nanocomposite membranes, and bio-inspired membranes such as hybrid protein-polymer biomimetic membranes, aligned nanotube membranes, and isoporous block copolymer membranes. A semi-quantitative ranking system was proposed considering projected performance enhancement (over state-of-the-art analogs) and state of commercial readiness. Performance enhancement was based on water permeability, solute selectivity, and operational robustness, while commercial readiness was based on known or anticipated material costs, scalability (for large scale water treatment applications), and compatibility with existing manufacturing infrastructure. Overall, bio-inspired membranes are farthest from commercial reality, but offer the most promise for performance enhancements; however, nanocomposite membranes offering significant performance enhancements are already commercially available. Zeolitic and catalytic membranes appear reasonably far from commercial reality and offer small to moderate performance enhancements. The ranking of each membrane nanotechnology is discussed along with the key commercialization hurdles for each membrane nanotechnology.

KEYWORDS

zeolite membrane; catalytic membrane; mixed-matrix membrane; nanocomposite membrane; thin film nanocomposite; biomimetic membrane; aligned carbon nanotube; block copolymer

TABLE OF CONTENTS

1. INTRODUCTION	4
2. CONVENTIONAL MEMBRANE MATERIALS	6
2.1. Inorganic Membranes.....	6
2.1.1. Mesoporous Ceramic Membranes	6
2.2. Organic Membranes	7
2.2.1. Integrally-Skinned Membranes	7
2.2.2. Thin Film Composite Membranes	9
3. NANOTECHNOLOGY-BASED MEMBRANE MATERIALS	12
3.1. Nanostructured Ceramic Membranes.....	12
3.1.1. Zeolite-Coated Ceramic Membranes.....	12
3.1.2. Reactive/Catalytic Ceramic Membranes	19
3.2 Inorganic-Organic Membranes	23
3.2.1. Mixed Matrix Membranes	23
3.2.2. Thin Film Nanocomposite Membranes	30
3.3. Biologically-Inspired Membranes.....	34
3.3.1. Aquaporin Membranes	34
3.3.2. Vertically Aligned Nanotube Membranes	36
3.3.3. Isoporous Block Copolymer Membranes	41
4. DISCUSSION AND CONCLUSIONS	48

1. INTRODUCTION

In the last century the global population quadrupled, while the world water demand increased sevenfold ¹. This global water challenge will become greater as the population and economies of developing countries expand; in the next forty years, the global population is expected to grow nearly 40%, and hence, domestic, agriculture, industry, and energy demands on water resources will continue to grow ². The World Water Council estimates that by 2030, 3.9 billion people will live in regions characterized as “water scarce” ³. In addition to overall water shortage, poor water quality is near crisis in many parts of the world. According to the World Health Organization, 1.1 billion people lack access to improved drinking water and 2.6 billion lack access to proper sanitation ⁴. As many as 2.2 million people die of diarrheal related disease every year most often caused by waterborne infections, and the majority of these cases are children under the age of 5 ². More than ever, existing fresh water resources need protection and new water resources must be developed in order to meet the world’s growing demand for clean water. This will require better water treatment technology.

Membranes are favored over many other technologies for water treatment because, in principle, they require no chemical additives or thermal inputs and they do not require regeneration of spent media. Although such an ideal membrane has not yet been realized in the 150 years since Maxwell theorized his magical ‘sorting demon,’ commercial membrane technologies can perform efficient, selective, and reliable separations ⁵. Pressure-driven membrane processes are the most widely used membrane technologies in water treatment applications ⁶; although, the use of gas separation, pervaporation, and electrochemical membrane processes for industrial and environmental separations have also increased dramatically in the past few decades ⁷.

Typically, pressure-driven membranes are classified according to characteristic pore size or their intended application (**Table 1**)^{5-6, 8}. Currently, membrane technology is commercially available for suspended solids, protozoa, and bacteria removal (microfiltration, MF), for virus and colloid removal (ultrafiltration, UF), for hardness, heavy metals, and dissolved organic matter removal (nanofiltration, NF), and for desalination, water reuse, and ultrapure water production (reverse osmosis, RO)⁶⁻⁷. While commercially available membranes perform well in many applications, the drive to protect existing water resources and to produce new water resources demands membranes with improved productivity, selectivity, fouling resistance, and stability available at lower cost and with fewer manufacturing defects. Better membranes require better materials.

Over the past decade, nanotechnology has rapidly changed from an academic pursuit to commercial reality; already nanotechnology concepts have led to new water treatment membranes that exceed state-of-the-art performance and enable new functionality, such as high permeability, catalytic reactivity, and fouling resistance. Herein, we present a brief overview of conventional materials used to prepare “state-of-the-art” pressure-driven membranes. This is followed by a critical review of current literature on nanotechnology-enabled water treatment membrane materials. Finally, we compare the “present day” merits and limitations of each water treatment membrane nanotechnology.

2. CONVENTIONAL MEMBRANE MATERIALS

2.1. Inorganic Membranes

2.1.1. Mesoporous Ceramic Membranes

As early as the 1940's inorganic membranes were developed for the enrichment of uranium. In the 1980's, the knowledge gained was applied for the formation of ceramic MF and UF membranes for industrial separations⁹. Generally, ceramic membranes are asymmetric in structure with a dense upper region atop a porous support (**Figure 1**). The mechanically stable support materials include, but are not limited to, alumina, silica, zirconia, mullite, oxide mixtures, and sintered metals¹⁰. Typical ceramic membranes are formed via the sol-gel process, in which particle dispersions are forced to agglomerate^{9,11}. The asymmetric structure is achieved by depositing particles of decreasing size and sintering at high temperature in order to achieve continuous, porous layers¹¹. Pore size and characteristics of the upper selective region may be tuned based upon the grain size and particle type selected⁹.

Post treatments are applied to alter the porosity of ceramic membranes. Mullite ($3\text{Al}_2\text{O}_3 \cdot 2\text{SiO}_2$) ceramic supports—formed through high temperature calcinations of kaoline clay—are desirable due to their enhanced mechanical strength. The extreme temperatures required for the formation of mullite allow for strong inter-crystalline bonds to form during the crystallization process. Free silica can be leached with a post treatment of strong alkali solution. The porosity of the resulting structure can be controlled by the leaching factors: time of leaching, concentration of leaching solution, and temperature at which leaching occurs¹². Coatings (of porous metals, metal oxides, and zeolites) can also be applied to ceramic membranes to further control performance with coating thickness, pore structure, and surface characteristics¹³.

With their enhanced mechanical, thermal, and chemical stability ceramic materials are well suited for challenging water purification processes, such as industrial wastewater, oil/water separations, and hazardous waste treatment¹². Flux through ceramic membranes is more easily recovered after fouling because ceramics can withstand harsh chemical and thermal cleaning methods¹⁴. Ceramics pose the opportunity for extended membrane lifetimes even under extreme fouling and cleaning conditions, which would destroy their polymeric counterparts. However, ceramics are typically considered too expensive for large-scale membrane applications, such as municipal drinking water production and wastewater treatment, so their application has been historically limited to relatively small-scale industrial separations not suitable for polymeric membranes^{11, 14-15}.

2.2. Organic Membranes

2.2.1. Integrally-Skinned Membranes

Porous polymeric membranes (i.e., MF/UF) have been applied to various water treatment processes, including water and wastewater filtration and as pretreatment for NF or RO membranes^{6, 8}. These membranes have an integrally skinned, often asymmetric structure consisting of an open porous support layer beneath a relatively thin, less porous skin layer of the same material (**Figure 2**)^{5, 8, 16-17}. The separation occurs at the skin layer while the support provides a nearly resistance-free path for water (and unrejected solutes carried in the permeating water) to exit the membrane. The highly selective top layer of MF/UF membranes, having pores ranging from ~0.01 to ~0.2 μm , is considered the active region of the membrane^{5, 8}.

Flat sheet forms of MF/UF membranes are formed through nonsolvent induced phase inversion of preformed polymers over a nonwoven support fabric, which provides mechanical

strength to the membrane. Alternatively, the phase inversion reaction can be carried out to form hollow fiber forms of MF/UF membranes. The phase inversion technique relies upon the controlled interaction of solvent and nonsolvent solutions to induce a phase separation transitioning a polymer from a liquid dispersion into a solid state^{5, 8, 18}. A recent review elucidates the details of this process¹⁹. A homogeneous polymer solution, containing polymer and solvent, is immersed into a nonsolvent coagulation bath and polymer solidification occurs during the miscible solvent and nonsolvent exchange^{5, 18}. Membrane characteristics vary with casting conditions, polymer selection, polymer concentration, the solvent/nonsolvent system and additives, and coagulation bath conditions^{5, 20-21}.

Cellulose acetate (CA) was one of the first polymers employed in aqueous membranes and continues to be employed to form membranes with properties ranging from MF to RO^{16, 22}. Other cellulosic derivatives include cellulose diacetate, triacetate, and regenerated cellulose. Cellulose acetate is obtained from cellulose – a naturally occurring linear compound found in wood pulp and cotton linters – via acetylation; CA is hydrophilic and produces smooth membrane surfaces with low fouling propensity²³⁻²⁴. Cellulosic membranes are also relatively easy to manufacture with a wide range of pore sizes and are relatively inexpensive²². Disadvantages of CA include limited temperature range (less than 30 °C) and pH range (approximately 3-5)⁵. A further operational limitation of CA membranes is their chlorine intolerance; continuous exposure of less than 1 mg·L⁻¹ of free chlorine will oxidize CA membranes opening the pores and causing a loss of selectivity, particularly in RO applications²⁵. Also, due to the cellulose backbone, CA membranes are biodegradable and can, in fact, be consumed by organisms growing in biofilms.

Other more widely applied MF/UF membrane polymers include polysulfone (PSf), polyethersulfone (PES), sulfonated PSf or PES, polyacrylonitrile (PAN), polypropylene (PP), polytetrafluoroethylene (PTFE, a.k.a., Teflon), and polyvinylidene fluoride (PVDF)¹¹. These materials exhibit excellent permeability, selectivity, and stability in water treatment applications. Polysulfone and PES membranes are among the most popular materials for UF membranes, as well as the standard support substrates used in formation of NF and RO composite membranes, while PP and PVDF are more popular materials for MF membranes.

2.2.2. Thin Film Composite Membranes

A major breakthrough in the field of membrane separations was the development of thin film composite membranes, which comprise an ultra-thin “barrier” layer polymerized *in situ* over a porous polymeric support membrane^{5, 26}. These membranes are often referred to generically as “interfacial composite,” “composite,” or “TFC” membranes, although TFC[®] is registered trademark of Koch Membrane Systems, Inc. in the US and other countries. The major advantage of TFC membranes over integrally skinned asymmetric membranes is that the chemistry, and hence, performance of the upper selective layer and the porous support layer can be independently selected to optimize composite membrane performance²⁷. In addition, more expensive monomers can be used to form the selective layer without dramatically increasing cost because this region only accounts for a small portion of the total material. The key factors driving the development of TFC membrane materials over the past 40-50 years was the pursuit of high flux, high selectivity RO membranes for seawater desalination. Along the way, low-pressure RO membranes for desalting brackish water and for reclaiming wastewater to nearly

ultrapure levels were developed along with NF membranes now used predominantly for water softening and dissolved organic removal.

Thin film composite membranes are born out of conventional asymmetric polymeric membranes and, thus, are structurally similar to those discussed above; however, in TFC membranes the support and active layers are composed of two distinct polymers. The porous layer is generally formed through phase inversion and the dense layer is applied through interfacial polymerization or coating (dip, spray, spin) followed by cross-linking^{5, 26}. Curing (heat, UV, chemical) is frequently applied to further of the extent of polymer cross-linking, which significantly impacts the stability, permeability, and selectivity of the thin film^{5, 21}. Thin film composite RO/NF membranes are most often formed on the surface of a microporous support membrane via interfacial polymerization (*i.e.*, *in situ* polycondensation).

A large number of TFC membranes have been successfully developed from different polymers such as polyurea, polyamide (PA), polyurea-amide, polyether-amide, and others^{26, 28-30}, most of which have shown excellent selectivity, in particular high salt selectivity and relatively high water permeability for RO applications. Polyamide chemistry, developed by Cadotte and others, was first applied in the 1960's when DuPont and Monsanto developed asymmetric, integrally-skinned hollow fibers for RO seawater desalination³¹. Polyamide TFC membranes continue to be employed because they yield good salt rejection, while overcoming the relatively low flux of their integrally skinned counterparts.

Microporous supports for TFCs may be prepared from PSf, PES, sulfonated PSf and PES, polyether ketones, PVDF, sulfonated PVDF, or PAN through any number of casting procedures cited in the literature^{25, 28, 32-33}. Polysulfone is the most widely used polymer for RO support membranes^{5, 34}. Additives such as poly(ethylene glycol) and polyvinylpyrrolidone (PVP) have

been made to PSf support membrane casting solutions to increase porosity of the support membrane skin layer, and thus, the composite membrane permeability³⁵⁻³⁷. Presumably, the *de facto* commercial TFC membrane is an interfacially polymerized PA thin film formed over a PSf membrane with molecular weight cutoff of about 60 kDa;^{25, 28-29, 32-33, 38-41} however, the exact chemistry of commercial TFC membrane supports and coating films are proprietary.

Interfacial polymerization of TFC membranes is accomplished as follows^{28-29, 32, 42}. The microporous support membrane is immersed in an aqueous solution containing the first reactant (*e.g.*, a diamine monomer). The substrate is placed in contact with an organic solution containing the second reactant (*e.g.*, a triacyl halide). The organic solution is chosen to be immiscible with the aqueous solution so that the reaction proceeds at the interface of the two solutions. A dense but very thin polymer layer forms over the support membrane surface, which inhibits further polyamide formation and stops the reaction. The selective layer formed is very thin, which provides high water permeability, but densely cross-linked, which provides high salt rejection. The most common TFC coating film chemistry explored in the open literature is based on the amine monomer 1,3-diaminobenzene or *m*-phenylenediamine (MPD) polymerized with 1,3,5-tricarbonyl chloride or trimesoyl chloride (TMC), other di/tri-acid chlorides, or combinations thereof. The standard NF membrane derives from piperazine or polypiperazine derivatives polymerized with TMC, other di/tri-acid chlorides, or combinations thereof. It is suspected that most differences in commercial TFC NF/RO membranes result from the use of different support membranes, interfacial polymerization additives, and physical/chemical post-treatments³⁹⁻⁵⁰.

One common goal of post-treatments is to reduce a TFC membrane's propensity for surface fouling. This can be achieved through surface modifications via graft polymerization induced by methods such as plasma exposure⁵¹⁻⁵², UV-photoinitiation⁵³, or redox initiation⁴².

Recently, Kim et al. produced nanostructured RO membranes through plasma induced graft polymerization, in which a PSf supported PA RO membrane is exposed to plasma at atmospheric pressure to prime the surface and then free-radical graft polymerization of a small, hydrophilic, water soluble monomer, poly(methacrylic acid) (PMAA), is applied ⁵². The nanostructured surface roughness of the PMAA film (5.2-7.1 nm thickness) is nearly three times that of the unmodified TFC membrane. Membrane permeability doubled, with negligible changes in salt rejection. The modified membranes appeared to resist gypsum scaling 2-5 times longer than a low-fouling commercial RO membrane. This appears to be the first appearance in the open literature of a plasma-induced graft polymerization process at atmospheric conditions, which makes it potentially compatible with conventional membrane manufacturing infrastructure.

3. NANOTECHNOLOGY-BASED MEMBRANE MATERIALS

3.1. Nanostructured Ceramic Membranes

3.1.1. Zeolite-Coated Ceramic Membranes

A current thrust in ceramic membrane development is to form membranes with water permeability on the range of UF membranes, but solute selectivity like that of NF or RO membranes ¹¹. In 2001, molecular dynamics simulations showed that zeolite membranes—previously applied solely for gas separations—may be applicable for aqueous osmotic separations ⁵⁴. Since then, thin zeolite membranes have been studied for RO desalination of brackish water as well as a variety of wastewaters ⁵⁵⁻⁶¹. For RO applications, ceramic alternatives offer the clear advantage of mechanical stability under high pressures and chemical stability to withstand disinfectants. In many wastewater treatment applications, ceramic membranes are more fouling-resistant and chemically stable than current polymeric membranes.

Zeolites are naturally occurring aluminosilicate minerals with highly uniform sub-nanometer and nanometer scale crystalline structures. Typical zeolite membranes are amorphous silicate, aluminosilicate or aluminophosphate crystalline structures formed via hydrothermal synthesis^{10,62}. Other synthesis methods include *in situ* layer-by-layer crystallization and dry gel conversion in the presence of a template-water vapor⁶³. Aluminosilicate crystals are intrinsically inert, imbuing these membranes with extreme thermal and chemical stability⁶¹. Zeolite crystals consist of a three-dimensional cross-linked (Si/Al)O₄ tetrahedral framework, in which each Al or Si atom occupies the vertex of a network connecting four oxygen atoms. The framework structure contains cavities that allow for the movement and containment of ions and water molecules⁶⁴. The containment of molecules in a given zeolite framework is a function of temperature, water content, ion type, and the ratio of Si to Al atoms in the matrix⁶⁵. Cronstedt, a Swedish mineralogist, first characterized these structures in 1756, terming them zeolites, a term with Greek roots meaning ‘boiling stones’, because of their inherent ability to give up water upon heating⁶⁵. Many natural zeolites can be produced synthetically, while additional structures, with no natural occurrence, have been synthesized and are characterized as zeolites based on their structures, such as zeolite-A produced by Linde Corporation⁶⁵.

A few common zeolite materials employed in membranes include MFI-type, sodalite (SOD), and Linde Type A (LTA). Zeolite ZSM-5 (MFI)—the most commonly applied zeolite in membranes—is composed of a unit cell with the chemical formula Na_nAl_nSi_{96-n}O_{192~16H₂O}(*n*~3)⁶⁵. The MFI structure contains straight channels in one direction and perpendicular sinusoidal channels that are not interconnected⁶¹. The drawback of employing MFI-type zeolites in porous membranes is that the crystals must be oriented with respect to the permeation direction. The hydrated form of SOD, referred to as hydroxyl sodalite⁶⁵, has also

been applied in membrane materials ¹⁰. This mineral has the chemical formula $\text{Na}_6\text{Al}_6\text{Si}_6\text{O}_{24}\cdot 8\text{H}_2\text{O}$ ⁶⁵. Sodalites are not mineralogically defined as zeolites, but feldspathoids because in nature salt molecules are contained in their frameworks. The SOD cage, often referred to as the β -cage, is quite common to zeolite structures and when crystalline networks are created with this cage structure zeolitic properties are exhibited. One common example is the zeolite-A (LTA) unit cell, defined by the chemical formula $\text{Na}_{12}\text{Al}_{12}\text{Si}_{12}\text{O}_{48}\cdot 27\text{H}_2\text{O}$ ⁶⁵. The LTA structure is composed of SOD cages (β -cages) connected by truncated cubo-octahedron (α -cages), forming an interconnected cage structure. The interconnected inner channel in LTA offers the opportunity for simplified membrane fabrication since crystal alignment is unnecessary.

Pore size and framework density are the primary factors of concern when considering zeolites for water separations; pore size determines ion selectivity and framework density determines water permeability. Atoms other than Si and Al can be substituted into the cage structures of zeolites via ion exchange to imbue alternate charge and structural properties. Since the ability to act as a molecular sieve is due to the channel widths, changing the atoms in the framework, and thus the channel widths, will change the sieve properties ⁶⁶. Additionally, both the ion and water molecule mobility through a zeolite depend upon the relative density of the framework structure; open porous structures will facilitate less hindered transport ⁶⁵. This is indicated by the framework density, defined as the number of Si or Al atoms per 1000 Å. Framework densities (normalized for ideal Si frameworks) are 18.4, 16.7, and 14.2 for MFI, SOD, and LTA, respectively ⁶⁷, implying that LTA would be expected to have the largest water mobility.

The Si:Al ratio of a zeolite cage is the most important factor affecting chemical stability, hydrophilic properties, and occurrence of inter-crystalline defects ⁶⁵ –all primary factors of

concern when engineering selective and robust water treatment membranes. An increase in Si:Al ratio implies a decrease in the overall surface charge on the framework. The MFI-type zeolites are capable of a large range of Si:Al ratios, from approximately 30 in the ZSM-5 form to nearly pure Si for the isomorphous silicate type MFI. Noack et al. find that as the Si:Al ratio decreases in MFI-type zeolites water permeability and selectivity for water increase; however, defects simultaneously increase until a point where selectivity is compromised⁶³.

Separations in zeolitic materials occur primarily through molecular sieving, competitive adsorption or ion exchange¹⁰. Ions with small hydrated radii diffuse more quickly through zeolite pore structures. Cationic adsorption occurs onto the negatively charged surface of zeolite membranes, and may enhance diffusion by establishing a charge gradient. Initially, adsorption occurs onto the pore walls. Inter-crystalline molecular sieving occurs when the electrical double layers of these adsorbed ions overlap and inhibit the passage of charged ions⁵⁵⁻⁵⁶. Hydrophilic zeolite membranes previously applied for gas separations are composed of a loose, thick zeolite film through which separation occurs⁶⁸⁻⁷¹. However, the new RO membranes being developed require an ultra-thin, dense layer and so pains must be taken to form nanoscale zeolite coatings to produce membranes with permeability on par with polymeric RO membranes.

Li et al. apply MFI-type zeolite membranes (thickness $\sim 3 \mu\text{m}$) for RO desalination (with 0.1 M NaCl feed solution at 2.07 MPa)⁵⁵. Water flux is $0.112 \text{ kg}\cdot\text{m}^{-2}\cdot\text{h}^{-1}$ with 76.7% Na^+ rejection. The membrane is also challenged with a complex solution, more reminiscent of real RO feed waters, and the resulting water flux and rejection are lower ($0.058 \text{ kg}\cdot\text{m}^{-2}\cdot\text{h}^{-1}$ with Na^+ rejection of 58.1%). The reduced rejection is attributed to double layer compression within intercrystal pores of the zeolite material due to the high ionic strength of the feed solution. Another study with similar MFI membranes reports higher flux and rejection values (>95% of

Na⁺ ions)⁵⁶. Higher trans-membrane pressure increases water permeation and decreases ion permeation, resulting in better separation performance. Higher operating temperature increases both water and salt permeation, but having a larger impact on salt permeation. This is due to the reduced viscosity of the feed solution and increased diffusivity of water molecules and salt ions⁵⁵. The effect of temperature is consistent with that observed for traditional polymeric RO membranes, absent the effects of polymer swelling at higher temperatures⁷². While these membranes served as a proof of concept, higher water flux and salt rejection are both needed for MFI-based RO membranes to be commercially viable.

Duke et al. prepare MFI-type membranes for seawater desalination via template-free secondary growth⁵⁷. Zeolite films are formed over alumina supports by dip coating in a silicalite suspension and grown under hydrothermal conditions. This method improves control over membrane formation and produces fewer defects by decoupling the deposition and crystal growth steps. Alumina content should influence surface hydrophobicity and charge⁶³; however, in this study surface charge did not vary with Si:Al ratio⁵⁷. In RO mode (with 0.5 wt.% sea salts at 700 kPa) rejection is highest (50%) in an alumina-free silicate membrane due to strong electrostatic shielding of Na⁺ ions by the monopolar surface, which maintains the ideal double layer for this application. Because the Si:Al ratio allows for tuning of the surface properties and the resultant electrostatic double layer such membranes could also be tuned for specific ion-selective applications, but further work is needed to fully understand the connection between zeolite chemistry and membrane performance.

Liu et al. form an α -alumina supported MFI-type zeolite membrane via *in situ* crystallization on the inner surface of tubular ceramic membranes for the removal of organics from produced water⁶¹. In RO (with 0.1 M NaCl solution at 2.76 MPa) the membranes produce

a water flux of $0.35 \text{ kg}\cdot\text{m}^{-2}\cdot\text{h}^{-1}$ with Na^+ rejection of 99.4%. Ion separation occurs via size exclusion of hydrated ions as well as Donnan exclusion at pore entries. When tested for produced water treatment the coated membranes exhibit a water flux of $0.33 \text{ kg}\cdot\text{m}^{-2}\cdot\text{h}^{-1}$ with an organics rejection of 96.5%. With non-electrolyte solutions zeolite membrane selectivity is dominated by molecular sieving and so very different rejections are seen for high and low dynamic molecular size compounds. This work produced high salt rejections, but higher permeability must concurrently be achieved for practical application of these zeolite membranes.

Kumakiri et al. synthesize A-type zeolite membranes via hydrothermal synthesis atop a porous α -alumina substrate⁶². The substrate is seeded with crystals, dipped in an alumina-silica solution, and crystallized at 80°C for 5 hours. This process is repeated multiple times until reasonable separation performance is achieved. The membranes tested for performance in RO (with 10 wt.% ethanol feed solution at 1.47 MPa and 30°C) have pure water flux of $0.14 \text{ kg}\cdot\text{m}^{-2}\cdot\text{h}^{-1}$. The membrane selectivity for the ethanol/water mixture is 44%. Flux varies linearly with applied pressure, while selectivity is not significantly influenced. Most significantly, the membrane is mechanically stable up to pressures as high as $50 \text{ kgf}\cdot\text{cm}^{-2}$ (4.90 MPa). If performance of these membranes can be made competitive, their mechanical strength will make them ideal in high-pressure applications.

Kazemimoghadam formed composite polycrystalline hydroxyl SOD membranes atop high porosity tubular mullite supports¹⁰. The active SOD layer was formed through hydrothermal growth by coating the ceramic support with crystal seeds ($\sim 0.4 \text{ nm}$ diameter), dipping it in a homogeneous aluminate-silicate gel, and treating it at 100°C to allow crystal growth. The zeolitic membrane was tested for performance as an RO membrane for water treatment at variable trans-membrane pressures (100 to 300 kPa), feed temperatures (20 to 60

°C), and feed rates (0.5 to 3 L·min⁻¹). Flux increased with trans-membrane pressure, temperature (due to resulting lower viscosity), and feed rates (due to enhanced turbulence and hydrodynamic effects). High permeability was achieved ($\sim 10^{-12}$ m·Pa⁻¹·s⁻¹), on the order of current polymeric seawater RO membranes; however, no salt rejection data was published. If competitive selectivity can also be achieved, these materials may offer new opportunities for RO membranes in high temperature, pressure, and fouling applications.

Here we normalized zeolite membrane water permeability (from each paper reviewed above) by zeolite film thickness and performed the same calculation for permeabilities typically reported for commercial polymeric RO membranes to produce a Darcy permeability—defined as ‘specific water permeability’ in **Table 2**. While the permeability of the relatively thick (~ 3 -50 μm) zeolite films formed to date do not compare to ultra-thin (~ 50 -250 nm) TFC RO membranes, the specific water permeability compares favorably in some cases. Specifically, the SOD membranes produced by Kazemimoghadam et al.¹⁰ appear to have specific water permeability 3 orders of magnitude lower than commercial seawater RO membranes. If defect free zeolite films could be formed with thickness of 0.2 μm , the resultant membrane would have a water permeability of $\sim 0.5 \times 10^{-10}$, which is equivalent to a tight polymeric UF membrane. Obviously, this could make zeolite-based RO membranes a viable alternative material for high flux RO membranes, but with dramatically enhanced thermal, mechanical, and chemical stability. The challenge remains improving control over crystal nucleation and growth to ensure defect free ultra-thin zeolite films, which may require abandoning or substantially modifying traditional hydrothermal synthesis methods⁶².

Perhaps other fields should be examined for insight into new fabrication approaches. For example, Öztürk and Akata present a method for the oriented assembly of zeolite-A monolayers

for nanoelectronics applications⁷³. E-beam lithography is combined with direct attachment to form patterned mono and double layers of zeolite-A nanocrystals (~250 nm) atop silicon wafers. A dilute PMMA solution is spun onto silicon wafer surfaces to form resist films (~400 and 850 nm thick). The films are pre-baked and then patterns are defined with e-beam lithography. Direct attachment is achieved by applying a zeolite powder to the silicon wafer, pressing the zeolites, and heating. The direct attachment method results in >90% coverage of the silicon surface, strong binding to the wafer, and strong organization with a cube face of each zeolite oriented parallel to the silicon surface. Coverage is limited by the degree of homogeneity of the synthesized nanocrystals and pattern resolution is limited by the size of the nanocrystal, implying further tunability of the procedure. While this method is likely too expensive for large-scale membrane fabrication, alternative low-cost direct attachment methods could be sought by examining the rich knowledge of inorganic thin films in other fields.

3.1.2. Reactive/Catalytic Ceramic Membranes

Reactive surfaces are applied in water treatment as semiconductor-based (e.g., titania, zinc oxide, ferric oxide) membranes activated by UV or sunlight to engage in redox processes for the degradation of organic compounds⁷⁴⁻⁷⁷. The application of photocatalysis to water treatment was first discussed by Carey et al. in 1976 when they recognized the ability to degrade polychlorobiphenyls (PCBs)⁷⁸. Semiconductor electronic properties are defined by having a filled valence band and an empty conduction band. In photocatalysis, semiconductors function by absorbing a photon of energy greater than their own bandgap energy, and creating an electron-hole pair via excitation of electrons from the conduction to the valence band^{74, 79}. Photocatalysis occurs when a semi-conductor nanoparticle is irradiated with an amount of

energy, $h\nu$, greater than its own bandgap energy, ΔE (**Figure 3**). These electron-hole pairs will either recombine (in a matter of nanoseconds) or react with the surrounding media. The latter is only possible if the electron and/or hole can be trapped in a surface defect or captured by an appropriate scavenger in the bulk media⁸⁰.

In bulk semiconductor materials, only the hole or electron is normally available for interaction; however, in nanoscale materials both are available at the surface allowing for high efficiency interactions. The mechanism by which oxidation of organic molecules in water is initiated at the particle surface is not yet fully understood, but theories include direct oxidation by the electron hole (positron), indirect oxidation via hydroxyl radicals produced on the surface or in the solution, or some combination thereof⁷⁴. Suspended nano-photocatalysts are applied for remediation of contaminants; the suspended state provides maximum surface area and activity⁸¹⁻⁸³. The key drawbacks of suspended processes are nanocatalyst recovery and regeneration (or disposal) of spent material. A clever approach is catalyst coated magnetic iron oxide nanoparticles, which would enable magnetic recovery of nanoparticles⁸⁴⁻⁸⁵.

Catalysts coatings have been formed on polymeric membranes to create reactive surfaces for enhanced separations while eliminating the complexity of catalyst recovery⁸⁶⁻⁹¹. Titania nanoparticles are highly photoactive and exhibit antimicrobial activity under UV light^{79, 92}. Water purification systems based on photolytic disinfection are currently available. Inactivation of pathogens occurs by DNA damage from UV irradiation and through the production of reactive oxygen species, in particular hydroxyl radicals, which damage the cell wall of organisms (inactivation by cell lysis). Molinari et al. altered commercially available porous polymeric membranes with a titania layer, by filtering a nanoparticle suspension through and applying UV/vis irradiation and show elevated (4-Nitrophenol) photodegradation⁸⁶. Madaeni and Ghaemi

form “self-cleaning” RO membranes with the addition of titania nanoparticles; the cleaning, as well as elevated flux, witnessed upon UV application are attributed to two concurrent phenomena: photocatalysis and ultra-hydrophilicity⁸⁸. To curtail the inevitable titania-catalyzed UV degradation of the organic parts of the conventional membranes, Mo et al. prepare PSf-supported self-cleaning PA/titania membranes through interfacial polymerization, which contain a layer of silicon dioxide between layers of cross-linked PA and titania⁸⁷. Flux recovery after 15 h of operation (with water cleansing and UV exposure every 3 h) is greater than 98% for these photocatalytic membranes, significantly higher than standard water treatment membranes.

Titania nanopowders are also applied to ceramic membrane surfaces, such as silica⁹³⁻⁹⁴, alumina⁹⁵, zeolites⁹⁶, and activated carbon⁹⁷, which are more stable than polymers under UV light and in the presence of reactive oxygen species. Choi et al. report on reactive membranes with titania coatings atop alumina supports⁹⁵. Acid and surfactant are employed in the sol-gel process to tailor the resulting membrane morphology and produce high efficiency films and composites. XRD analysis reveals anatase crystals throughout the thin film with crystalline size of 8-10 nm. This size range is known to produce the optimum catalytic activity because it is the point where the blue shift occurs favoring surface recombination of electron-hole pairs and allowing for the maximum number of active sites per mass of catalyst⁹⁸. The structure of these films is highly porous and interconnected, enabling a high surface area for both adsorption and photocatalytic activity on the titania surface. Three dip-coatings are sufficient to create a defect-free skin layer (~0.9 μm thick); while more layers may be desirable to provide more active area, each layer also increases processing time and cost⁹⁵. The resulting membrane has water permeability of $6.71 \text{ L}\cdot\text{m}^{-2}\cdot\text{bar}^{-1}\cdot\text{h}^{-1}$ and molecular weight cut-off of ~12 kDa. The overall permeability is high considering that the Al_2O_3 substrate has a relatively low permeability (11.0

$\text{L}\cdot\text{m}^{-2}\cdot\text{bar}^{-1}\cdot\text{h}^{-1}$); even higher permeability may be achieved with more permeable ceramic supports (*e.g.*, mullite).

Catalytic ozonation is used for natural organic matter and organic compound removal in water and wastewater treatment; when combined with a catalytic metal oxide other substances can be degraded such as phenols, aromatic hydrocarbons, and humic substances⁹⁹⁻¹⁰². Karnik et al. exhibit the potential for catalytic membranes in combined ozonation/UF for disinfection byproduct removal¹⁰³. Commercially available ceramic membranes (composed of a mixture of alumina, zirconia, and titania) are coated via the layer-by-layer technique with iron oxide nanoparticles (4-6 nm diameter). The coating layer has negligible resistance, witnessed by unchanged membrane permeability. The membranes serve as catalysts in the ozone degradation of natural organic matter and disinfection by-products. Specifically, total trihalomethanes and halogenic acetic acids, are removed up to 90 and 85%, respectively. The proposed mechanism by which this degradation occurs is the decomposition of ozone on the iron oxide coating surfaces, enhancing hydroxyl radical production and, thus, degradation¹⁰⁴⁻¹⁰⁵.

The major limitation of photocatalysis is the fast recombination of the produced electron-hole pairs. This limits degradation of organics and inactivation of organisms with complex, dense cell wall structures, such as bacterial endospores that require longer exposure times^{79, 106}. When immobilized in membranes or in reactive surfaces, the active area is reduced, further limiting the photoactivity⁸⁵. Research shows that doping the particles with ions increases the photoactivity by separating the photo-induced charges and enhancing surface availability¹⁰⁶⁻¹⁰⁸. For disinfection applications, reactive oxygen species production that ultimately leads to cell wall compromise and cell demise is limited by the ability for the nanoparticle to maintain electron-hole pairs^{79, 109}. Krishna et al. coat multi-walled carbon nanotubes (CNTs) (known to

have large surface area and substantial photon-generated electron trapping capacity) with titania in order to delay recombination⁷⁹. Titania-coated CNTs display two times the inactivation rate of commercially available titania alone when tested on *B. cereus* spores.

Both zeolite and catalyst-coated membranes face similar challenges as have always faced ceramic water treatment membranes, that is, high manufacturing cost and low packing density relative to polymeric membranes. An additional hindrance of photocatalytic water treatment is the energy demand for irradiating the surfaces. To minimize this, solar induced photocatalytic surfaces have been investigated and applied^{91, 110}. Reactive surface-mediated photocatalysis for water treatment shows promise, particularly for the purpose of small-scale production where solar energy can be utilized.

3.2 Inorganic-Organic Membranes

3.2.1. Mixed Matrix Membranes

Mixed matrix membranes seek to take advantage of both the low cost and ease of fabrication of organic polymeric membranes and the mechanical strength and functional properties of inorganic materials. Zimmerman et al. first discussed mixed matrix membranes in the 1990's as a way to push the limitations of polymeric membranes for gas separations¹¹¹. Mixed matrix membranes including inorganic molecular sieves, such as zeolites and silicalite, embedded within a polymer matrix are employed to provide preferential flow paths for the target species to pass through¹¹²⁻¹¹⁵. The formation of continuous pathways of fast diffusion molecular sieves is theorized to occur at a volume fraction of filler material known as the 'percolation threshold'. At this point, target molecules can traverse the entire membrane cross-section through the filler^{111 116-117 118}. Above certain high volume fractions, defects tend to occur at the polymer-

filler interface limiting selectivity¹¹¹. Mixed matrix membranes present an opportunity for tunable water treatment membranes as well, through increased selectivity, targeted functionalities, and improved thermal, chemical and mechanical stability. The interplay between enhanced properties and defect formation must be balanced to derive positive benefits without compromising the integrity of the membrane.

Micron-sized inorganic particles are added to typical porous water treatment membranes to achieve enhanced selectivity, as well as other functional properties¹¹⁹⁻¹²³. Inorganic fillers in porous membranes are shown to inhibit macrovoid formation, increase pore interconnectivity, and improve mechanical strength¹²⁰. Such morphological and mechanical changes are desirable to avoid compaction of membranes during high-pressure separations. One example of this is the Zirfon® UF membrane, composed of an asymmetric PSf membrane with zirconia (ZrO_2) particles^{120, 122}. These membranes exhibit elevated permeability without compromise of particle retention^{120, 122}. The increased permeability is due to grain disturbances that occur when zirconia content is sufficiently high (~40 wt.%) during phase inversion formation of the top layer and increase pore distribution preferentially at the particle-matrix interface^{119, 122}. Aerts et al. report that as zirconia particle (~0.9 μm) content increases, elastic strain in Zirfon® UF membranes decreases, producing a more mechanically robust membrane¹¹⁹. Wara et al. dispersed ceramic alumina particles (~0.34 μm) in CA membranes during phase inversion, observing reduced macrovoids and, thus, increased selectivity¹²¹.

Today, mixed matrix membranes comprising nanoparticle fillers are emerging. These membranes are also referred to as polymer-nanocomposite membranes. Isodimensional nanoparticles are commonly used as nanocomposite fillers as they provide the highest surface area per unit volume. Nanoparticles for membrane applications are most often prepared through

the sol-gel process, which yields high purity samples and allows for control over size, composition, and surface chemistry ¹²⁴⁻¹²⁵. Additional formation processes include: inert gas condensation, pulsed laser ablation, spark discharge generation, ion sputtering, spray pyrolysis, laser pyrolysis, photothermal synthesis, thermal plasma synthesis, flame synthesis, low-temperature reactive synthesis, flame spray pyrolysis, mechanical alloying/milling, mechanochemical synthesis, and electrodeposition ¹²⁴. The favorable characteristics of nanoparticles can be exploited, similar to micron-scale inorganic particles, by directly including these particles in the casting solution.

Attention to nanoparticles for environmental applications has grown as their ability to preferentially disinfect, adsorb, and degrade pollutants in aqueous solutions is realized ^{6, 124, 126-128}. Metal oxide nanoparticles, specifically magnesium oxide (MgO) particles, inactivate Gram-positive bacteria, Gram-negative bacteria, and spore cells ¹²⁶. Alumina nanoparticles are useful as an adsorbent for nickel [Ni(II)] in aqueous solutions ¹²⁹. Iron oxide, aluminum oxide, and titanium oxide nanoparticles adsorb heavy metals ¹²⁴. Zero-valent iron nanoparticles have been applied for the removal of halogenated hydrocarbons, radionuclides, and organic compounds ¹³⁰⁻¹³². Such nanoparticles pose an efficient alternative to activated carbon for water and wastewater treatment, with increased surface area and activity due to their nanoscale characteristics ¹²⁴. Nanocomposite membranes have been researched for a variety of goals, including targeted degradation, enhanced flux and selectivity, decreased fouling propensity, and increased thermal and mechanical stability ¹³³⁻¹⁴², while maintaining the ease of fabrication and low cost of their fully polymeric counterparts.

Targeted degradation can be achieved with addition of nanoparticles to polymeric membranes, particularly for reductive dechlorination processes ¹⁴³⁻¹⁴⁵. Bi-metallic nanoparticles

(e.g., Fe/Pd, Fe/Ni, Mg/Pd) are applied for pollutant degradation, wherein the first zero-valent metal, often iron, serves as an electron donor and is actually responsible for degrading the target compound while the second metal serves as a catalyst to promote the reaction through hydrogenation¹⁴⁵⁻¹⁵⁰. Wu et al. employ CA supported palladium-coated iron nanoparticles (~10 nm; 1.9 wt.% Pd) formed through microemulsion to facilitate trichloroethylene decomposition and find that dechlorination is significantly enhanced¹⁴³⁻¹⁴⁴. Smuleac et al. show elevated degradation of 2,2'-dichlorobiphenyl with PVDF membranes containing similar Fe/Pd nanoparticles (~20-30 nm) formed through *in situ* polymerization¹⁴⁵. In the latter case, nanoparticles are formed within the polymeric matrix through an ion exchange with Fe²⁺, followed by reduction to Fe⁰, and deposition of Pd. *In situ* formation of nanoparticles inhibits agglomerate formation, a common issue when nanoparticles are dispersed in membrane casting solutions¹⁵¹. Good dispersion of nanoparticles is required to reap benefits for mixed matrix membranes; in some cases, membranes containing nanoparticle agglomerates perform worse than the unmodified membranes with no fillers at all¹⁵².

Particles that alter the surface properties of membranes can change separation performance and fouling behavior^{23, 134, 153}. Yan et al. add alumina nanoparticles (~10 nm; 19 wt.%) to casting solution during phase inversion of PVDF to form mixed matrix UF membranes¹³⁴. While pore density and size are not altered, hydrophilicity, water permeability, fouling resistance, flux recovery, and mechanical stability increase¹³⁴. Maximous and Nakhla prepare PES UF membranes with alumina nanoparticles (~0.48 nm; 0.01-0.05 wt.%) and find that membrane fouling and flux decline are reduced¹³⁵. Fan et al. add polyaniline (PANI) nanofibers to commercial UF membranes (1-15 wt.%) and find increases in water permeability, selectivity, and surface wettability¹³⁶⁻¹³⁷. Antifouling nature improves and flux recovery increases (to as

high as 90%) with particle additions in the blended membranes¹³⁶. Furthermore, flux recovery could be achieved with a simply water cleanse, implying that adsorption to these improved surfaces is much weaker than to unmodified membranes¹³⁷.

Particles with antimicrobial properties can help reduce biofouling of membranes¹⁵⁴. Silver nanoparticles are excellent bacteriocides^{138, 155-157}. Silver nanoparticle coatings are now widely applied as antibacterial safeguards in many consumer products¹⁵⁷. Morones et al. study the activity of nanoscale silver particles embedded in a carbon matrix towards four types of Gram-negative bacteria and find that all four are inactivated due to interaction with the silver nanoparticles¹³⁸; however, only those particles freed from the carbon matrix are able to interact with the cell membranes, enter the cells, and effectively inactivate them. Biofilm formation is successfully reduced in nano-silver containing membranes due to the successive release of ionic silver over the lifetime of a membrane¹³³.

In order to ensure sustained ion release, silver nanoparticles incorporated in membranes must be fully reduced to the zero-valent state¹⁵⁸. Taurozzi et al. find that when PSf membranes are formed with silver nanoparticles included in the casting solution—both following *ex situ* reduction of the nanoparticles prior to addition to the casting solution and with *in situ* reduction during casting—water permeability increased, with negligible reduction in solute rejection¹³³. Enhanced performance is attributed to macrovoid broadening and increased pore size and pore density due to the presence of nanoparticles. Because nanosilver dissolves rapidly in water, long-term testing is needed to quantify the lifetime of these membranes and to understand the impacts of defect formation due silver dissolution.

Mixed matrix membranes have been formed with the addition of nanotubes^{34, 159-160}. Carbon nanotubes exhibit antimicrobial activity¹⁶¹; thus, presenting an opportunity for improved

disinfection or antifouling membranes. Bundling is often an issue, especially with single-walled CNTs, due to the van der Waals interactions between nanotubes and the fact that they are insoluble in water and organic solvents; this hinders the application for large scale fabrication of membrane materials¹⁶². Lin et al. recommend functionalizing CNTs with polymer groups that are structurally similar to the bulk polymer matrix to aid nanotube dispersion and homogenous membrane properties¹⁶⁰.

Choi et al. cast multi-walled CNT/PSf mixed matrix membranes by nonsolvent induced phase inversion³⁴. Nanotubes are pretreated with acid to aid in dispersion throughout the solvent. Surface hydrophilicity of the membranes increases with the presence of CNTs due to the carboxylic acid groups that form on CNT surfaces during acid pretreatment. Pore size increases with nanotube additions up to 1.5 wt.% and then decreases, becoming smaller than pure PSf at 4 wt.%. Water permeability and rejection, however, increased with nanotube additions as high as 4 wt.%, likely because the improved hydrophilicity and resulting anti-fouling ability plays the dominant role in membrane performance. Brunet et al. formed nanotube/polymer membranes by dispersing multi-walled CNTs (4 wt.%) throughout a PSf/PVP polymer matrix via phase inversion¹⁵⁹. PVP seemed to aid in the dispersion of CNTs throughout the membrane casting solution. Mechanical stability (indicated by the degree of elongation to failure) is enhanced in the mixed matrices with well-dispersed nanotubes; however, the presence of CNT aggregates seems to reduce stability. The blended membranes did not display the desired antimicrobial activity because the contact between organisms and the CNTs stabilized in the polymer matrix is not sufficient to enable inactivation. Future applications may attempt to expose CNTs to solution for antimicrobial applications.

Inorganic fillers additionally enhance the thermal and mechanical stability of polymeric membranes by reducing the impacts of heating and membrane compaction. Compaction occurs during the initial stages of membrane operation, resulting in irrecoverable flux decline¹⁶³. The majority of compaction is known to occur in the bulk macrovoid region of asymmetric membranes¹⁶⁴ and so adding mechanically strong fillers to this region is thought to assist in reduced structural losses. Ebert et al. demonstrate increased stability of poly(vinylidene fluoride) (PVDF) membranes when titania nanoparticles are included as inorganic fillers in the phase inversion casting solution¹⁶⁵. Filled membranes exhibit higher thermal stability (as witnessed by minimal change in pore distribution following heat treatment) and less compaction (as seen by minimal structural changes after pressure application in the filled membranes). Calculations show an 83% decrease in pore volume in pure PVDF membranes, but only a 17% decrease in PVDF/titania membranes following compaction¹⁶⁵. In another study, silica and zeolite nanocomposite-PSf supported RO membranes are shown to experience less compaction than pure PSf supported membranes¹⁶⁶. In general, the nanocomposite-PSf supported membranes have higher initial water permeation and less flux decline during compaction. Electron microscopy images verify that the nanocomposite-PSf supports resist the deleterious impacts of compaction by maintaining open surface pores better than the pure PSf supported RO membrane.

Mixed matrix membranes can also be formed by dispersing polymeric structures within inorganic matrices. Arkas et al. synthesized organo-silicon dendritic networks within a porous ceramic membrane and showed the resultant filter was effective at removing toxic polycyclic aromatic compounds from water¹⁶⁷. Dendrimers are polymers with a high level of branching and symmetric structure of central core, repeating polymer units, and terminal functional groups. While dendritic polymer synthesis is more tedious than conventional polymers, the tunable

functional groups and tendency to form nanocavities make them desirable for functional membrane applications. The filters are capable of reducing polycyclic aromatics in water to a few ppb. The filters are also regenerated by acetonitrile washing thanks to the chemical stability of the ceramic backbone.

Nanoparticle-containing mixed matrix membranes, *a.k.a.*, nanocomposite membranes, have the potential to provide novel functionalities, enhanced performance, and heightened stability while maintaining the ease of membrane fabrication. While nanoparticle mixed matrix membranes are not yet commercially available, the micron-scale predecessors would seem to have paved the way for advances in this technology. As industrial-scale nanoparticle production grows, costs of these materials will come down and many of the research level innovations may make their way into the marketplace.

3.2.2. Thin Film Nanocomposite Membranes

Nanoparticle additions have been made to the thin films of TFC RO membranes in order to take advantage of the properties of the nanomaterials. Addition of nanoparticles to interfacial polymerization processes or surface attachment via self-assembly has introduced the concept of thin film nanocomposite (TFN) membranes, which offer potential benefits of enhanced separation performance, reduced fouling, antimicrobial activity, and other novel functionality¹⁶⁸⁻¹⁷³. As with TFC membranes, TFN membrane performance can be fine-tuned with nanoparticle additions to the support membrane (see mixed matrices, **Section 3.2.1**), the coating film, or both.

Zeolite nanoparticle-based TFN RO membranes attempt to leverage the molecular sieving properties of zeolites^{168, 173}. By casting molecular sieves in the thin film of an RO membrane, where diffusion controls the transport process, the goal is to essentially reach the

percolation threshold in the dense selective layer with an individual particle (**Figure 4**). Jeong et al. cast zeolite-polyamide thin films atop PSf support membranes by dispersing zeolite nanoparticles in the TMC solution prior to interfacial polymerization¹⁶⁸. Water permeability of zeolite TFN membranes increases as much as 80% over identically cast TFC membranes at the highest TFN particle loading (0.4 wt.%), with rejections consistently above 90%. Pure water permeability increases even for pore-filled zeolites, although permeability increases more for pore-opened zeolites supporting the role of molecular sieving. These results appear to imply a combination of effects contribute to the permeability enhancement born out of zeolite fillers.

Lind et al. similarly cast TFN membranes also containing LTA nanoparticles (0.2 wt.%) in the thin film through interfacial polymerization and characterized membrane structure, morphology, and separation characteristics¹⁶⁹. The presence of zeolite nanoparticles results in higher permeability, greater negative surface charge, and thicker membranes regardless of particle size used (97, 212, and 286 nm). Larger nanoparticles produce membranes with highly favorable surface properties, while smaller nanoparticles increased permeability more by increasing the characteristic pore size. All TFN membranes reported are less cross-linked than pure polyamide TFC counterparts, suggesting another potential mechanism by which TFN membrane permeability is enhanced. This work implies that the addition of nanoparticles can be tailored to particular membrane applications with the selection of nanoparticle size and type.

Later, TFN membranes were cast by Lind et al. by including sodium- and silver-exchanged LTA nanoparticles (~140 nm; 0.4 wt.%) in the PA polymerization reaction¹⁷³. Increased pure water permeation is found in both TFNs, with more significant increases, as much as 66%, with silver zeolites; rejection (tested with NaCl and PEG) is not affected. Silver-zeolites not only provided more hydrophilic surfaces, but also actively inhibit biofouling due to the

antimicrobial nature of nanosilver. Lee et al. prepared composite PA thin film NF membranes with titania (~60 nm) nanoparticles in the skin layer through interfacial polymerization¹⁷⁰. As titania concentration increases towards 5 wt.%, water flux increases and decreases salt rejection, suggesting significant defects formed in the nanocomposite coating film.

Carbon nanotubes have attracted attention for novel environmental applications. Brady-Estévez et al. demonstrate the use of CNTs for the removal of viral and bacterial pathogens from water at low pressure inputs¹⁷⁴. A thin coating of bundled single-walled CNTs (maximum gap ~0.3 μm) is overlaid on the surface of a PVDF microporous membrane (5 μm pore size). After passing water through the filter all *E. coli* cells (~2 μm) are removed, likely due to size exclusion. More importantly, a fluorescence-based viability test proves that nearly 80% of the bacteria are inactivated after 20 min contact time (an 8-fold increase over the uncoated microporous membrane). This result is confirmed with a metabolic activity test that finds only 6% of the *E. coli* cells are metabolically active following interaction with the filter. Viral pathogen removal is exhibited by passing a suspension containing a model virus, MS2 bacteriophage (~27 nm), through the filter. Size exclusion is not enough to explain the virus removal seen, even with the presence of the nanoporous coating. Results of viral inactivation by the CNT-coated filter are conclusive, yet vary with CNT layer thickness indicating a lower limit of contact time required for inactivation. Full virus removal (5-7 log removal) is observed with a 6 μm skin layer; 3.2-log removal is seen with a thin 2 μm layer. Such uses of CNTs offer an exciting opportunity for use in disinfection and water filtration.

Enhanced hydrophilicity, and thus, reduced fouling is a goal of many TFN studies. Luo et al. produce PES UF membranes dip-coated with titania nanoparticles and find contact angle reduction from 39.6 to 19.2°¹⁷⁵. The same group cast films with controlled titania contents (5,

10, and 15 wt.%) and find the largest reduction in contact angle at 10 wt.% (from 79.6 to 41.2°); at the higher 15 wt.% contact angle reduction dropped off (to 73.8°) possibly because of nanoparticle agglomeration¹⁷². This beneficial breakpoint points toward the existence of optimum particle loading depending on starting materials. Bae et al. form titania nanocomposite polymer membranes through electrostatic self-assembly and again find reductions in fouling, including reductions in initial sharp flux decline and eventual irreversible fouling¹⁷¹. It is found that pore size and water permeability slightly decrease¹⁷¹, but depending on application the anti-fouling capacity may outweigh this loss.

Here, we predict the performance of nanocomposite thin films using a Maxwell mixing model and the relative permeabilities of the filler nanoparticle and thin film polymer coupled with the fractional content of each. Theoretically, the permeability of TFNs containing impermeable nanoparticles (e.g., titania nanoparticles) decreases, while the permeability of TFNs employing permeable nanoparticles (e.g., SOD-zeolite nanoparticles) increases (**Figure 5**). Any nanoparticle with water permeability higher than that of the polymer matrix can increase the permeability of the resulting nanocomposite membrane by providing preferential flow paths through the cross-section. The filler fraction required for reasonable enhancements will depend upon the intrinsic permeabilities of both phases. Conversely, impermeable nanoparticles can only reduce the water permeability of a membrane because they reducing the area available for permeation through the polymer film. However, impermeable fillers can increase membrane permeability through defect formation, which may also compromise solute rejection. This is a simple analysis, but the concept must be kept in mind as research continues on nanocomposite materials. For certain applications, a loss in permeability may be overcome by the benefits of super-hydrophilic or antimicrobial nanoparticles that significantly reduce membrane fouling, but

in general reduced permeability is not a desirable feature. Cost considerations are also important, while antimicrobial and zeolite nanoparticles are expensive, zeolite TFNs have shown higher flux at extremely low loadings such that the cost increase may be minimal.

3.3. Biologically-Inspired Membranes

3.3.1. Aquaporin Membranes

Aquaporins are the protein channels that control water flux across biological membranes. Agre et al. won a Nobel prize for discovering the first of these proteins, which they named Aquaporin-1 (AQP1), in 1993¹⁷⁶. This first characterized aquaporin is found widely in human tissues with the purpose of rapid, passive transport of water across cell membranes. Such transport channels exist in the cells of species in all three domains of life. A single trans-membrane protein is ~120 kDa in size, with a tetramer structure composed of four channels¹⁷⁷. These channels are responsible for the physiological plumbing of our bodies, including our red blood cells, our brain, and our kidneys. Water movement in aquaporins is mediated by selective, rapid diffusion caused by osmotic gradients¹⁷⁸⁻¹⁷⁹. The hourglass shape of AQP1, with selective extracellular and intracellular vestibules at each end, allows water molecules to pass rapidly in a single-file line, while excluding proteins^{178, 180}.

Zhu et al. produced a fundamental study to simulate water permeation in AQP1¹⁸¹. Two factors involved in water transport are defined: osmotic permeability, p_f , molecular movement due to concentration differences resulting in net mass transfer, and diffusion permeability, p_d , random movement of molecules resulting in no net transfer. In the theory, water molecules transport in single-file through a narrow aquaporin channel; a constant number of molecules are assumed to occupy the channel at all times and the water molecules are assumed to move

together in discrete translocations, or hops (**Figure 6**). In the case of diffusion permeability dominated movement, a “permeation event” involves the movement of two molecules between opposite reservoirs. This requires that a molecule moves all the way through a channel and is different than a hop. The ratio of p_f/p_d is, in fact, the number of effective steps a water molecule must move in order to permeate a channel.

The highly selective water permeability of aquaporin channels is an interesting concept when considering water treatment membranes. Biological lipid bilayers containing aquaporins transport water and maintain selectivity that far surpasses all commercial RO membranes. Single aquaporins transfer water molecules at rates of $2\text{-}8 \times 10^9$ molecules per second¹⁷⁷. Kaufman et al. predict that a membrane with 75% coverage of aquaporins could have a hydraulic permeability in the range of $2.5 \times 10^{-11} \text{ m}\cdot\text{Pa}^{-1}\cdot\text{s}^{-1}$, an order of magnitude higher than commercial seawater RO membranes¹⁷⁷.

Kumar et al. include Aquaporin-Z from *E. coli* bacterial cells in a polymeric membrane¹⁸². This aquaporin is selected based on the ability for high water permeation and high selectivity. In addition, it is easy to purify and multiply using a recombinant *E. coli* strain. A symmetric triblock copolymer with a high hydrophobic to hydrophilic block ratio is selected, reminiscent of a lipid-bilayer membrane. The resulting protein-polymer membrane demonstrates over an order of magnitude increase in water permeability over a purely polymeric membrane, as well as full rejection of glucose, glycerol, salt, and urea. These results demonstrate that aquaporins are functional for synthetic applications.

The transport across biological membranes is driven by an osmotic pressure (or salt concentration) gradient, rather than a mechanical applied pressure gradient as in industrial filtration processes. Kaufman et al. demonstrate supported lipid bilayers formed atop dense water

permeable NF membranes that can be operated under a mechanical driving force as RO membranes (**Figure 7**)¹⁷⁷. NF membranes are chosen as the support because of their high permeability and low surface roughness that allowed for minimal distortion of the lipid bilayer. Aquaporin solutions (of protein PM28, the integral protein of a spinach leaf plasma membrane) are deposited onto commercially available NF membranes (NF-270 and NTR-7450) via vesicle fusion. Electrostatic interactions are tailored to optimize surface coverage with the lipid bilayer; formation on NTR-7450 at pH 2 with a low ionic strength solution and with the NF membrane surface and the protein vesicles having opposite charges produces the best results. Full, defect-free coverage is implied by the decrease in permeability of the composite membrane (from ~ 30 to $\sim 2 \times 10^{-12}$ m \cdot Pa $^{-1} \cdot$ s $^{-1}$). Further work must be done to further optimize the formation of such structures and their resulting permeability and selectivity; however, this work demonstrates the potential for incorporation of biological aquaporins into pressure-driven RO membranes in the future. At this time, aquaporin-based membranes are not commercially available due to the difficulties of attaining large quantities of proteins and producing large areas of membrane material, but research continues in this area. A synthetic approach to producing and purifying aquaporin samples in large quantities might improve practical implementation. Furthermore, techniques to simplify the fabrication and produce mechanically robust membranes will bring the promise of these materials to reality.

3.3.2. Vertically Aligned Nanotube Membranes

Nanotubes have attracted attention because of their many unique properties¹⁸³⁻¹⁸⁴. Carbon nanotubes exhibit a fast mass transport reminiscent of aquaporin water transport in which water transport is 2-5 times higher than theoretical predictions by the Hagen-Poiseuille equation

¹⁸⁵⁻¹⁸⁶, and gas transport is over an order of magnitude larger than Knudsen diffusion predictions ¹⁸⁶. The striking flow rate has been studied with molecular dynamic simulations and attributed to atomic smoothness and molecular ordering, in which water molecules are passed through CNTs in a one dimensional single-file procession ¹⁸⁷⁻¹⁸⁸. This finding implies significant advantages of aligned CNT membranes over conventional membranes through reduced hydraulic driving pressure, and therefore, lower energy costs; however, this will not be the case in desalination applications where productivity is limited by osmotic pressure via the ‘thermodynamic restriction’¹⁸⁹. Carbon nanotube-based membranes may also have longer lifetimes than conventional membrane materials due to the excellent mechanical properties that CNTs exhibit ¹⁹⁰⁻¹⁹¹.

When CNTs act as the selective layer they can form an array of high flux molecular sieves within a polymer matrix (**Figure 8**) at the surface of a membrane. Kim et al. fabricate aligned CNT/polymer membranes that allow for efficient gas separation processing; CNTs allow for increased selectivity and gas flux due to their intrinsic properties ¹⁹². Highly selective, high flux membranes provide a more efficient, lower energy option ⁷. It is the hope that water treatment analogues to these membranes will be produced with similar materials.

Most uniform, aligned nanotube arrays to date are produced through chemical vapor deposition (CVD) ¹⁹³⁻¹⁹⁸. Fornasiero et al. attempted to model and study biological porin ion transport with sub-2 nm diameter CNTs as surrogates ¹⁹⁸. Aligned CNTs are grown through CVD on a silicon surface and then encapsulated through conformal deposition of silicon nitride to form composite membrane structures. The CNTs are adapted by fixing negatively charged functional groups at the ends in order to mimic porin structure and the selectivity region at the openings, which dictates ion transport. Pressure-driven NF is coupled with capillary

electrophoresis for ion concentration analysis in the filtrate. Ion exclusion is found to be as high as 98%. The results show ion transport is dominated by Donnan type rejection based on electrostatic interactions between membrane surface charge and particle charge rather than steric effect¹⁹⁸.

Gao et al. grow dense arrays of titanium carbide crystal-filled, aligned CNTs (inner diameter 10-100 nm) atop a titanium substrate through CVD with a simultaneous solid state reaction¹⁹³. Choi et al. produce uniform (10 nm diameter) aligned CNTs atop nickel deposited silicon substrates through microwave plasma-enhanced CVD; it is found that the nickel thin film characteristics largely control the growth rate and resulting diameter and density of CNTs¹⁹⁴. Maeron et al. produce aligned CNT films (20-28 nm diameter; 20-35 μm thick) atop silicon chips through CVD with gaseous acetylene and nitrogen¹⁹⁷. Overall perpendicular alignment of multi-wall CNTs on the preformed substrate is seen and attributed to high nanotube density, although the individual nanotubes are curved. Yoshikawa et al. produce thin, narrow, uniform, vertically aligned CNTs (2.5-6.0 nm diameter; 20-90 μm length) atop commercial aluminum foil using catalyst-supported CVD¹⁹⁶.

Holt et al. produce gap-free sub-2 nm diameter aligned double-walled CNT membranes (1.3-2 nm pores determined by size exclusion) through an automated and reproducible microelectromechanical system fabrication, using catalytic CVD¹⁸⁶. Pore densities are as high as 0.25×10^{12} pores per cm^2 ¹⁸⁶, the highest example to date. Water flux through these CNT membranes is found to be at least 3 orders of magnitude higher than theoretical, Hagan-Poiseuille predictions¹⁸⁶. These nanoporous membranes offer opportunities for extreme selectivity, without compromising water permeation. While aligned CNT membranes show

promise, alignment via CVD is expensive, sensitive, and not yet applicable for large-scale fabrication.

Films of aligned CNTs have also been produced through self-assembly approaches^{192, 199-200}. Heer et al. accomplish this by drawing aqueous suspension of CNTs (~10 nm diameter; 1-5 μm length) through a 0.2 μm pore ceramic filter and then transferring the deposit to a Teflon surface¹⁹⁹. After rubbing the surface with Teflon or aluminum foil the tubes reorient perpendicular to the surface. The vertically aligned structure is confirmed by electron microscopy images. A magnetic alignment approach for macroscopic film formation, involving high pressure filtration of suspended single-walled CNTs in a magnetic field, is applied by Casavant et al. to produce (125 cm^2 of 10 μm thick) aligned CNT membranes²⁰⁰. Theoretical calculations are confirmed to show that the magnetic alignment was primarily a function of tube diameter, rather than magnetic field. Kim et al. prepare CNT/polymer composite membranes, having similar gas transport properties to nanotube composites prepared through CVD, by passing a single-walled CNT suspended solution through a PTFE filter in order to align nanotubes; a PSf coating is applied in order to maintain perpendicular orientation and impart mechanical strength¹⁹².

Srivastava et al. exhibit the potential for CNT filters in two important environmental applications: the separation of heavy hydrocarbons from petroleum during crude oil post-distillation and the removal of microbial contaminants from drinking water²⁰¹. Macroscale hollow carbon cylinders are produced with densely packed, radially aligned, micron-length multi-walled CNTs through the continuous spray pyrolysis method. To confirm the bio-adsorption of contaminants, namely *E. coli* (2-5 μm), *Staphylococcus aureus* (~1 μm), and the poliovirus (~25 nm), from drinking water, unfiltered biological suspension and post-treatment

filtrate are incubated in both solid and liquid media and then plated; biological growth is seen in the unfiltered samples, but none is found in the filtrate. These biofilters offer not only an efficient means for treatment, but also an economical means. Due to the strong mechanical and thermal stability, CNT filters can be cleaned (by ultrasonication and autoclaving) and reused, whereas conventional water filtration membranes are typically disposed off at the end of one use due to permanent damage from biofouling and inability to withstand cleaning.

A 2007 molecular dynamics simulation by Corry points out the importance of the type of CNT selected for membrane production²⁰². Results show that narrow CNTs with an “armchair” structure – those classified as (5,5) and (6,6)-type nanotubes – might completely reject ions due to the large energy barrier at the nanotube openings created by stable hydrogen bond formation. Larger (7,7)- and (8,8)-type nanotubes will not select against ions in this way. Water on the other hand, forms no stable hydrogen bonds with any CNT types and permeates rapidly. While extreme permeation enhancements are often predicted (as much as 3 orders of magnitude over current membranes), these predictions have been made assuming maximum coverage of CNTs per unit area, but it is not clear that such high packing densities are practically possible. Using the results of this simulation and assuming the CNT packing density achieved experimentally to date (with double-walled CNTs) by Holt et al.¹⁸⁶, Corry projects flux enhancements of 2-fold and 4-fold over a commercially available seawater RO membrane with (5,5) and (6,6) aligned CNT membranes, respectively,²⁰².

A comparison of the achievable performance of aligned nanotube membranes versus current polymeric seawater RO membranes is presented (**Figure 9**), similar to that shown for TFN membranes above, but here including permeability projections compiled by Corry²⁰² and maximum coverage demonstrated by Holt et al.¹⁸⁶. At a fractional content of 0.03% in an

impermeable matrix, a CNT membrane will exceed the commercially available SWRO standard. This limit is within the previously achieved range, but thus far no large-scale aligned CNT membranes have been fabricated. Carbon nanotubes promise mimicry of biological aquaporin channels, with a material producible in large quantities; however, fabrication of large areas of these materials stands in the way of commercial application. Both aquaporin- and CNT- based membranes are limited by their cost and lack of scalability; however, this was also the case for polymeric membranes 50 years ago, so the scale-up issues may be resolved over time if performance enhancements prove practically achievable.

3.3.3. Isoporous Block Copolymer Membranes

One advance aimed at solving the issue of scale up and manufacturing of membranes with uniform, aligned nanopores involves block copolymer self-assembly²⁰³. In 1994, François and his research team formulated an emulsion method whereby water droplets condense on a rapidly cooled polymer surface in a humid environment to create porous structures²⁰⁴⁻²⁰⁵. Water molecules arrange themselves on the surface and polymer precipitates around them. Finally, evaporation of the water droplets occurs, leaving a honeycomb pore structure. This idea is widely applied²⁰⁶⁻²⁰⁹, yet a full understanding of the molecular level activity has yet to be reached. Self-assembly, defined as the “autonomous organization of components into patterns or structures without human intervention²⁰³,” of block copolymers show promise for translating ‘bottom-up’ synthesis methods into large-scale manufacturing processes, which is needed for practical water treatment membranes.

Block copolymers are macromolecules composed of multiple block polymeric species with the ability to self-assemble into highly ordered structures when placed in a selective solvent

^{208, 210-212}. Block copolymer self-assembly provides the opportunity for narrow pore size distributions and high porosities, as well as sharp molecular weight cut-off. In self-assembly, the characteristic differences between blocks will cause separation into microphases during polymerization. An analogy can be drawn to the hydrophobic effect in which natural amphiphilic molecules, such as phospholipids, become ordered in water with a compact hydrophobic region surrounded by dispersed hydrophilic segments in order to reach a thermodynamically favorable arrangement ²¹². Similarly, when water is added to a system of block copolymers dissolved in an aqueous solution, the blocks will align with the hydrophobic ends precipitating and the hydrophilic ends remaining extended in solution ²⁰⁸. Furthermore, when any selective solvent is added to a solvent-nonsolvent system consisting of macromolecules of two distinct regions – one soluble, the other insoluble – a predictable arrangement will form based on the respective interactions of each polymer with the solvent ²¹².

The geometry of block copolymer nanostructures is determined by the molecular weights of the blocks and the ordering depends upon the concentrations of the blocks and the insoluble to soluble ratio ^{210, 212}. At a certain point, known as the critical aggregation concentration (CAC), the blocks will go from dispersed unimers to self-assembled isotropic structures ²¹². The ratio of the insoluble volume to the total volume occupied by the copolymer can generally determine the resultant structure the macromolecule will attain in solvent. If the insoluble volume is less than 33% of the total volume, spherical micelles (hydrophobic core with a hydrophilic corona) will form (**Figure 10**), between 33 and 50% cylindrical micelles form, and then up to the theoretical point of 100% insoluble fraction a membrane (composed of two monolayers) will form ^{210, 212}. Reverse micelles can also be formed with a hydrophilic inner core when nonsolvent, rather than a solvent, is added to the system ²¹³⁻²¹⁴. Additionally, these same ideas can be expanded beyond

diblock copolymers to multi-block systems²¹². By varying the concentrations and conditions under which self-assembly occurs various structures can be formed, including densely packed cylindrical pores ideal for water separation membranes²¹⁵. Techniques for producing such membranes involve phase inversion (which is successful, but expensive as the block copolymer is used for both the support and the selective layers), shear aligning (which typically produces thicker than desired films), and controlled substrate-polymer interactions (which are effective, but difficult to control in large-scale production)²¹⁶. In theory, aligned cylinders formed through nanostructuring of block copolymers could enable a fully polymeric analog to aquaporin or aligned CNT membranes, providing an opportunity to take advantage of nanopore performance, while maintaining ease and economy of large-scale polymeric membrane fabrication.

Self-assembly for bottom-up structure formation can result in membranes containing defects due to the various factors²¹⁷. One particularly interesting characteristic of copolymers is that they are “soft” meaning that they tolerate a large amount of such imperfections and still assemble relatively homogeneously. While imperfections may be seen as a major limitation in some applications, for aqueous membrane materials where total homogeneity is not a requirement this soft nature poses processing and manufacturing advantages. Dove points out that while micellar assemblies are soft and may be reverted to unimers with a change in conditions, there is the opportunity to cause selective crosslinking²¹⁰, which enhances the mechanical, thermal, and chemical stability of the membranes^{5, 207}. The soft nature also means that minimal external fields – electrical or shear – will impact the arrangement²¹². This could have implications for auto-arranging of materials on demand and an opportunity for self-cleaning membranes.

Peinemann et al. demonstrate the ability to combine block copolymer self-assembly with conventional phase inversion to achieve highly ordered, asymmetric porous membranes composed solely of block copolymer materials²¹¹. This process is very complex involving both thermodynamic and kinetic factors: during fabrication, block copolymers will align in order to obtain a thermodynamically favorable, low energy arrangement. However, perpendicular arrangement is difficult to guarantee throughout the thickness of copolymer membranes. Predictions of arrangement must take into account the factors of solvent composition, selectivity, and concentration^{211, 217}. In their one step process, Peinemann's group achieves a non-ordered porous structure—typical of polymeric membranes—overlaid with a 200-300 nm thick dense layer of aligned nanocylinders, with a pore density of 240×10^{12} and an effective pore diameter of 8 nm²¹¹. Water flux through these membranes is $20 \text{ l} \cdot \text{m}^{-2} \cdot \text{h}^{-1}$ at 0.5 bar with 82% rejection of ~ 7 nm albumin²¹¹. One-step fabrication holds promise for large-scale production. Peinmann holds a patent for the process of block (di- and tri-) copolymer membranes for separation applications, including UF and NF²¹⁸.

Phillip et al. report fabrication of a 100 μm thick, nanoporous block copolymer membrane with tunable selectivity, narrow pore size distribution (~ 14 nm), and a 40% void fraction²¹⁹. Membranes are formed using the “doubly reactive” block polymer²¹⁹ combined with selective etching of a single block²²⁰. The process allows for simplified alignment because the block polymer acts as a structural template during crosslinking²¹⁹. Water permeability was lower than predicted, but did increase linearly with applied pressure. If the membrane thickness is decreased to 0.5 μm , the membrane would become competitive (at $5600 \text{ gal} \cdot \text{ft}^{-2} \cdot \text{day}^{-1}$ with a 200 kPa pressure drop) with typical membranes formed through phase inversion. Flux was found to decrease with pH of permeate by as much as 60% (from pH 2 to 12). The molecular weight

cut-off of the membrane was found to correlate with the molecular weight of the etchable block employed, implying further tuning of such membranes for target separation applications is possible.

Another route for employing block copolymers is to form a thin layer atop a sacrificial substrate and then transfer it to a functional support layer. Using copolymers for upper layer alone provides large cost savings and may pose an advantage for large-scale production²²¹. This is fiscally appealing as block copolymers are more costly than typical polymers used in membrane formation. Yang et al. created a NF membrane, with an 80 nm thick top layer of 15 nm diameter cylindrical pores atop a (250 μm) conventional support, capable of filtering viruses²²². This approach holds benefits of a highly tunable top layer, with pores ranging from 10 to 40 nm, and the reliability of conventional supports. The process is limited in its scalability because of the difficulty of transferring films without damage to the porous structure.

To avoid complications in the transfer step, self-assembly of block copolymers directly atop functional supports has been attempted. Here, separate tailoring of the support and selective layers allow for novel membrane fabrication. Fierro et al. employ block copolymer membranes in direct formation atop a conventional porous support and study the impact of polymer selection on physical characteristics²⁰⁶. To predict the assembly outcome the affinity of the substrate for each block employed must be considered, as the substrate tends to be selective towards one of the block units. Orientation of the self-assembly is strongly impacted by the surface composition and roughness on which assembly is initiated^{206, 223}. Phillip et al. fabricate membranes with a 4 μm thin film of monodisperse, 24 nm diameter vertically aligned, hexagonally-packed cylinders directly atop a commercially available microporous support membrane in a single step of controlled evaporation. Ultraviolet light (254 nm) is applied to ensure full adhesion between the

copolymer film and commercial support layer. UV also promotes crosslinking between micelles. A single block is selectively etched to form the open pores. Water permeability in UF testing is lower than expected likely because the pores were not aligned or etched through the full length of the thin film. Membrane rejection of 100 kDa polyethylene oxide is over 93%. This evaporative self-assembly method provides an opportunity for economical scalability by using a simple fabrication process and selecting a commercially available, mechanically robust support layer. In addition, the dual material membrane means that characteristics of support structure and thin film selectivity can be independently fine-tuned with respect to applications.

Li et al. employ a homopolymer (i.e., polyacrylic acid) to guide self-assembly of their diblock copolymer system. Ordered nanoporous films are formed directly atop various polymeric and ceramic porous supports via spin coating followed by solvent evaporation²²⁴. The addition of the homopolymer allowed for the desired pore structure to be achieved under various casting conditions (humidity, substrate, solvent, film thickness) with no need for thermal or solvent treatments. The homopolymer is then selectively removed. In NF tests, liquid permeability ranges from 1.2-1.6 L·m⁻²·bar⁻¹·h⁻¹, increasing with homopolymer content. Molecular weight cut-off of the membranes is determined to be 400-500 Da (defined for 90% rejection of polyethylene glycol). Interestingly, while the homopolymer is necessary to attain self-assembly of cylindrical pores, it can be removed with a simple water soak without changing the pore structure implying that it is not chemically stable in the self-assembled structure. The use of such homopolymer additives presents an opportunity for simple and scalable fabrication of membranes with highly tunable performance characteristics.

Multiblock or star copolymers enable more predictable alignment atop commercial substrates by compensating for the discrepancy in substrate affinity between blocks with a

symmetric arrangement. It is predicted that more complex structures result in a reduced thermodynamic loss due to conformational entropy and provide an opportunity for more specific nanoscale tuning of structures^{204, 206, 225}. Stratford et al. simulate a method for producing what they termed Bijels (bicontinuous interfacially jammed emulsion gels), which are self-assembled three dimensional structures formed through liquid-liquid interfacial sequestering of particles to form a matrix²²⁵. Stratford's predicted kinetic path is applied, using the emulsion technique first presented by François' group²⁰⁴, by Chen's group to prepare tunable porous structures with self-assembling ABA triblock amphiphilic copolymers into a highly ordered honeycomb film²²⁶. With honeycomb structures it is consistently found that the hydrophobic-hydrophilic ratio of the blocks determines the ordering and size of pores; namely, the regularity of pores decreases with increasing hydrophilic block content and pore diameter increased with increasing hydrophobic block length^{205, 208, 226}. The ability to tune pore size with hydrophobic block selection and water content²⁰⁸ is intuitive based on the proposed formation path in the emulsion technique²⁰⁴. Beattie et al. form similar matrices through reversible addition-fragmentation chain transfer^{205, 227}. Kabuto et al. experiment with honeycomb formation using a commercially available polymer and create an asymmetric membrane with a top layer of ordered 3 nm pores²⁰⁷. Upon cross-linking the honeycomb surface inverts from hydrophobic to hydrophilic, allowing for filtration through the pores²⁰⁷. As a further understanding of the mechanisms at play in formation is reached, this highly ordered and predictable membrane formation process will gain exposure in the membrane field.

Membranes with aligned nanopores formed by self-assembly of block copolymers during phase inversion offer a significant promise as fully polymeric analogs to aquaporin and aligned CNT membranes. In principle, these structures could be fine-tuned for water filtration

applications, but may also serve as more ideal support substrates for high-flux, high-selectivity forward and reverse osmosis membranes for desalination and osmotic power production.

4. DISCUSSION

The aims of nanotechnology-enabled water treatment membranes encompass many different goals and performance enhancements. Chemically stable ceramic membranes have been modified for high selectivity NF and potentially RO membranes with zeolite thin film coatings. Self-cleaning and catalytic membranes have been formed with antimicrobial and photocatalytic nanoparticle coatings. Mixed matrix membranes offer enhanced separation performance, fouling resistance, and mechanical stability for filtration applications and as support membranes for TFC or TFN membranes. Thin film nanocomposites seek to produce compaction resistant membranes with silica, fouling-resistant membranes with nanosilver, self-cleaning photocatalytic membranes with titania nanoparticles, or highly permeable and selective membranes with molecular sieve zeolites. Biologically inspired membranes—aquaporins, aligned CNTs, and block copolymers—seek to simultaneously improve selectivity and permeability. Each of these innovative materials concepts promises unique performance enhancements and each has unique hurdles to overcome before it is commercially viable.

Here, we ranked the aforementioned membrane nanotechnologies based on two categories: (1) performance enhancement and (2) state of commercial readiness and three sub-categories within each category. Performance sub-categories considered potential enhancements in membrane (a) permeability, (b) selectivity, and (c) robustness over the current state-of-the-art. Robustness encompasses chemical, mechanical, and thermal stability as well as fouling resistance and enhanced cleanability. Commercial readiness sub-categories included (1)

anticipated material costs, (2) manufacturing scalability, and (3) apparent time to commercialization. Those membrane nanotechnologies that promise significant performance improvements over current industry standard membranes were ranked positive, those that offer lower performance were ranked negative, and those that did not change the performance (or if no information was available) were given a neutral score. Membrane nanotechnologies close to commercial reality, cheaper than the state-of-the-art, and capable of being produced using existing membrane manufacturing infrastructure were ranked positive, those judged oppositely were ranked negative, and those not promising change in the specific metric (or if no information was available) were given a neutral score. The scores given to each membrane nanotechnology reviewed above are shown in **Table 3**.

Reactive/catalytic and zeolite coated ceramic membranes promise improved performance with marginal changes in current inorganic membrane fabrication methods (i.e., low cost impact). However, these innovations are not out of the laboratory yet and will most likely be limited by the same factors that have always limited ceramic membranes—high capital cost and low membrane area density relative to polymeric membrane equivalents. Ceramic membranes with reactive surfaces have been proven effective in laboratory studies, but more research needs to be done to produce commercially viable systems. While negligible improvement to productivity for such membranes has been shown, selectivity can be increased with catalyzed degradation of target compounds. Additionally, reactive surfaces have been shown to be biofouling resistant and so an enhancement in robustness is promised. For these reasons, the ratings of 0 (no improvement) to productivity and +1 (slight improvement) to both selectivity and robustness are assigned. These membranes show no major changes in commercial viability when compared to current ceramic membranes and so neutral ratings are applied in all categories

of time to commercialization. The materials and production cost roughly the same amount as current ceramics and the materials discussed here are between laboratory and pilot-scale testing, but none are known to be commercially available as of yet.

Zeolitic coatings promise the ability to tune the molecular selectivity of ceramic membranes. Thanks to the extreme stability of inorganic materials, these membranes may have a future in desalination and purification of challenging wastewaters (needs currently met primarily by polymeric membranes); however, the synthesis of zeolite films must be improved to obtain thinner layers and achieve competitive water permeability without sacrificing selectivity. In terms of potential performance enhancements, zeolitic coatings are given a -1 rating for productivity because currently these achieve lower flux than commercially available materials. These were rated neutral in terms of selectivity since rejections comparable to current membranes have been shown. These materials were given a +1 rating for robustness, however, because they pose a more chemically and thermally stable alternative to current membranes typically applied for high pressure and complex water separations. Similar to reactive/catalytic surfaces, zeolitic coatings are given neutral scores for commercial viability, with the exception of cost effectiveness. The materials to produce fully zeolitic coatings made presumably cost more than typical polymer membrane materials and ceramic materials and so a -1 rating is assigned.

Mixed matrix membranes and TFNs offer significant performance enhancements with minimal changes to current manufacturing processes. All inorganic-organic materials evaluated offer a significant productivity enhancement when tested against current 'state of the art' membranes. Mixed matrices and zeolite TFNs show no significant change to membrane selectivity; however, nanoparticle TFNs do show some decrease in selectivity due to defect formation and so these are given a -1 rating for selectivity. All inorganic-organic materials also

show an enhancement in robustness, through either compaction resistance or hydrophilic, anti-fouling surfaces due to the presence of filler materials, earning them a +1 rating for robustness. Mixed matrix membranes and nanoparticle TFNs both receive ratings of -1 for cost effectiveness due to the added cost of filler materials. Thin film nanocomposites containing zeolites, however, have been shown in the literature to improve on all aspects of performance using only small amounts of relatively inexpensive filler materials and so were rated neutral for cost effectiveness. All materials in this category are given a +1 rating for scalability since all can be produced through current polymeric membrane processes by simply adding nanoparticles to the casting or coating solutions. While mixed matrices have been seen at the laboratory scale only, earning them a neutral score for time to commercialization, early stages of TFN membranes are now commercially available, earning them a +1 score.

Biologically-inspired membranes all promise extremely high performance enhancements, but are currently far from commercial reality. Aquaporin-based membranes promise to revolutionize membranes with at least an order of magnitude increase in flux over the current membranes available, earning them a rating of +3 for productivity. Aligned nanotubes and isoporous block copolymer membranes have also been predicted and shown to reach extreme flux enhancements, earning them a +2 rating for productivity. All biologically-inspired membranes promise to alter the bounds of membrane selectivity with extremely narrow pore distributions. The regular morphology of these membrane materials earns them a +2 for selectivity. Both aquaporin and nanotube-based membranes show no significant changes in membrane robustness if cast within or atop polymeric matrices; however, at this stage pure block copolymer membranes tested are less mechanically stable than current polymeric membranes available. Both aquaporins and nanotubes are expensive to purify and have not yet been formed

in large membrane areas and so both receive a –1 rating for cost effectiveness and scalability. Aquaporins are difficult to attain in large quantities and few studies have shown the ability to form uniform coatings of protein membranes for industrial applications. Aligned CNT films have been produced uniformly, but only over small surfaces. At this point, both materials are in the laboratory production phase and so earn neutral scores for time to commercialization. Block copolymer materials are not significantly more costly than current polymeric membranes, particularly since research is moving towards using the specialized polymers for the selective layers only and so these receive a neutral score for cost. Because self-assembled block copolymer membranes can be formed through typical membrane fabrication processes with current infrastructure they earn a +1 for scalability. Aligned block copolymer membranes are in stages of early development and ideal polymer systems must still be found to achieve the outcomes promised, earning them a –1 for time to commercialization. However, if the polymerization conditions can be mastered so that fabrication of these structures can occur reliably and at large scales with minor changes to infrastructure, they will pose a promising, low-cost, fully polymeric counterpart to high performance aquaporin and CNT membranes. Biologically-inspired membranes promise the greatest separation performance enhancements; however, their cost and robustness are unproven and they appear most challenging to produce for large commercial applications. However, this was also the case for polymeric membranes 40-50 years ago and these scale-up issues can be resolved if the performance enhancements promised by these exiting materials prove practically achievable.

While each technology clearly has its own merits, an overall ranking is proposed here by summing the three scores from each category and plotting the total scores for performance enhancement against commercial viability (**Figure 11**). The ideal technology offers both

revolutionary performance enhancements and is already commercially available (upper right quadrant). Biologically-inspired membranes promise the greatest potential performance enhancements and are farthest from commercial reality, while zeolite TFN membranes offer moderate performance enhancement and appear nearest to commercial viability. The other materials offer noteworthy performance enhancement while remaining far from commercial reality. None of the membrane nanotechnologies fell in the optimal (upper right) quadrant of the chart, but this could change over time as biologically inspired membrane technology matures.

Readers should note that we propose this ranking methodology as a means to provoke critical thought rather than as an endorsement or indictment of any specific membrane nanotechnology. We realize limitations are inherent to any such ranking system. The most obvious limitation is that our assessment represents a ‘snapshot in time’ of the technology landscape, which is ever changing. While our intent is to provide an objective evaluation of the technologies, we realize that our ranking may be somewhat subjective. Regardless of the current ranking, each membrane nanotechnology concept described has the potential to revolutionize water treatment to varying degrees, but each material must be developed, matched to the ideal application, and fine-tuned to produce commercially available membranes.

ACKNOWLEDGMENTS

This publication is based on work supported in part by Award No. KUS-C1-018-02, made by King Abdullah University of Science and Technology (KAUST), in addition to the NSF Graduate Research Fellowship, UCLA Cota Robles Fellowship, and the UCLA Faculty Women’s Club Russell and Sallie O’Neill Memorial Scholarship.

REFERENCES

1. *Human Development Report 2006. Chapter 4*, United Nations Development Programme (UNDP), 2006.
2. *Coping with water scarcity. Challenge of the twenty-first century*, United Nations (UN) Water. Food and Agricultural Association (FAO), 2007.
3. *Urban Urgency, Water Caucus Summary*, World Water Council (WWC), Marseille, France, 2007.
4. *Progress on Sanitation and Drinking-Water*, World Health Organization(WHO)/United Nations International Children's Fund (UNICEF) Joint Monitoring Programme for Water Supply and Sanitation, 2010.
5. M. Mulder, *Basic Principles of Membrane Technology*, Kluwer Academic Publishers, London, 1996.
6. M. Ulbricht, Advanced functional polymer membranes, *Polymer*, 2006, **47**, 2217-2262.
7. P. Bernardo, E. Drioli and G. Golemme, Membrane gas separation: A review/state of the art, *Ind. Eng. Chem. Res.*, 2009, **48**, 4638-4663.
8. R. E. Kesting, The 4 Tiers of Structure in integrally skinned phase inversion membranes and their relevance to various separation regimes, *J. Appl. Polym. Sci.*, 1990, **41**, 2739-2752.
9. R. R. Bhave, *Inorganic Membranes: Synthesis, Characteristics, and Applications*, Van Nostrand Reinhold, New York, NY, 1991.
10. M. Kazemimoghadam, New nanopore zeolite membranes for water treatment, *Desalination*, 2010, **251**, 176-180.
11. E. Hoek and A. Jawor, Nano-filtration separations, in *Dekker Encyclopedia of Nanoscience and Nanotechnology*, 2002.
12. J. Benito, M. Sanchez, P. Pena and M. Rodríguez, Development of a new high porosity ceramic membrane for the treatment of bilge water, *Desalination*, 2007, **214**, 91-101.
13. M. H. Hassan, J. D. Way, P. M. Thoen and A. C. Dillon, Single-component and mixed-gas transport in a silica hollow-fiber membrane, *J. Membrane Sci.*, 1995, **104**, 27-42.
14. R. Faibish and Y. Cohen, Fouling-resistant ceramic-supported polymer membranes for ultrafiltration of oil-in-water microemulsions, *J. Membrane Sci.*, 2001, **185**, 129-143.
15. R. Faibish and Y. Cohen, Fouling and rejection behavior of ceramic and polymer-modified ceramic membranes for ultrafiltration of oil-in-water emulsions and microemulsions, *Colloid Surface A*, 2001, **191**, 27-40.
16. S. Loeb and S. Sourirajan, *High flow semipermeable membrane for separation of water from saline solution*, US Patent, US3133132 (1964).
17. R. Kesting, *Synthetic Polymeric Membranes*, McGraw-Hill, New York, NY, 1971.
18. T-H. Young and L-W. Chen, Pore formation mechanism of membranes from phase inversion process, *Desalination*, 1995, **103**, 233-247.
19. G. Guillen, Y. Pan, M. Li and E. M. V. Hoek, A review of nonsolvent induced phase separation membrane formation and characterization, *Desalination*, 2010, *submitted/in review*.
20. I. C. Kim, H. G. Yun and K. H. Lee, Preparation of asymmetric polyacrylonitrile membrane with small pore size by phase inversion and post-treatment process, *J. Membrane Sci.*, 2002, **199**, 75-84.

21. A. K. Ghosh, B. H. Jeong, X. F. Huang and E. M. V. Hoek, Impacts of reaction and curing conditions on polyamide composite reverse osmosis membrane properties, *J. Membrane Sci.*, 2008, **311**, 34-45.
22. M. Sivakumar, D. R. Mohan and R. Rangarajan, Studies on cellulose acetate-polysulfone ultrafiltration membranes II. Effect of additive concentration, *J. Membrane Sci.*, 2005, **268**, 208-219.
23. M. Kabsch-Korbutowicz, K. Majewska-Nowak and T. Winnicki, Analysis of membrane fouling in the treatment of water solutions containing humic acids and mineral salts, *Desalination*, 1999, **126**, 179-185.
24. M. Elimelech, X. Zhu, A. Childress and S. Hong, Role of membrane surface morphology in colloidal fouling of cellulose acetate and composite aromatic polyamide reverse osmosis membranes, *J. Membrane Sci.*, 1997, **127**, 101-109.
25. M. Cheryan, *Ultrafiltration and Microfiltration Handbook*, Technomic Publishing Co., Inc., Lancaster, UK, 1998.
26. J. E. Cadotte, R. J. Petersen, R. E. Larson and E. E. Erickson, New thin-film composite seawater reverse-osmosis membrane, *Desalination*, 1980, **32**, 25-31.
27. A. P. Rao, N. V. Desai and R. Rangarajan, Interfacially synthesized thin film composite RO membranes for seawater desalination, *J. Membrane Sci.*, 1997, **124**, 263-272.
28. H. Hachisuka and K. Ikeda, *Reverse osmosis composite membrane and reverse osmosis treatment method for water using the same*, US Patent, US6413425 (2002).
29. W. E. Mickols, *Composite membrane and method for making the same*. US Patent, US6562266 (2003).
30. R. J. Petersen, Composite reverse-osmosis and nanofiltration membranes, *J. Membrane Sci.*, 1993, **83**, 81-150.
31. A. I. Schafer, A. G. Fane and T. D. Waite, *Nanofiltration Principles and Applications*, Elsevier Advanced Technology, New York, NY, 2005.
32. W. Zhang, G. H. He, P. Gao and G. H. Chen, Development and characterization of composite nanofiltration membranes and their application in concentration of antibiotics, *Separ. Purif. Technol.*, 2003, **30**, 27-35.
33. C. Linder, M. Nemas, M. Perry and R. Ketraro, *Coated membranes*, US Patent, US5028337 (1991).
34. J. H. Choi, J. Jegal and W. N. Kim, Fabrication and characterization of multi-walled carbon nanotubes/polymer blend membranes, *J. Membrane Sci.*, 2006, **284**, 406-415.
35. A. L. Ahmad, M. Sarif and S. Ismail, Development of an integrally skinned ultrafiltration membrane for wastewater treatment: effect of different formulations of PSf/NMP/PVP on flux and rejection, *Desalination*, 2005, **179**, 257-263.
36. M. J. Han and S. T. Nam, Thermodynamic and rheological variation in polysulfone solution by PVP and its effect in the preparation of phase inversion membrane, *J. Membrane Sci.*, 2002, **202**, 55-61.
37. K. W. Lee, B. K. Seo, S. T. Nam and M. J. Han, Trade-off between thermodynamic enhancement and kinetic hindrance during phase inversion in the preparation of polysulfone membranes, *Desalination*, 2003, **159**, 289-296.
38. E. M. V. Hoek, *Colloidal fouling mechanisms in reverse osmosis and nanofiltration*, Ph.D. Dissertation, Yale University, New Haven, CT, 2002.

39. A. P. Rao, S. V. Joshi, J. J. Trivedi, C. V. Devmurari and V. J. Shah, Structure-performance correlation of polyamide thin film composite membranes: Effect of coating conditions on film formation, *J. Membrane Sci.*, 2003, **211**, 13-24.
40. I. C. Kim and K. H. Lee, Preparation of interfacially synthesized and silicone-coated composite polyamide nanofiltration membranes with high performance, *Ind. Eng. Chem. Res.*, 2002, **41**, 5523-5528.
41. S. Y. Kwak, S. H. Kim and S. S. Kim, Hybrid organic/inorganic reverse osmosis (RO) membrane for bactericidal anti-fouling. 1. Preparation and characterization of TiO₂ nanoparticle self-assembled aromatic polyamide thin-film-composite (TFC) membrane, *Environ. Sci. Technol.*, 2001, **35**, 2388-2394.
42. V. Freger, Nanoscale heterogeneity of polyamide membranes formed by interfacial polymerization, *Langmuir*, 2003, **19**, 4791-4797.
43. M. Hirose, H. Ito and Y. Kamiyama, Effect of skin layer surface structures on the flux behaviour of RO membranes, *J. Membrane Sci.*, 1996, **121**, 209-215.
44. C. K. Kim, J. H. Kim, I. J. Roh and J. J. Kim, The changes of membrane performance with polyamide molecular structure in the reverse osmosis process, *J. Membrane Sci.*, 2000, **165**, 189-199.
45. V. Freger, J. Gilron and S. Belfer, TFC polyamide membranes modified by grafting of hydrophilic polymers: an FT-IR/AFM/TEM study, *J. Membrane Sci.*, 2002, **209**, 283-292.
46. M. Kurihara, Y. Fusaoka, T. Sasaki, R. Bairinji and T. Uemura, Development of cross-linked fully aromatic polyamide ultra-thin composite membranes for seawater desalination, *Desalination*, 1994, **96**, 133-143.
47. S. Y. Kwak and D. W. Ihm, Use of atomic force microscopy and solid-state NMR spectroscopy to characterize structure-property-performance correlation in high-flux reverse osmosis (RO) membranes, *J. Membrane Sci.*, 1999, **158**, 143-153.
48. S. Y. Kwak, Relationship of relaxation property to reverse osmosis permeability in aromatic polyamide thin-film-composite membranes, *Polymer*, 1999, **40**, 6361-6368.
49. S. Y. Kwak, S. G. Jung, Y. S. Yoon and D. W. Ihm, Details of surface features in aromatic polyamide reverse osmosis membranes characterized by scanning electron and atomic force microscopy, *J. Polym. Sci. B*, 1999, **37**, 1429-1440.
50. I. J. Roh, S. Y. Park, J. J. Kim and C. K. Kim, Effects of the polyamide molecular structure on the performance of reverse osmosis membranes, *J. Polym. Sci. B*, 1998, **36**, 1821-1830.
51. Y. Yang, L. Wan and Z. Xu, Surface hydrophilization for polypropylene microporous membranes: A facile interfacial crosslinking approach, *J. Membrane Sci.*, 2009, **326**, 372-381.
52. M. Kim, N. Lin, G. Lewis and Y. Cohen, Surface nano-structuring of reverse osmosis membranes via atmospheric pressure plasma-induced graft polymerization for reduction of mineral scaling propensity, *J. Membrane Sci.*, 2010, **354**, 142-149.
53. G. Kang, Y. Cao, H. Zhao and Q. Yuan, Preparation and characterization of crosslinked poly(ethylene glycol) diacrylate membranes with excellent antifouling and solvent-resistant properties, *J. Membrane Sci.*, 2008, **318**, 227-232.
54. J. Lin and S. Murad, A computer simulation study of the separation of aqueous solutions using thin zeolite membranes, *Mol. Phys.*, 2001, **99**, 1175-1181.

55. L. Li, J. Dong, T. Nenoff and R. Lee, Desalination by reverse osmosis using MFI zeolite membranes, *J. Membrane Sci.*, 2004, **243**, 401-404.
56. L. Li, J. Dong and T. Nenoff, Transport of water and alkali metal ions through MFI zeolite membranes during reverse osmosis, *Separ. Purif. Technol.*, 2007, **53**, 42-48.
57. M. Duke, J. O'Brien-Abraham, N. Milne, B. Zhu, J. Lin and J. Diniz da Costa, Seawater desalination performance of MFI type membranes made by secondary growth, *Separ. Purif. Technol.*, 2009, **68**, 343-350.
58. J. Lu, N. Liu, L. Li and R. Lee, Organic fouling and regeneration of zeolite membrane in wastewater treatment, *Separ. Purif. Technol.*, 2010, **72**, 203-207.
59. L. Li and R. Lee, Purification of produced water by ceramic membranes: Material screening, process design and economics, *Separ. Purif. Technol.*, 2009, **44**, 3455-3484.
60. L. Li, N. Liu, B. McPherson and R. Lee, Enhanced water permeation of reverse osmosis through MFI-type zeolite membranes with high aluminum contents, *Ind. Eng. Chem. Res.*, 2007, **46**, 1584-1589.
61. N. Liu, L. Li, B. McPherson and R. Lee, Removal of organics from produced water by reverse osmosis using MFI-type zeolite membranes, *J. Membrane Sci.*, 2008, **325**, 357-361.
62. I. Kumakiri, T. Yamaguchi and S. Nakao, Application of a Zeolite A membrane to reverse osmosis process, *J. Chem. Eng. Jpn.*, 2000, **33**, 333-336.
63. M. Noack, P. Kölsch, V. Seefeld, P. Toussaint, G. Georgi and J. Caro, Influence of the Si/Al-ratio on the permeation properties of MFI-membranes, *Micropor. Mesopor. Mat.*, 2005, **79**, 329-337.
64. R. F. Lobo, *Handbook of Zeolite Science and Technology*, Marcel Dekker, Inc., New York, NY, 2003.
65. A. Dyer, *An Introduction to Zeolite Molecular Sieves*, John Wiley & Sons Ltd., Chichester, UK, 1988.
66. Y. Li, T. Chung and S. Kulprathipanja, Novel Ag⁺-zeolite/polymer mixed matrix membranes with a high CO₂/CH₄ selectivity, *AIChE J.*, 2007, **53**, 610-616.
67. C. Baerlocher and L. B. McCusker, *Database of Zeolite Structures*, <http://www.iza-structure.org/databases/>.
68. W. Yuan, Y. Lin and W. Yang, Molecular sieving MFI-Type zeolite membranes for pervaporation separation of xylene isomers, *J. Am. Chem. Soc.*, 2004, **126**, 4776-4777.
69. Y. Li, H. Chen, J. Liu and W. Yang, Microwave synthesis of LTA zeolite membranes without seeding, *J. Membrane Sci.*, 2006, **277**, 230-239.
70. M. Lovallo, A. Gouzinis and M. Tsapatsis, Synthesis and characterization of oriented MFI membranes prepared by secondary growth, *AIChE J.*, 2004, **44**, 1903-1913.
71. M. Kondo, M. Komori, H. Kita and K. Okamoto, Tubular-type pervaporation module with Zeolite NaA membrane, *J. Membrane Sci.*, 1997, **133**, 133-141.
72. V. Freger, Swelling and morphology of the skin layer of polyamide composite membranes: An atomic force microscopy study, *Environ. Sci. Technol.*, 2004, **38**, 3168-3175.
73. S. Ozturk and B. Akata, Oriented assembly and nanofabrication of Zeolite A monolayers, *Micropor. Mesopor. Mat.*, 2009, **126**, 228-233.
74. D. Bahnemann, Photocatalytic water treatment: Solar energy applications, *Sol. Energy*, 2004, **77**, 445-459.

75. E. Pramauro, A. Prevot, M. Vincenti and R. Gamberini, Photocatalytic degradation of naphthalene in aqueous TiO₂ dispersions: Effect of nonionic surfactants, *Chemosphere*, 1998, **36**, 1523-1542.
76. B. Prevot, Analytical monitoring of photocatalytic treatments. Degradation of 2, 3, 6-trichlorobenzoic acid in aqueous TiO₂ dispersions, *Talanta*, 1999, **48**, 847-857.
77. M. Hoffmann, S. Martin, W. Choi and D. Bahnemann, Environmental applications of semiconductor photocatalysis, *Chem. Rev.*, 1995, **95**, 69-96.
78. J. Carey, J. Lawrence and H. Tosine, Photodechlorination of PCB's in the presence of titanium dioxide in aqueous suspensions, *B. Environ. Contam. Tox.*, 1976, **16**, 697-701.
79. V. Krishna, S. Pumprueg, S. H. Lee, J. Zhao, W. Sigmund, B. Koopman and B. M. Moudgil, Photocatalytic disinfection with titanium dioxide coated multi-wall carbon nanotubes, *Process Saf. Environ.*, 2005, **83**, 393-397.
80. G. Rothenberger, J. Moser, M. Graetzel, N. Serpone and D. Sharma, Charge carrier trapping and recombination dynamics in small semiconductor particles, *J. Am. Chem. Soc.*, 1985, **107**, 8054-8059.
81. A. Modestov and O. Lev, Photocatalytic oxidation of 2, 4-dichlorophenoxyacetic acid with titania photocatalyst. Comparison of supported and suspended TiO₂, *J. Photoch. Photobio. A*, 1998, **112**, 261-270.
82. S. Horikoshi, H. Hidaka and N. Serpone, Environmental remediation by an integrated microwave/UV-illumination method. 1. Microwave-assisted degradation of Rhodamine-B dye in aqueous TiO₂ dispersions, *Environ. Sci. Technol*, 2002, **36**, 1357-1366.
83. A. Prevot, C. Baiocchi, M. Brussino, E. Pramauro, P. Savarino, V. Augugliaro, G. Marci and L. Palmisano, Photocatalytic degradation of acid blue 80 in aqueous solutions containing TiO₂ suspensions, *Environ. Sci. Technol*, 2001, **35**, 971-976.
84. W. Fu, H. Yang, M. Li, L. Chang, Q. Yu, J. Xu and G. Zou, Preparation and photocatalytic characteristics of core-shell structure TiO₂/BaFe₁₂O₁₉ nanoparticles, *Mater. Lett.*, 2006, **60**, 2723-2727.
85. Y. Ao, J. Xu, D. Fu, L. Ba and C. Yuan, Deposition of anatase titania onto carbon encapsulated magnetite nanoparticles, *Nanotechnology*, 2008, **19**, 405604.
86. R. Molinari, M. Mungari, E. Drioli, A. Di Paola, V. Loddo, L. Palmisano and M. Schiavello, Study on a photocatalytic membrane reactor for water purification, *Catal. Today*, 2000, **55**, 71-78.
87. J. Mo, S. H. Son, J. Jegal, J. Kim and Y. H. Lee, Preparation and characterization of polyamide nanofiltration composite membranes with TiO₂ layers chemically connected to the membrane surface, *J. Appl. Polym. Sci.*, 2007, **105**, 1267-1274.
88. S. S. Madaeni and N. Ghaemi, Characterization of self-cleaning RO membranes coated with TiO₂ particles under UV irradiation, *J. Membrane Sci.*, 2007, **303**, 221-233.
89. A. Rahimpour, S. S. Madaeni, A. H. Taheri and Y. Mansourpanah, Coupling TiO₂ nanoparticles with UV irradiation for modification of polyethersulfone ultrafiltration membranes, *J. Membrane Sci.*, 2008, **313**, 158-169.
90. Y. Mansourpanah, S. S. Madaeni, A. Rahimpour, A. Farhadian and A. H. Taheri, Formation of appropriate sites on nanofiltration membrane surface for binding TiO₂ photo-catalyst: Performance, characterization and fouling-resistant capability, *J. Membrane Sci.*, 2009, **330**, 297-306.
91. M. Moosemiller, C. Hill and M. Anderson, Physicochemical properties of supported-Al₂O₃ and TiO₂ ceramic membranes, *Separ. Sci. Technol.*, 1989, **24**, 641-657.

92. C. Burda, Y. Lou, X. Chen, A. Samia, J. Stout and J. Gole, Enhanced nitrogen doping in TiO₂ nanoparticles, *Nano Lett.*, 2003, **3**, 1049-1051.
93. I. Ilisz, A. Dombi, K. Mogyorósi and I. Dékány, Photocatalytic water treatment with different TiO₂ nanoparticles and hydrophilic/hydrophobic layer silicate adsorbents, *Colloid Surface A*, 2003, **230**, 89-97.
94. W. Dong, C. Lee, X. Lu, Y. Sun, W. Hua, G. Zhuang, S. Zhang, J. Chen, H. Hou and D. Zhao, Synchronous role of coupled adsorption and photocatalytic oxidation on ordered mesoporous anatase TiO₂-SiO₂ nanocomposites generating excellent degradation activity of RhB dye, *Appl. Catal. B-Environ.*, 2009.
95. H. Choi, E. Stathatos and D. Dionysiou, Sol-gel preparation of mesoporous photocatalytic TiO₂ films and TiO₂/Al₂O₃ composite membranes for environmental applications, *Appl. Catal. B-Environ.*, 2006, **63**, 60-67.
96. S. Fukahori, H. Ichiura, T. Kitaoka and H. Tanaka, Capturing of bisphenol A photodecomposition intermediates by composite TiO₂-zeolite sheets, *Appl. Catal. B-Environ.*, 2003, **46**, 453-462.
97. J. Matos, J. Laine and J. Herrmann, Effect of the type of activated carbons on the photocatalytic degradation of aqueous organic pollutants by UV-irradiated titania, *J. Catal.*, 2001, **200**, 10-20.
98. Z. Zhang, C. Wang, R. Zakaria and J. Ying, Role of particle size in nanocrystalline TiO₂-based photocatalysts, *J. Phys. Chem. B*, 1998, **102**, 10871-10878.
99. F. Beltran, F. Rivas and R. Montero-de-Espinosa, Ozone-enhanced oxidation of oxalic acid in water with cobalt catalysts. 1. Homogeneous catalytic ozonation, *Ind. Eng. Chem. Res.*, 2003, **42**, 3210-3217.
100. B. Legube and K. Leitner, Catalytic ozonation: A promising advanced oxidation technology for water treatment, *Catal. Today*, 1999, **53**, 61-72.
101. L. Liotta, M. Gruttadauria, G. Di Carlo, G. Perrini and V. Librando, Heterogeneous catalytic degradation of phenolic substrates: Catalysts activity, *J. Haz. Mater.*, 2009, **162**, 588-606.
102. R. Gracia, J. Aragües and J. Ovelleiro, Study of the catalytic ozonation of humic substances in water and their ozonation byproducts, *Ozone-Sci. Eng.*, 1996, **18**, 195-208.
103. B. Karnik, S. Davies, M. Baumann and S. Masten, Fabrication of catalytic membranes for the treatment of drinking water using combined ozonation and ultrafiltration, *Environ. Sci. Technol.*, 2005, **39**, 7656-7661.
104. J. Ma and N. Graham, Degradation of atrazine by manganese-catalysed ozonation: Influence of humic substances, *Water Res.*, 1999, **33**, 785-793.
105. J. Ma and N. Graham, Degradation of atrazine by manganese-catalysed ozonation: Influence of radical scavengers, *Water Res.*, 2000, **34**, 3822-3828.
106. G. Liu, X. Zhang, Y. Xu, X. Niu, L. Zheng and X. Ding, Effect of ZnFe₂O₄ doping on the photocatalytic activity of TiO₂, *Chemosphere*, 2004, **55**, 1287-1291.
107. X. Qiu and C. Burda, Chemically synthesized nitrogen-doped metal oxide nanoparticles, *Chem. Phys.*, 2007, **339**, 1-10.
108. Y. Bessekhoud, D. Robert, J. Weber and N. Chaoui, Effect of alkaline-doped TiO₂ on photocatalytic efficiency, *J. Photoch. Photobio. A*, 2004, **167**, 49-57.
109. L. Brunet, D. Y. Lyon, E. M. Hotze, P. J. J. Alvarez and M. R. Wiesner, Comparative photoactivity and antibacterial properties of C-60 fullerenes and titanium dioxide nanoparticles, *Environ. Sci. Technol.*, 2009, **43**, 4355-4360.

110. V. Augugliaro, C. Baiocchi, A. Bianco Prevot, E. García-López, V. Loddo, S. Malato, G. Marci, L. Palmisano, M. Pazzi and E. Pramauro, Azo-dyes photocatalytic degradation in aqueous suspension of TiO₂ under solar irradiation, *Chemosphere*, 2002, **49**, 1223-1230.
111. C. Zimmerman, A. Singh and W. Koros, Tailoring mixed matrix composite membranes for gas separations, *J. Membrane Sci.*, 1997, **137**, 145-154.
112. R. Mahajan, R. Burns, M. Schaeffer and W. J. Koros, Challenges in forming successful mixed matrix membranes with rigid polymeric materials, *J. Appl. Polym. Sci.*, 2002, **86**, 881-890.
113. R. Mahajan, D. Q. Vu and W. J. Koros, Mixed matrix membrane materials: An answer to the challenges faced by membrane based gas separations today? *J. Chin. Inst. Chem. Eng.*, 2002, **33**, 77-86.
114. M. D. Jia, K. V. Peinemann and R. D. Behling, Molecular-sieving effect of the zeolite-filled silicone-rubber membranes in gas permeation, *J. Membrane Sci.*, 1991, **57**, 289-296.
115. L. Y. Jiang, T. S. Chung and S. Kulprathipanja, Fabrication of mixed matrix hollow fibers with intimate polymer-zeolite interface for gas separation, *AIChE J.*, 2006, **52**, 2898-2908.
116. S. Kirkpatrick, Percolation and conduction, *Rev. Mod. Phys.*, 1973, **45**, 574-588.
117. H. Frisch and J. Hammersley, Percolation processes and related topics, *J. Ind. Appl. Math.*, 1963, **11**, 894-918.
118. J. Ottino and N. Shah, Analysis of transient sorption and permeation of small molecules in multiphase polymer systems, *Polym. Eng. Sci.*, 2004, **24**, 153-162.
119. P. Aerts, A. R. Greenberg, R. Leysen, W. B. Krantz, V. E. Reinsch and P. A. Jacobs, The influence of filler concentration on the compaction and filtration properties of Zirfon®-composite ultrafiltration membranes, *Separ. Purif. Technol.*, 2001, **22-3**, 663-669.
120. P. Aerts, S. Kuypers, I. Genne, R. Leysen, J. Mewis, I. F. J. Vankelecom and P. A. Jacobs, Polysulfone-ZrO₂ surface interactions. The influence on formation, morphology and properties of zirfon-membranes, *J. Phys. Chem. B*, 2006, **110**, 7425-7430.
121. N. M. Wara, L. F. Francis and B. V. Velamakanni, Addition of alumina to cellulose-acetate membranes. *J. Membrane Sci.*, 1995, **104**, 43-49.
122. I. Genne, S. Kuypers and R. Leysen, Effect of the addition of ZrO₂ to polysulfone based UF membranes, *J. Membrane Sci.*, 1996, **113**, 343-350.
123. A. Bottino, G. Capannelli and A. Comite, Preparation and characterization of novel porous PVDF-ZrO₂ composite membranes, *Desalination*, 2002, **146**, 35-40.
124. Y. C. Sharma, V. Srivastava, V. K. Singh, S. N. Kaul and C. H. Weng, Nano-adsorbents for the removal of metallic pollutants from water and wastewater, *Environ. Technol.*, 2009, **30**, 583-609.
125. D. M. Fernandes, R. Silva, A. A. W. Hechenleitner, E. Radovanovic, M. A. C. Melo and E. A. G. Pineda, Synthesis and characterization of ZnO, CuO and a mixed Zn and Cu oxide, *Mater. Chem. and Phys.*, 2009, **115**, 110-115.
126. P. K. Stoimenov, R. L. Klinger, G. L. Marchin and K. J. Klabunde, Metal oxide nanoparticles as bactericidal agents, *Langmuir*, 2002, **18**, 6679-6686.
127. N. Savage and M. S. Diallo, Nanomaterials and water purification: Opportunities and challenges, *J. Nanopart. Res.*, 2005, **7**, 331-342.
128. Z. R. Yue and J. Economy, Nanoparticle and nanoporous carbon adsorbents for removal of trace organic contaminants from water, *J. Nanopart. Res.*, 2005, **7**, 477-487.

129. Y. C. Sharma, V. Srivastava, S. N. Upadhyay and C. H. Weng, Alumina nanoparticles for the removal of Ni(II) from aqueous solutions. *Ind. Eng. Chem. Res.*, 2008, **47**, 8095-8100.
130. J. G. Darab, A. B. Amonette, D. S. D. Burke, R. D. Orr, S. M. Ponder, B. Schrick, T. E. Mallouk, W. W. Lukens, D. L. Caulder and D. K. Shuh, Removal of pertechnetate from simulated nuclear waste streams using supported zerovalent iron, *Chem. Mater.*, 2007, **19**, 5703-5713.
131. S. M. Ponder, J. G. Darab and T. E. Mallouk, Remediation of Cr(VI) and Pb(II) aqueous solutions using supported, nanoscale zero-valent iron, *Environ. Sci. Technol.*, 2000, **34**, 2564-2569.
132. S. M. Ponder, J. G. Darab, J. Bucher, D. Caulder, I. Craig, L. Davis, N. Edelstein, W. Lukens, H. Nitsche, L. F. Rao, D. K. Shuh and T. E. Mallouk, Surface chemistry and electrochemistry of supported zerovalent iron nanoparticles in the remediation of aqueous metal contaminants, *Chem. Mater.*, 2001, **13**, 479-486.
133. J. S. Taurozzi, H. Arul, V. Z. Bosak, A. F. Burban, T. C. Voice, M. L. Bruening and V. V. Tarabara, Effect of filler incorporation route on the properties of polysulfone-silver nanocomposite membranes of different porosities, *J. Membrane Sci.*, 2008, **325**, 58-68.
134. L. Yan, Y. S. Li and C. B. Xiang, Preparation of poly(vinylidene fluoride)(PVDF) ultrafiltration membrane modified by nano-sized alumina (Al_2O_3) and its antifouling research, *Polymer*, 2005, **46**, 7701-7706.
135. N. Maximous, G. Nakhla, W. Wan and K. Wong, Preparation, characterization and performance of Al_2O_3 /PES membrane for wastewater filtration, *J. Membrane Sci.*, 2009, **341**, 67-75.
136. Z. F. Fan, Z. Wang, M. R. Duan, J. X. Wang and S. C. Wang, Preparation and characterization of polyaniline/polysulfone nanocomposite ultrafiltration membrane, *J. Membrane Sci.*, 2008, **310**, 402-408.
137. Z. F. Fan, Z. Wang, N. Sun, J. X. Wang and S. C. Wang, Performance improvement of polysulfone ultrafiltration membrane by blending with polyaniline nanofibers, *J. Membrane Sci.*, 2008, **320**, 363-371.
138. J. R. Morones, J. L. Elechiguerra, A. Camacho, K. Holt, J. B. Kouri, J. T. Ramirez and M. J. Yacaman, The bactericidal effect of silver nanoparticles, *Nanotechnology*, 2005, **16**, 2346-2353.
139. T. H. Bae and T. M. Tak, Effect of TiO_2 nanoparticles on fouling mitigation of ultrafiltration membranes for activated sludge filtration, *J. Membrane Sci.*, 2005, **249**, 1-8.
140. X. C. Cao, J. Ma, X. H. Shi and Z. J. Ren, Effect of TiO_2 nanoparticle size on the performance of PVDF membrane, *Appl. Surf. Sci.*, 2006, **253**, 2003-2010.
141. J. F. Li, Z. L. Xu, H. Yang, L. Y. Yu and M. Liu, Effect of TiO_2 nanoparticles on the surface morphology and performance of microporous PES membrane, *Appl. Surf. Sci.*, 2009, **255**, 4725-4732.
142. S. S. Hosseini, Y. Li, T. S. Chung and Y. Liu, Enhanced gas separation performance of nanocomposite membranes using MgO nanoparticles, *J. Membrane Sci.*, 2007, **302**, 207-217.
143. L. Wu, M. Shamsuzzoha and S. M. C. Ritchie, Preparation of cellulose acetate supported zero-valent iron nanoparticles for the dechlorination of trichloroethylene in water, *J. Nanoparticle Res.*, 2005, **7**, 469-476.

144. L. F. Wu and S. M. C. Ritchie, Enhanced dechlorination of trichloroethylene by membrane-supported Pd-coated iron nanoparticles, *Environ. Prog.*, 2008, **27**, 218-224.
145. V. Smuleac, L. Bachas and D. Bhattacharyya, Aqueous-phase synthesis of PAA in PVDF membrane pores for nanoparticle synthesis and dichlorobiphenyl degradation, *J. Membrane Sci.*, 2009, **346**, 310-317.
146. Y. Shih, Y. Chen, M. Chen, Y. Tai and C. Tso, Dechlorination of hexachlorobenzene by using nanoscale Fe and nanoscale Pd/Fe bimetallic particles, *Colloid Surface A*, 2009, **332**, 84-89.
147. Y. Han, W. Li, M. Zhang and K. Tao, Catalytic dechlorination of monochlorobenzene with a new type of nanoscale Ni (b)/Fe (b) bimetallic catalytic reductant, *Chemosphere*, 2008, **72**, 53-58.
148. D. Meyer and D. Bhattacharyya, Impact of membrane immobilization on particle formation and trichloroethylene dechlorination for bimetallic Fe/Ni nanoparticles in cellulose acetate membranes, *J. Phys. Chem. B*, 2007, **111**, 7142-7154.
149. B. Zhu and T. Lim, Catalytic reduction of chlorobenzenes with Pd/Fe nanoparticles: Reactive sites, catalyst stability, particle aging, and regeneration., *Environ. Sci. Technol.*, 2007, **41**, 7523-7529.
150. E. Hadnagy, L. Rauch and K. Gardner, Dechlorination of polychlorinated biphenyls, naphthalenes and dibenzo-p-dioxins by magnesium/palladium bimetallic particles, *J. Environ. Sci. Heal. A*, 2007, **42**, 685-695.
151. J. S. Baker and L. Y. Dudley, Biofouling in membrane systems—A review, *Desalination*, 1998, **118**, 81-89.
152. M. Z. Rong, M. Q. Zhang, Y. X. Zheng, H. M. Zeng, R. Walter and K. Friedrich, Structure-property relationships of irradiation grafted nano-inorganic particle filled polypropylene composites, *Polymer*, 2001, **42**, 167-183.
153. N. A. Ochoa, M. Masuelli and J. Marchese, Effect of hydrophilicity on fouling of an emulsified oil wastewater with PVDF/PMMA membranes, *J. Membrane Sci.*, 2003, **226**, 203-211.
154. D. Lee, R. E. Cohen and M. F. Rubner, Antibacterial properties of Ag nanoparticle loaded multilayers and formation of magnetically directed antibacterial microparticles, *Langmuir*, 2005, **21**, 9651-9659.
155. I. Sondi and B. Salopek-Sondi, Silver nanoparticles as antimicrobial agent: A case study on E-coli as a model for Gram-negative bacteria, *J. Colloid Interf. Sci.*, 2004, **275**, 177-182.
156. J. Fabrega, S. R. Fawcett, J. C. Renshaw and J. R. Lead, Silver nanoparticle impact on bacterial growth: Effect of pH, concentration, and organic matter. *Environ. Sci. Technol.*, 2009, **43**, 7285-7290.
157. C. Marambio-Jones and E. M. V. Hoek, A review of the antibacterial effects of silver nanomaterials and potential implications for human health and the environment, *J. Nanoparticle Res.*, 2010, **12**, 1-21.
158. V. V. Tarabara, in *Nanotechnology Applications for Clean Water*, eds. N. Savage, M. Diallo, J. Duncan, A. Street and R. Sustich, William Andrew Inc., Norwich, NY, 2009, pp. 59-75.
159. L. Brunet, D. Y. Lyon, K. Zodrow, J. C. Rouch, B. Caussat, P. Serp, J. C. Remigy, M. R. Wiesner and P. J. J. Alvarez, Properties of membranes containing semi-dispersed carbon nanotubes, *Environ. Eng. Sci.*, 2008, **25**, 565-575.

160. Y. Lin, M. Meziani and Y. Sun, Functionalized carbon nanotubes for polymeric nanocomposites, *J. Mater. Chem.*, 2007, **17**, 1143-1148.
161. S. Kang, M. Pinault, L. D. Pfefferle and M. Elimelech, Single-walled carbon nanotubes exhibit strong antimicrobial activity, *Langmuir*, 2007, **23**, 8670-8673.
162. P. Ajayan, Nanotubes from carbon, *Chem. Rev.*, 1999, **99**, 1787-1800.
163. K. M. Persson, V. Gekas and G. Tragardh, Study of membrane compaction and its influence on ultrafiltration water permeability, *J. Membrane Sci.*, 1995, **100**, 155-162.
164. G. Jonsson, Methods for determining the selectivity of reverse osmosis membranes, *Desalination*, 1978, **24**, 19-37.
165. K. Ebert, D. Fritsch, J. Koll and C. Tjahjawiguna, Influence of inorganic fillers on the compaction behaviour of porous polymer based membranes, *J. Membrane Sci.*, 2004, **233**, 71-78.
166. M. M. Pendergast, J. M. Nygaard, A. K. Ghosh, E. M. V. Hoek, Using nanocomposite membrane materials to understand and control reverse osmosis membrane compaction, *Desalination*, 2010, **261**, 255-263.
167. M. Arkas, D. Tsiourvas and C. M. Paleos, Organosilicon dendritic networks in porous ceramics for water purification, *Chem. Mater.*, 2005, **17**, 3439-3444.
168. B. H. Jeong, E. M. V. Hoek, Y. S. Yan, A. Subramani, X. F. Huang, G. Hurwitz, A. K. Ghosh and A. Jawor, Interfacial polymerization of thin film nanocomposites: A new concept for reverse osmosis membranes, *J. Membrane Sci.*, 2007, **294**, 1-7.
169. M. Lind, A. Ghosh, A. Jawor, X. Huang, W. Hou, Y. Yang and E. Hoek, Influence of Zeolite Crystal Size on Zeolite-Polyamide Thin Film Nanocomposite Membranes, *Langmuir*, 2009, **25**, 10139-10145.
170. H. S. Lee, S. J. Im, J. H. Kim, H. J. Kim, J. P. Kim and B. R. Min, Polyamide thin-film nanofiltration membranes containing TiO₂ nanoparticles, *Desalination*, 2008, **219**, 48-56.
171. T. H. Bae, I. C. Kim and T. M. Tak, Preparation and characterization of fouling-resistant TiO₂ self-assembled nanocomposite membranes, *J. Membrane Sci.*, 2006, **275**, 1-5.
172. M. L. Luo, W. Tang, J. Q. Zhao and C. S. Pu, Hydrophilic modification of poly(ether sulfone) used TiO₂ nanoparticles by a sol-gel process, *J. Mater. Process. Tech.*, 2006, **172**, 431-436.
173. M. L. Lind, B. H. Jeong, A. Subramani, X. F. Huang and E. M. V. Hoek, Effect of mobile cation on zeolite-polyamide thin film nanocomposite membranes, *J. Mater. Res.*, 2009, **24**, 1624-1631.
174. A. S. Brady-Estevéz, S. Kang and M. Elimelech, A single-walled-carbon-nanotube filter for removal of viral and bacterial pathogens, *Small*, 2008, **4**, 481-484.
175. M. L. Luo, J. Q. Zhao, W. Tang and C. S. Pu, Hydrophilic modification of poly(ether sulfone) ultrafiltration membrane surface by self-assembly of TiO₂ nanoparticles, *Appl. Surf. Sci.*, 2005, **249**, 76-84.
176. P. Agre, S. Sasaki and M. J. Chrispeels, Aquaporins: A family of water channel proteins, *Am. J. Physiol-Renal*, 1993, **265**, F461.
177. Y. Kaufman, A. Berman and V. Freger, Supported lipid bilayer membranes for water purification by reverse osmosis, *Langmuir*, 2010, **26**, 7388-7395.
178. P. Agre, *Aquaporin Water Channels*, Nobel Lecture, Stockholm, SE, 2003.
179. A. Meinild, D. Klaerke and T. Zeuthen, Bidirectional water fluxes and specificity for small hydrophilic molecules in Aquaporins 0-5, *J. Biol. Chem.*, 1998, **273**, 32446.

180. P. Agre, G. M. Preston, B. L. Smith, J. S. Jung, S. Raina, C. Moon, W. B. Guggino and S. Nielsen, Aquaporin CHIP: The archetypal molecular water channel, *Am. J. Physiol-Renal*, 1993, **265**, F463-476.
181. F. Q. Zhu, E. Tajkhorshid and K. Schulten, Theory and simulation of water permeation in Aquaporin-1, *Biophysical Journal*, 2004, **86**, 50-57.
182. M. Kumar, M. Grzelakowski, J. Zilles, M. Clark and W. Meier, Highly permeable polymeric membranes based on the incorporation of the functional water channel protein Aquaporin Z, *P. Natl. Acad. Sci. USA*, 2007, **104**, 20719-20724.
183. T. W. Ebbesen, Carbon nanotubes, *Annu. Rev. Mater. Sci.*, 1994, **24**, 235-264.
184. T. W. Ebbesen, Nanotubes, nanoparticles, and aspects of fullerene related carbons, *J. Phys. Chem. Solids*, 1997, **58**, 1979-1982.
185. S. Ahadian and Y. Kawazoe, An artificial intelligence approach for modeling and prediction of water diffusion inside a carbon nanotube. *Nanoscale Res. Lett.*, 2009, **4**, 1054-1058.
186. J. K. Holt, H. G. Park, Y. M. Wang, M. Stadermann, A. B. Artyukhin, C. P. Grigoropoulos, A. Noy and O. Bakajin, Fast mass transport through sub-2-nanometer carbon nanotubes, *Science*, 2006, **312**, 1034-1037.
187. G. Hummer, J. C. Rasaiah and J. P. Noworyta, Water conduction through the hydrophobic channel of a carbon nanotube, *Nature*, 2001, **414**, 188-190.
188. A. Kalra, S. Garde and G. Hummer, Osmotic water transport through carbon nanotube membranes, *P. Natl. Acad. Sci. USA*, 2003, **100**, 10175-10180.
189. L. Song, J. Y. Hu, S. L. Ong, W. J. Ng, M. Elimelech and M. Wilf, Emergence of thermodynamic restriction and its implications for full-scale reverse osmosis processes, *Desalination*, 2003, **155**, 213-228.
190. J. P. Salvetat, G. A. D. Briggs, J. M. Bonard, R. R. Bacsá, A. J. Kulik, T. Stockli, N. A. Burnham and L. Forro, Elastic and shear moduli of single-walled carbon nanotube ropes, *Phys. Rev. Lett.*, 1999, **82**, 944-947.
191. J. P. Salvetat, A. J. Kulik, J. M. Bonard, G. A. D. Briggs, T. Stockli, K. Metenier, S. Bonnamy, F. Beguin, N. A. Burnham and L. Forro, Elastic modulus of ordered and disordered multiwalled carbon nanotubes, *Adv. Mater.*, 1999, **11**, 161-165.
192. S. Kim, J. R. Jinschek, H. Chen, D. S. Sholl and E. Marand, Scalable fabrication of carbon nanotube/polymer nanocomposite membranes for high flux gas transport, *Nano Lett.*, 2007, **7**, 2806-2811.
193. Y. Gao, J. Liu, M. Shi, S. H. Elder and J. W. Virden, Dense arrays of well-aligned carbon nanotubes completely filled with single crystalline titanium carbide wires on titanium substrates, *Appl. Phys. Lett.*, 1999, **74**, 3642-3644.
194. Y. C. Choi, Y. M. Shin, Y. H. Lee, B. S. Lee, G. S. Park, W. B. Choi, N. S. Lee and J. M. Kim, Controlling the diameter, growth rate, and density of vertically aligned carbon nanotubes synthesized by microwave plasma-enhanced chemical vapor deposition, *Appl. Phys. Lett.*, 2000, **76**, 2367-2369.
195. A. Huczko, Synthesis of aligned carbon nanotubes, *Appl. Phys. A-Mater.*, 2002, **74**, 617-638.
196. N. Yoshikawa, T. Asari, N. Kishi, S. Hayashi, T. Sugai and H. Shinohara, An efficient fabrication of vertically aligned carbon nanotubes on flexible aluminum foils by catalyst-supported chemical vapor deposition, *Nanotechnology*, 2008, **19**, 245607.

197. P. Mauron, C. Emmenegger, A. Zuttel, C. Nutzenadel, P. Sudan and L. Schlapbach, Synthesis of oriented nanotube films by chemical vapor deposition, *Carbon*, 2002, **40**, 1339-1344.
198. F. Fornasiero, H. G. Park, J. K. Holt, M. Stadermann, C. P. Grigoropoulos, A. Noy and O. Bakajin, Ion exclusion by sub-2-nm carbon nanotube pores, *P. Natl. Acad. Sci. USA*, 2008, **105**, 17250-17255.
199. W. A. deHeer, W. S. Basca, C. T. Gerfin, R. Humphrey-Baker, L. Forro and D. Ugarte, Aligned carbon nanotube films: Production and optical and electronic properties, *Science*, 1995, **268**, 845-847.
200. M. J. Casavant, D. A. Walters, J. J. Schmidt and R. E. Smalley, Neat macroscopic membranes of aligned carbon nanotubes, *J. Appl. Phys.*, 2003, **93**, 2153-2156.
201. A. Srivastava, O. N. Srivastava, S. Talapatra, R. Vajtai and P. M. Ajayan, Carbon nanotube filters, *Nat. Mater.*, 2004, **3**, 610-614.
202. B. Corry, Designing carbon nanotube membranes for efficient water desalination, *J. Phys. Chem. B*, 2008, **112**, 1427-1434.
203. G. M. Whitesides and B. Grzybowski, Self-assembly at all scales, *Science*, 2002, **295**, 2418-2421.
204. G. Widawski, M. Rawiso and B. Francois, Self-organized honeycomb morphology of star-polymer polystyrene films, *Nature*, 1994, **369**, 387-389.
205. D. Beattie, K. H. Wong, C. Williams, L. A. Poole-Warren, T. P. Davis, C. Barner-Kowollik and M. H. Stenzel, Honeycomb-structured porous films from polypyrrole-containing block copolymers prepared via RAFT polymerization as a scaffold for cell growth, *Biomacromolecules*, 2006, **7**, 1072-1082.
206. D. Fierro, K. Buhr, C. Abetz, A. Boschetti-de-Fierro and V. Abetz, New insights into the control of self-assembly of block copolymer membranes, *Aust. J. Chem.* 2009, **62**, 885-890.
207. T. Kabuto, Y. Hashimoto and O. Karthaus, Thermally stable and solvent resistant mesoporous honeycomb films from a crosslinkable polymer, *Adv. Funct. Mater.*, 2007, **17**, 3569-3573.
208. C. Rodriguez-Abreu and M. Lazzari, Emulsions with structured continuous phases, *Curr. Opin. Colloid In.*, 2008, **13**, 198-205.
209. H. Yabu, Y. Hirai and M. Shimomura, Electroless plating of honeycomb and pincushion polymer films prepared by self-organization, *Langmuir*, 2006, **22**, 9760-9764.
210. A. Dove, Controlled ring-opening polymerisation of cyclic esters: polymer blocks in self-assembled nanostructures, *Chem. Commun.*, 2008, **2008**, 6446-6470.
211. K. V. Peinemann, V. Abetz and P. F. W. Simon, Asymmetric superstructure formed in a block copolymer via phase separation, *Nat. Mater.*, 2007, **6**, 992-996.
212. T. Smart, H. Lomas, M. Massignani, M. V. Flores-Merino, L. R. Perez and G. Battaglia, Block copolymer nanostructures, *Nano Today*, 2008, **3**, 38-46.
213. R. O'Reilly, C. Hawker and K. Wooley, Cross-linked block copolymer micelles: functional nanostructures of great potential and versatility, *Chem. Soc. Rev.*, 2006, **35**, 1068-1083.
214. H. Jung, K. Price and D. McQuade, Synthesis and characterization of cross-linked reverse micelles, *Polymer*, 1993, **34**, 4969.
215. W. Phillip, M. Hillmyer and E. Cussler, Cylinder orientation mechanism in block copolymer thin films upon solvent evaporation, *Macromolecules*, 2010, **43**, 7763-7770.

216. W. Phillip, B. O'Neill, M. Rodwogin, M. Hillmyer, E. Cussler, Self-assembled block copolymer thin films as water filtration membranes, *ACS Appl. Mater. Interface*, 2010, **2**, 847-853.
217. J. Y. Cheng, A. M. Mayes and C. A. Ross, Nanostructure engineering by templated self-assembly of block copolymers, *Nat. Mater.*, 2004, **3**, 823-828.
218. K. V. Peinemann, P. F. Abetz, W. Simon, G. Johannsen, G., *Isoporous membrane and method of production thereof*, US Patent, US0173694 (2009).
219. W. A. Phillip, M. Amendt, B. O'Neill, L. Chen, M. A. Hillmyer and E. L. Cussler, Diffusion and flow across nanoporous polydicyclopentadiene-based membranes. *ACS Appl. Mater. Interface*, 2009, **1**, 472-480.
220. L. Chen, W. A. Phillip, E. L. Cussler and M. A. Hillmyer, Robust nanoporous membranes templated by a doubly reactive block copolymer, *J. Am. Chem. Soc.*, 2007, **129**, 13786-13787.
221. M. J. Fasolka and A. M. Mayes, Block copolymer thin films: Physics and applications, *Annu. Rev. Mater. Res.*, 2001, **31**, 323-355.
222. S. Y. Yang, I. Ryu, H. Y. Kim, J. K. Kim, S. K. Jang and T. P. Russell, Nanoporous membranes with ultrahigh selectivity and flux for the filtration of viruses, *Adv. Mater.*, 2006, **18**, 709-712.
223. K. Fukunaga, T. Hashimoto, H. Elbs and G. Krausch, Self-assembly of a lamellar ABC triblock terpolymer thin film. Effect of substrates, *Macromolecules*, 2003, **36**, 2852-2861.
224. X. Li, C. Fustin, N. Lefèvre, J. Gohy, S. De Feyter, J. De Baerdemaeker, W. Egger and I. Vankelecom, Ordered nanoporous membranes based on diblock copolymers with high chemical stability and tunable separation properties, *J. Mater. Chem*, 2010, **20**, 4333-4339.
225. K. Stratford, R. Adhikari, I. Pagonabarraga, J. C. Desplat and M. E. Cates, Colloidal jamming at interfaces: A route to fluid-bicontinuous gels, *Science*, 2005, **309**, 2198-2201.
226. X. Yao, H. W. Yao, Y. T. Li and G. Chen, Preparation of honeycomb scaffold with hierarchical porous structures by core-crosslinked core-corona nanoparticles, *J. Colloid Interf. Sci.*, 2009, **332**, 165-172.
227. J. S. Wang and K. Matyjaszewski, Controlled living radical polymerization-atom-transfer radical polymerization in the presence of transition-metal complexes. *J. Am. Chem. Soc.*, 1995, **117**, 5614-5615.
228. G. Guillen and E. M. V. Hoek, Modeling the impacts of feed spacer geometry on reverse osmosis and nanofiltration processes, *Chem. Eng. J.*, 2009, **149**, 221-231.

TABLES

Table 1. Membrane characterizations by pore type and target species

Pore Type (size range, nm)	Membrane Type (pore size, nm)	Species ^c	Dimensions ^c (nm)
Macropores (> 50)	Microfiltration^a (50 - 500)	yeasts & fungi	1 000 - 10 000
		bacteria	300 - 10 000
		oil emulsions	100 - 10 000
Mesopores (2 - 50)	Ultrafiltration^a (2 - 50)	colloidal solids	100 - 1 000
		viruses	30 - 300
		proteins/polysaccharides	3 - 10
		humics/nucleic acids	< 3
Micropores (0.2 - 2)	Nanofiltration^a (≤ 2) Reverse Osmosis^b (0.3-0.6) Forward Osmosis^b (0.3-0.6)	common antibiotics	0.6 - 1.2
		organic antibiotics	0.3 - 0.8
		inorganic ions	0.2 - 0.4
		water	0.2

^a See reference ⁶.^b See reference ⁸.^c See reference ⁵.

Table 2. Performance comparison of organic and inorganic membranes

Membrane Type	Test Temp (°C)	Film Thickness (μm)	Water Permeability (m·Pa ⁻¹ ·s ⁻¹)	Specific Water Permeability (m ² ·Pa ⁻¹ ·s ⁻¹)	Solute Type (concentration)	Solute Rejection (%)	Solute Permeability (m·s ⁻¹)	Reference
SWRO *	20	~0.2	~3×10 ⁻¹²	~0.6×10 ⁻¹⁸	NaCl (32 g/l)	> 99.5	~2×10 ⁻⁸	228
BWRO	20	~0.1	~10×10 ⁻¹²	~1×10 ⁻¹⁸	NaCl (2 g/l)	99.0	~7×10 ⁻⁸	228
HFRO	20	~0.1	~20×10 ⁻¹²	~2×10 ⁻¹⁸	NaCl (0.5-1.5 g/l)	98.5	~1×10 ⁻⁷	228
NF	20	~0.05	~40×10 ⁻¹²	~2×10 ⁻¹⁸	MgSO4 (0.5 g/l)	95.0	~10×10 ⁻⁷	228
MFI	20	~3	~0.01×10 ⁻¹²	~0.04×10 ⁻¹⁸	NaCl (0.1 M)	76.7	7×10 ⁻⁷	55
MFI	30	~3	~0.03×10 ⁻¹²	~0.1×10 ⁻¹⁸	NaCl (0.1 M)	98.0	2×10 ⁻⁷	56
MFI	20	~1.2	~0.03×10 ⁻¹²	~0.04×10 ⁻¹⁸	NaCl (0.1 M)	99.4	0.6×10 ⁻⁷	61
SOD	20	~50	~2×10 ⁻¹²	~100×10 ⁻¹⁸	none tested	-	-	10
LTA	30	~5	~0.03×10 ⁻¹²	~0.1×10 ⁻¹⁸	none tested	-	-	62

*Commercial polymeric seawater RO (SWRO), brackish water RO (BWRO), high-flux RO (HFRO)

Table 3. Comparison of nanotechnology-enabled technologies

Nanotechnology-Enabled Membrane Concept		Potential Performance Enhancement			Potential Commercial Viability		
		Productivity	Selectivity	Robustness	Cost Effectiveness	Scalability	Time to Commercialization
Nanostructured Ceramic Membranes	Reactive/Catalytic Surfaces	0	+	+	0	0	0
	Zeolitic Coatings	-	0	+	-	0	0
Inorganic-Organic Membranes	Mixed Matrices	+	0	+	-	+	0
	Nanoparticle TFNs	+	-	+	-	+	+
	Zeolite TFNs	+	0	+	0	+	+
Biologically-Inspired Membranes	Aquaporins	+++	++	0	-	-	0
	Aligned Nanotubes	++	++	0	-	-	0
	Block Copolymers	++	++	-	0	+	-

LIST OF FIGURES

Figure 1. Conceptual depiction of the asymmetric structure of an inorganic membrane.

Figure 2. Conceptual cross-section of an asymmetric, integrally skinned membrane.

Figure 3. Schematic of nanoparticle mediated photocatalysis. Adapted from ⁷⁴.

Figure 4. Conceptual cross-section of a membrane containing molecular sieves throughout the polymeric thin film, providing preferential flow paths for water as indicated by arrows. Adapted from ¹⁶⁸.

Figure 5. Theoretical projection of the possibilities for thin films containing nanoparticles (permeable and impermeable) compared to current polymeric seawater RO membranes.

Figure 6. Molecular ordering of water molecules being transported through nanoscale channels (aquaporins and carbon nanotubes) as predicted by molecular dynamics simulations. Adapted from ¹⁸⁷.

Figure 7. Conceptual cross-sectional image of a semi-permeable lipid bi-layer membrane cast atop a nanofiltration-type support membrane. Adapted from ¹⁷⁷.

Figure 8. Conceptual image of an array of aligned nanotubes embedded in a nonporous polymeric matrix.

Figure 9. Theoretical projection of the possibilities for aligned carbon nanotube membranes compared to current polymeric seawater RO membranes.

Figure 10. Di-block copolymer micelle formation upon reaching the critical micelle concentration. Adapted from ²²⁶.

Figure 11. Comparison of the potential performance and commercial viability of nanotechnology-enabled membrane advances based on review of current literature. Performance enhancement relates to permeability, selectivity, and robustness, while commercial viability relates to material cost, scalability, and compatibility with existing manufacturing infrastructure.

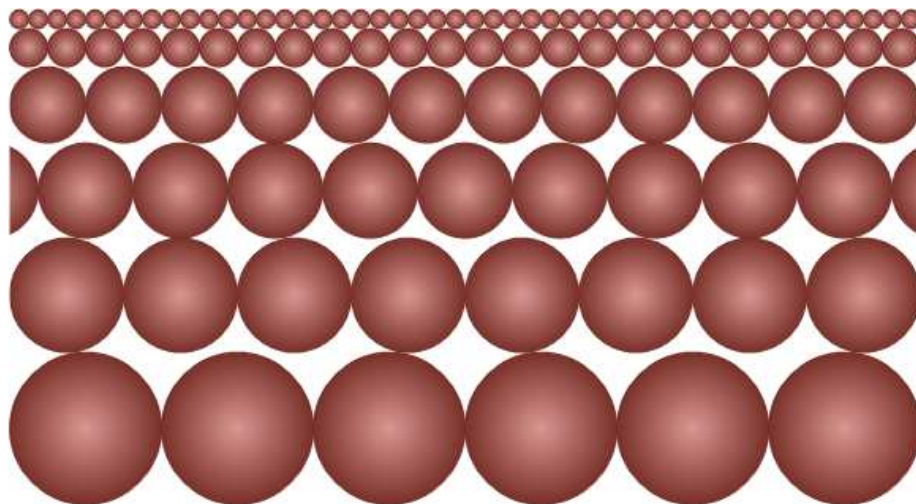
FIGURES

Figure 1. Conceptual depiction of the asymmetric structure of an inorganic membrane.

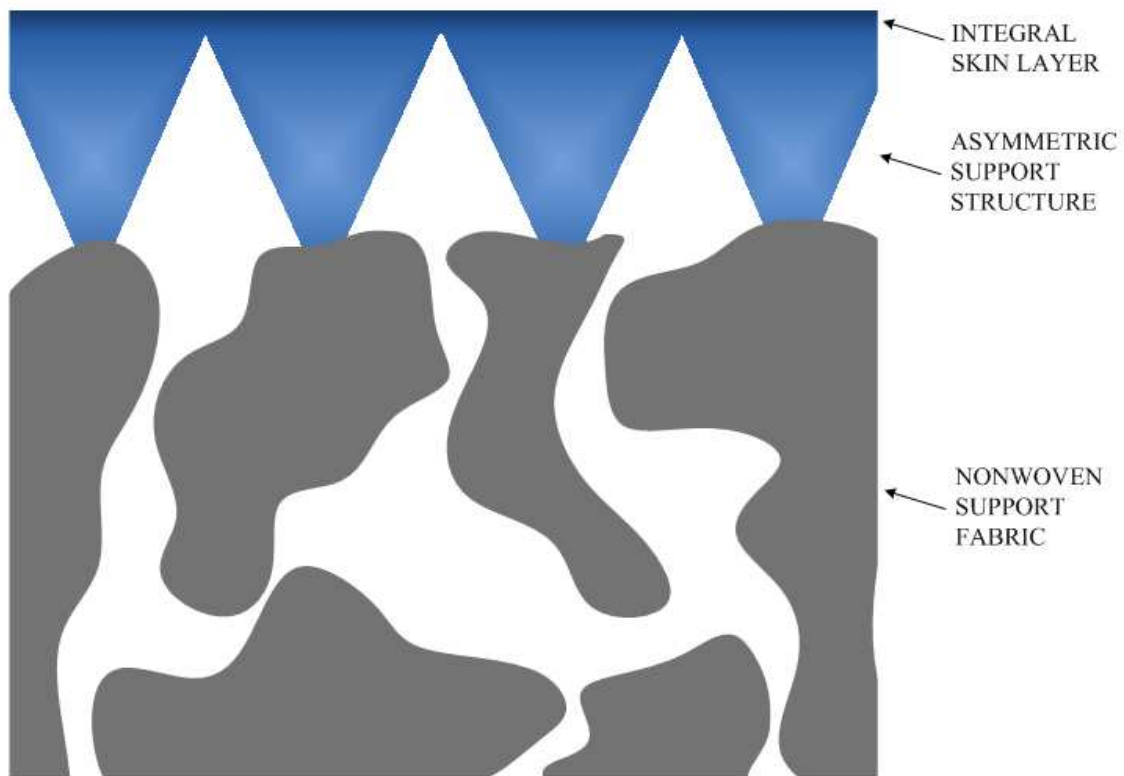


Figure 2. Conceptual cross-section of an asymmetric, integrally skinned membrane.

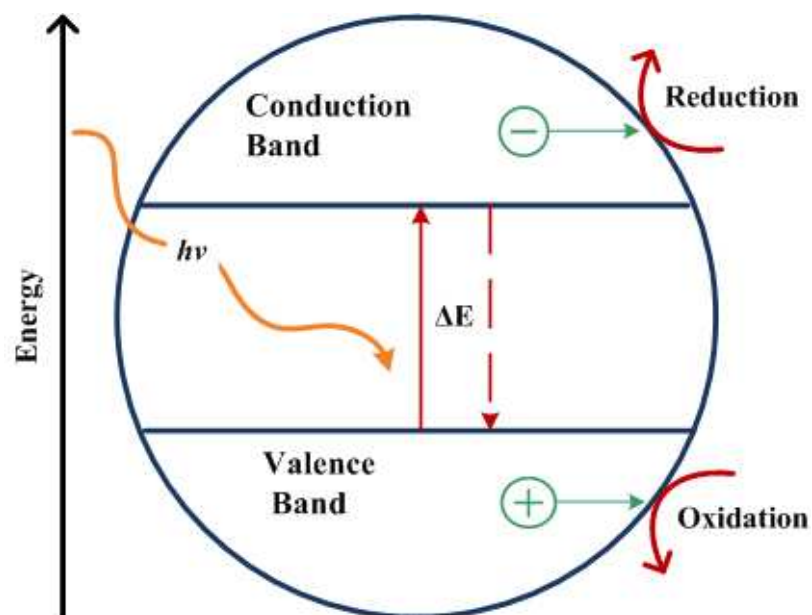


Figure 3. Schematic of nanoparticle mediated photocatalysis. Adapted from ⁷⁴.

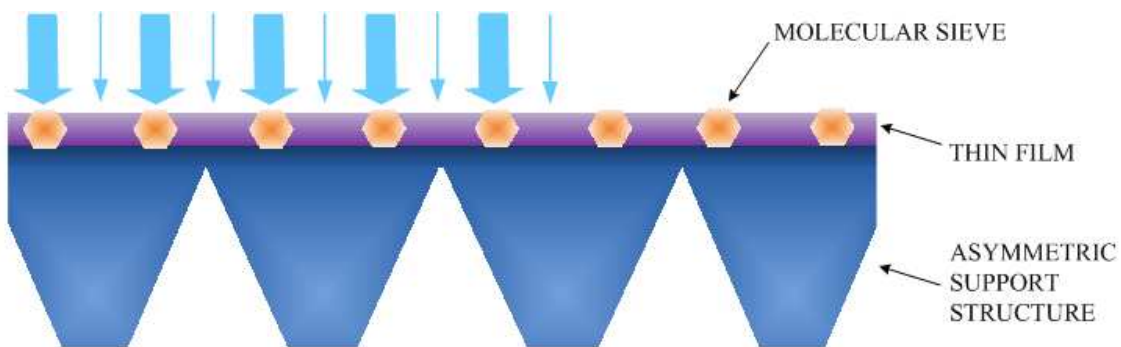


Figure 4. Conceptual cross-section of a membrane containing molecular sieves throughout the polymeric thin film, providing preferential flow paths for water as indicated by arrows. Adapted from ¹⁶⁸.

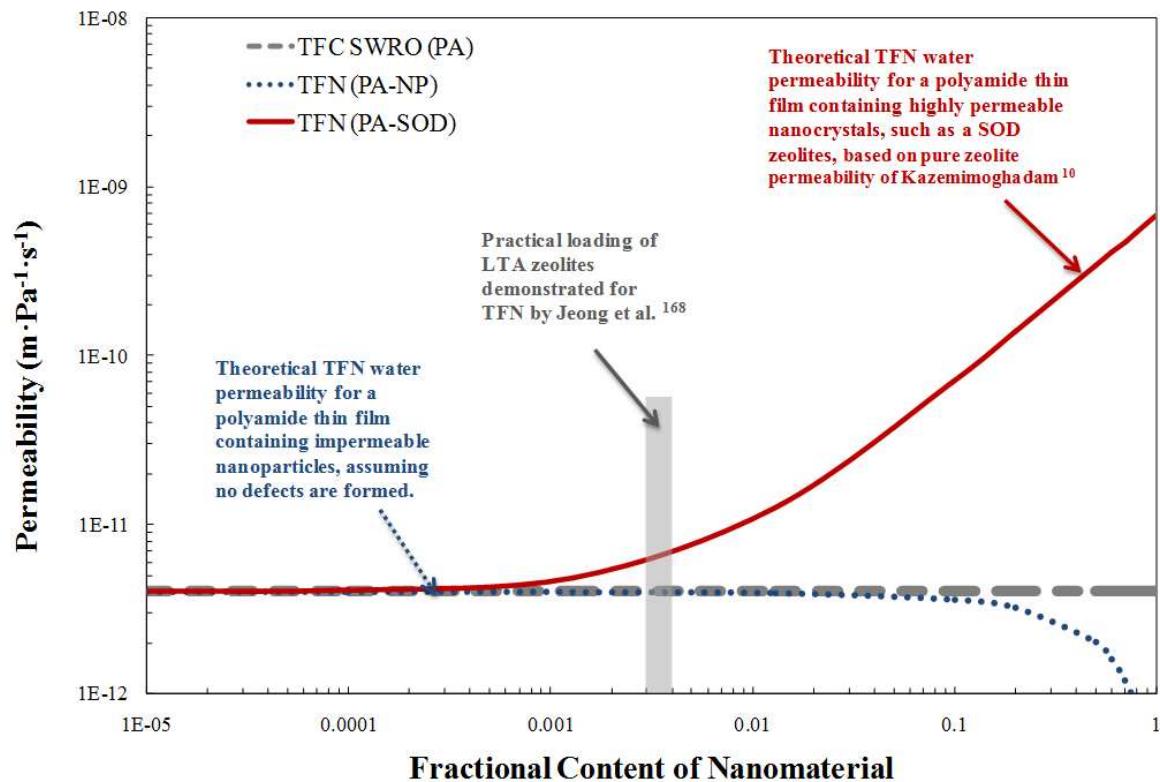


Figure 5. Theoretical projection of the possibilities for thin films containing nanoparticles (permeable and impermeable) compared to current polymeric seawater reverse osmosis membranes.

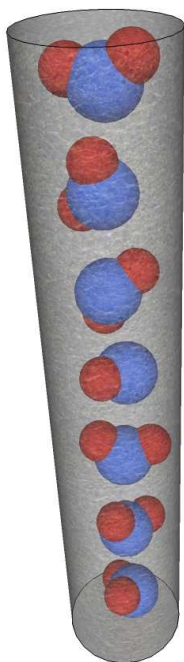


Figure 6. Molecular ordering of water molecules being transported through nanoscale channels (aquaporins and carbon nanotubes) as predicted by molecular dynamics simulations. Adapted from ¹⁸⁷.

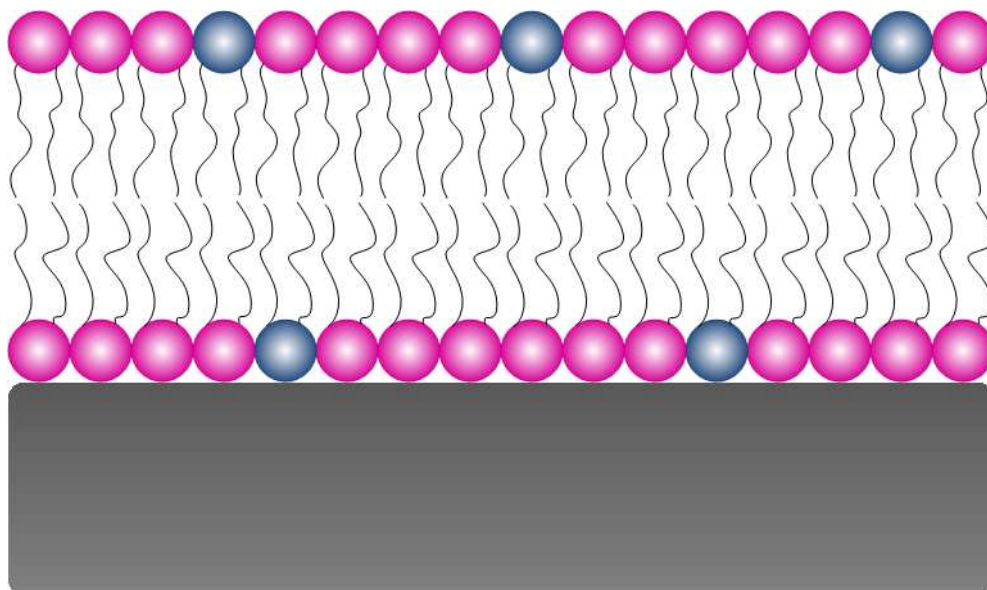


Figure 7. Conceptual cross-sectional image of a semi-permeable lipid bi-layer membrane cast atop a nanofiltration-type support membrane. Adapted from ¹⁷⁷.

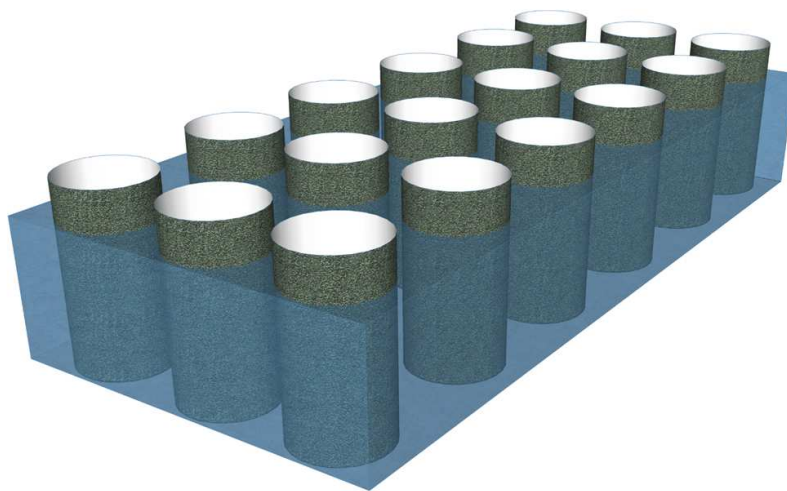


Figure 8. Conceptual image of an array of aligned nanotubes embedded in a nonporous polymeric matrix.

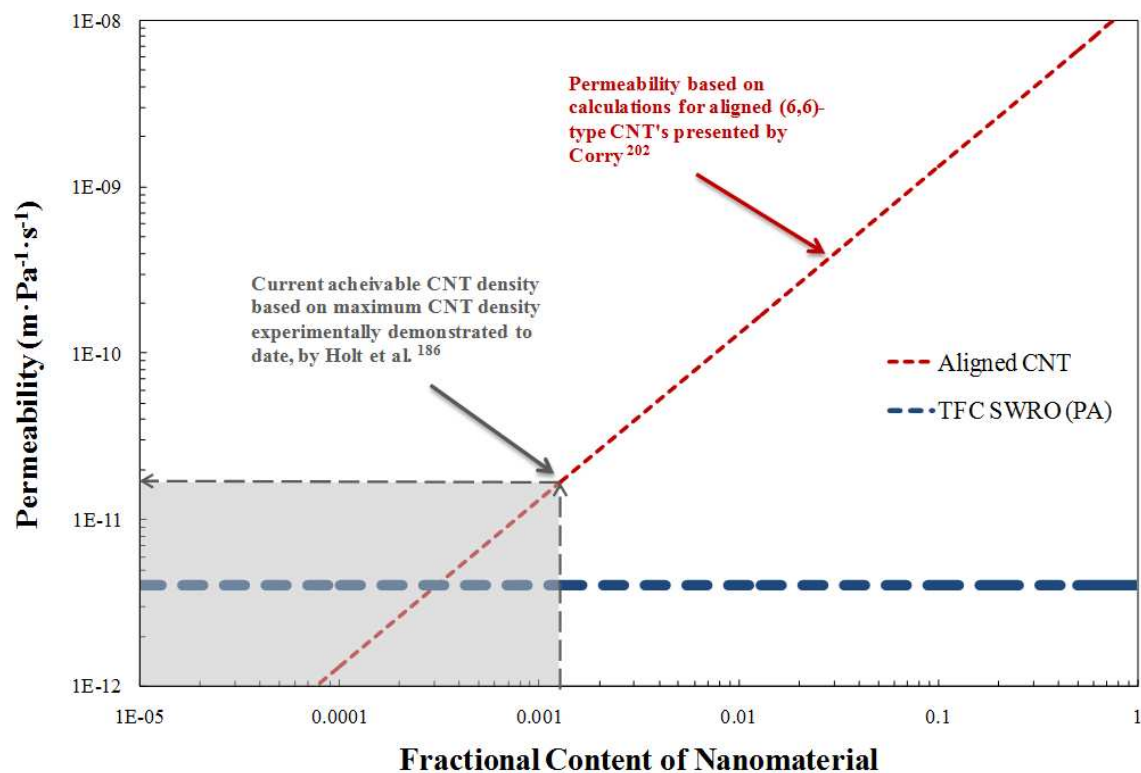


Figure 9. Theoretical projection of the possibilities for aligned carbon nanotube membranes compared to current polymeric seawater reverse osmosis membranes.

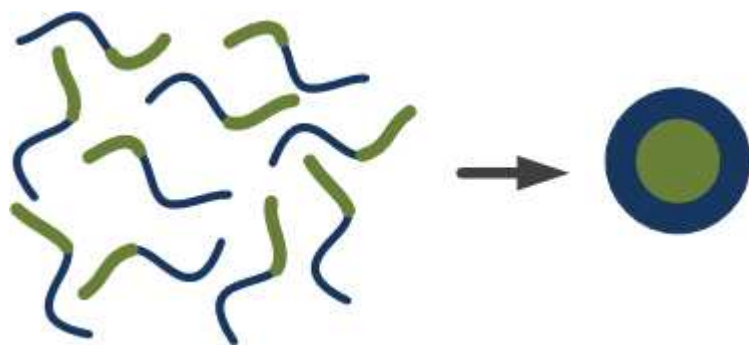


Figure 10. Di-block copolymer micelle formation upon reaching the critical micelle concentration. Adapted from ²²⁶.

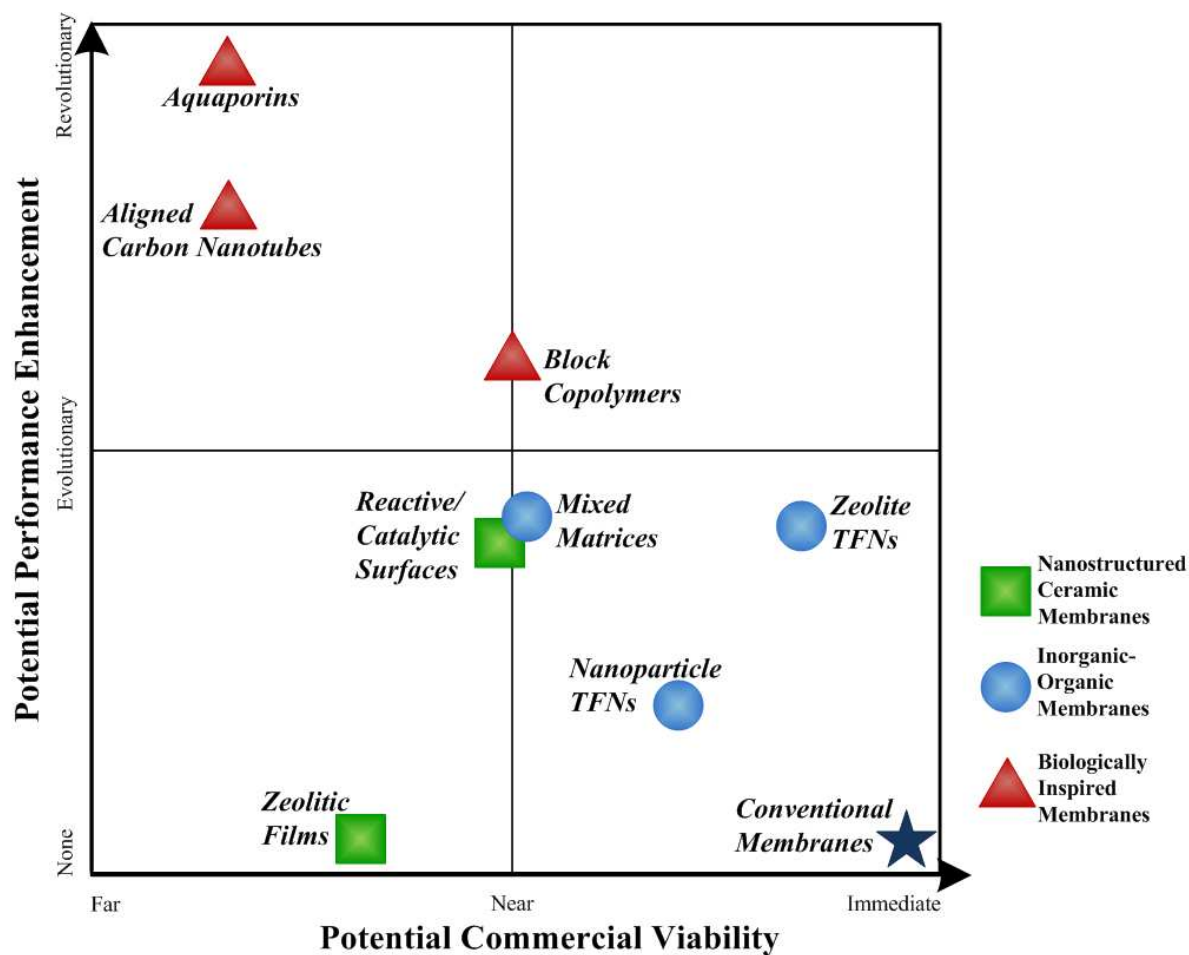


Figure 11. Comparison of the potential performance and commercial viability of nanotechnology-enabled membrane advances based on review of current literature. Performance enhancement relates to permeability, selectivity, and robustness, while commercial viability relates to material cost, scalability, and compatibility with existing manufacturing infrastructure.

A REVIEW OF WATER TREATMENT MEMBRANE NANOTECHNOLOGIES

by

*MaryTheresa M. Pendergast, Eric M.V. Hoek**

Department Civil & Environmental Engineering and California NanoSystems
Institute, University of California, Los Angeles, California, USA

Submitted to

Energy and Environmental Science

January 26, 2011

* Corresponding author contact: University of California, Los Angeles; 5732-G Boelter Hall;
P.O. Box 951593; Los Angeles, California, 90095-1593, USA; Tel: (310) 206-3735; Fax: (310)
206-2222; E-mail: emvhoek@ucla.edu

ABSTRACT

Nanotechnology is being used to enhance conventional ceramic and polymeric water treatment membrane materials through various avenues. Among the numerous concepts proposed, the most promising to date include zeolitic and catalytic nanoparticle coated ceramic membranes, hybrid inorganic-organic nanocomposite membranes, and bio-inspired membranes such as hybrid protein-polymer biomimetic membranes, aligned nanotube membranes, and isoporous block copolymer membranes. A semi-quantitative ranking system was proposed considering projected performance enhancement (over state-of-the-art analogs) and state of commercial readiness. Performance enhancement was based on water permeability, solute selectivity, and operational robustness, while commercial readiness was based on known or anticipated material costs, scalability (for large scale water treatment applications), and compatibility with existing manufacturing infrastructure. Overall, bio-inspired membranes are farthest from commercial reality, but offer the most promise for performance enhancements; however, nanocomposite membranes offering significant performance enhancements are already commercially available. Zeolitic and catalytic membranes appear reasonably far from commercial reality and offer small to moderate performance enhancements. The ranking of each membrane nanotechnology is discussed along with the key commercialization hurdles for each membrane nanotechnology.

KEYWORDS

zeolite membrane; catalytic membrane; mixed-matrix membrane; nanocomposite membrane; thin film nanocomposite; biomimetic membrane; aligned carbon nanotube; block copolymer

TABLE OF CONTENTS

1. INTRODUCTION	4
2. CONVENTIONAL MEMBRANE MATERIALS	6
2.1. Inorganic Membranes.....	6
2.1.1. Mesoporous Ceramic Membranes.....	6
2.2. Organic Membranes	7
2.2.1. Integrally-Skinned Membranes	7
2.2.2. Thin Film Composite Membranes.....	9
3. NANOTECHNOLOGY-BASED MEMBRANE MATERIALS	12
3.1. Nanostructured Ceramic Membranes.....	12
3.1.1. Zeolite-Coated Ceramic Membranes.....	12
3.1.2. Reactive/Catalytic Ceramic Membranes	19
3.2 Inorganic-Organic Membranes	23
3.2.1. Mixed Matrix Membranes.....	23
3.2.2. Thin Film Nanocomposite Membranes	30
3.3. Biologically-Inspired Membranes.....	34
3.3.1. Aquaporin Membranes	34
3.3.2. Vertically Aligned Nanotube Membranes.....	36
3.3.3. Isoporous Block Copolymer Membranes	41
4. DISCUSSION AND CONCLUSIONS	48

1. INTRODUCTION

In the last century the global population quadrupled, while the world water demand increased sevenfold ¹. This global water challenge will become greater as the population and economies of developing countries expand; in the next forty years, the global population is expected to grow nearly 40%, and hence, domestic, agriculture, industry, and energy demands on water resources will continue to grow ². The World Water Council estimates that by 2030, 3.9 billion people will live in regions characterized as “water scarce” ³. In addition to overall water shortage, poor water quality is near crisis in many parts of the world. According to the World Health Organization, 1.1 billion people lack access to improved drinking water and 2.6 billion lack access to proper sanitation ⁴. As many as 2.2 million people die of diarrheal related disease every year most often caused by waterborne infections, and the majority of these cases are children under the age of 5 ². More than ever, existing fresh water resources need protection and new water resources must be developed in order to meet the world’s growing demand for clean water. This will require better water treatment technology.

Membranes are favored over many other technologies for water treatment because, in principle, they require no chemical additives or thermal inputs and they do not require regeneration of spent media. Although such an ideal membrane has not yet been realized in the 150 years since Maxwell theorized his magical ‘sorting demon,’ commercial membrane technologies can perform efficient, selective, and reliable separations ⁵. Pressure-driven membrane processes are the most widely used membrane technologies in water treatment applications ⁶; although, the use of gas separation, pervaporation, and electrochemical membrane processes for industrial and environmental separations have also increased dramatically in the past few decades ⁷.

Typically, pressure-driven membranes are classified according to characteristic pore size or their intended application (**Table 1**)^{5-6, 8}. Currently, membrane technology is commercially available for suspended solids, protozoa, and bacteria removal (microfiltration, MF), for virus and colloid removal (ultrafiltration, UF), for hardness, heavy metals, and dissolved organic matter removal (nanofiltration, NF), and for desalination, water reuse, and ultrapure water production (reverse osmosis, RO)⁶⁻⁷. While commercially available membranes perform well in many applications, the drive to protect existing water resources and to produce new water resources demands membranes with improved productivity, selectivity, fouling resistance, and stability available at lower cost and with fewer manufacturing defects. Better membranes require better materials.

Over the past decade, nanotechnology has rapidly changed from an academic pursuit to commercial reality; already nanotechnology concepts have led to new water treatment membranes that exceed state-of-the-art performance and enable new functionality, such as high permeability, catalytic reactivity, and fouling resistance. Herein, we present a brief overview of conventional materials used to prepare “state-of-the-art” pressure-driven membranes. This is followed by a critical review of current literature on nanotechnology-enabled water treatment membrane materials. Finally, we compare the “present day” merits and limitations of each water treatment membrane nanotechnology.

2. CONVENTIONAL MEMBRANE MATERIALS

2.1. Inorganic Membranes

2.1.1. Mesoporous Ceramic Membranes

As early as the 1940's inorganic membranes were developed for the enrichment of uranium. In the 1980's, the knowledge gained was applied for the formation of ceramic MF and UF membranes for industrial separations⁹. Generally, ceramic membranes are asymmetric in structure with a dense upper region atop a porous support (**Figure 1**). The mechanically stable support materials include, but are not limited to, alumina, silica, zirconia, mullite, oxide mixtures, and sintered metals¹⁰. Typical ceramic membranes are formed via the sol-gel process, in which particle dispersions are forced to agglomerate^{9,11}. The asymmetric structure is achieved by depositing particles of decreasing size and sintering at high temperature in order to achieve continuous, porous layers¹¹. Pore size and characteristics of the upper selective region may be tuned based upon the grain size and particle type selected⁹.

Post treatments are applied to alter the porosity of ceramic membranes. Mullite ($3\text{Al}_2\text{O}_3 \cdot 2\text{SiO}_2$) ceramic supports—formed through high temperature calcinations of kaoline clay—are desirable due to their enhanced mechanical strength. The extreme temperatures required for the formation of mullite allow for strong inter-crystalline bonds to form during the crystallization process. Free silica can be leached with a post treatment of strong alkali solution. The porosity of the resulting structure can be controlled by the leaching factors: time of leaching, concentration of leaching solution, and temperature at which leaching occurs¹². Coatings (of porous metals, metal oxides, and zeolites) can also be applied to ceramic membranes to further control performance with coating thickness, pore structure, and surface characteristics¹³.

With their enhanced mechanical, thermal, and chemical stability ceramic materials are well suited for challenging water purification processes, such as industrial wastewater, oil/water separations, and hazardous waste treatment¹². Flux through ceramic membranes is more easily recovered after fouling because ceramics can withstand harsh chemical and thermal cleaning methods¹⁴. Ceramics pose the opportunity for extended membrane lifetimes even under extreme fouling and cleaning conditions, which would destroy their polymeric counterparts. However, ceramics are typically considered too expensive for large-scale membrane applications, such as municipal drinking water production and wastewater treatment, so their application has been historically limited to relatively small-scale industrial separations not suitable for polymeric membranes^{11, 14-15}.

2.2. Organic Membranes

2.2.1. Integrally-Skinned Membranes

Porous polymeric membranes (i.e., MF/UF) have been applied to various water treatment processes, including water and wastewater filtration and as pretreatment for NF or RO membranes^{6, 8}. These membranes have an integrally skinned, often asymmetric structure consisting of an open porous support layer beneath a relatively thin, less porous skin layer of the same material (**Figure 2**)^{5, 8, 16-17}. The separation occurs at the skin layer while the support provides a nearly resistance-free path for water (and unrejected solutes carried in the permeating water) to exit the membrane. The highly selective top layer of MF/UF membranes, having pores ranging from ~0.01 to ~0.2 μm , is considered the active region of the membrane^{5, 8}.

Flat sheet forms of MF/UF membranes are formed through nonsolvent induced phase inversion of preformed polymers over a nonwoven support fabric, which provides mechanical

strength to the membrane. Alternatively, the phase inversion reaction can be carried out to form hollow fiber forms of MF/UF membranes. The phase inversion technique relies upon the controlled interaction of solvent and nonsolvent solutions to induce a phase separation transitioning a polymer from a liquid dispersion into a solid state^{5, 8, 18}. A recent review elucidates the details of this process¹⁹. A homogeneous polymer solution, containing polymer and solvent, is immersed into a nonsolvent coagulation bath and polymer solidification occurs during the miscible solvent and nonsolvent exchange^{5, 18}. Membrane characteristics vary with casting conditions, polymer selection, polymer concentration, the solvent/nonsolvent system and additives, and coagulation bath conditions^{5, 20-21}.

Cellulose acetate (CA) was one of the first polymers employed in aqueous membranes and continues to be employed to form membranes with properties ranging from MF to RO^{16, 22}. Other cellulosic derivatives include cellulose diacetate, triacetate, and regenerated cellulose. Cellulose acetate is obtained from cellulose – a naturally occurring linear compound found in wood pulp and cotton linters – via acetylation; CA is hydrophilic and produces smooth membrane surfaces with low fouling propensity²³⁻²⁴. Cellulosic membranes are also relatively easy to manufacture with a wide range of pore sizes and are relatively inexpensive²². Disadvantages of CA include limited temperature range (less than 30 °C) and pH range (approximately 3-5)⁵. A further operational limitation of CA membranes is their chlorine intolerance; continuous exposure of less than 1 mg·L⁻¹ of free chlorine will oxidize CA membranes opening the pores and causing a loss of selectivity, particularly in RO applications²⁵. Also, due to the cellulose backbone, CA membranes are biodegradable and can, in fact, be consumed by organisms growing in biofilms.

Other more widely applied MF/UF membrane polymers include polysulfone (PSf), polyethersulfone (PES), sulfonated PSf or PES, polyacrylonitrile (PAN), polypropylene (PP), polytetrafluoroethylene (PTFE, a.k.a., Teflon), and polyvinylidene fluoride (PVDF)¹¹. These materials exhibit excellent permeability, selectivity, and stability in water treatment applications. Polysulfone and PES membranes are among the most popular materials for UF membranes, as well as the standard support substrates used in formation of NF and RO composite membranes, while PP and PVDF are more popular materials for MF membranes.

2.2.2. Thin Film Composite Membranes

A major breakthrough in the field of membrane separations was the development of thin film composite membranes, which comprise an ultra-thin “barrier” layer polymerized *in situ* over a porous polymeric support membrane^{5,26}. These membranes are often referred to generically as “interfacial composite,” “composite,” or “TFC” membranes, although TFC[®] is registered trademark of Koch Membrane Systems, Inc. in the US and other countries. The major advantage of TFC membranes over integrally skinned asymmetric membranes is that the chemistry, and hence, performance of the upper selective layer and the porous support layer can be independently selected to optimize composite membrane performance²⁷. In addition, more expensive monomers can be used to form the selective layer without dramatically increasing cost because this region only accounts for a small portion of the total material. The key factors driving the development of TFC membrane materials over the past 40-50 years was the pursuit of high flux, high selectivity RO membranes for seawater desalination. Along the way, low-pressure RO membranes for desalting brackish water and for reclaiming wastewater to nearly

ultrapure levels were developed along with NF membranes now used predominantly for water softening and dissolved organic removal.

Thin film composite membranes are born out of conventional asymmetric polymeric membranes and, thus, are structurally similar to those discussed above; however, in TFC membranes the support and active layers are composed of two distinct polymers. The porous layer is generally formed through phase inversion and the dense layer is applied through interfacial polymerization or coating (dip, spray, spin) followed by cross-linking^{5, 26}. Curing (heat, UV, chemical) is frequently applied to further of the extent of polymer cross-linking, which significantly impacts the stability, permeability, and selectivity of the thin film^{5, 21}. Thin film composite RO/NF membranes are most often formed on the surface of a microporous support membrane via interfacial polymerization (*i.e.*, *in situ* polycondensation).

A large number of TFC membranes have been successfully developed from different polymers such as polyurea, polyamide (PA), polyurea-amide, polyether-amide, and others^{26, 28-30}, most of which have shown excellent selectivity, in particular high salt selectivity and relatively high water permeability for RO applications. Polyamide chemistry, developed by Cadotte and others, was first applied in the 1960's when DuPont and Monsanto developed asymmetric, integrally-skinned hollow fibers for RO seawater desalination³¹. Polyamide TFC membranes continue to be employed because they yield good salt rejection, while overcoming the relatively low flux of their integrally skinned counterparts.

Microporous supports for TFCs may be prepared from PSf, PES, sulfonated PSf and PES, polyether ketones, PVDF, sulfonated PVDF, or PAN through any number of casting procedures cited in the literature^{25, 28, 32-33}. Polysulfone is the most widely used polymer for RO support membranes^{5, 34}. Additives such as poly(ethylene glycol) and polyvinylpyrrolidone (PVP) have

been made to PSf support membrane casting solutions to increase porosity of the support membrane skin layer, and thus, the composite membrane permeability³⁵⁻³⁷. Presumably, the *de facto* commercial TFC membrane is an interfacially polymerized PA thin film formed over a PSf membrane with molecular weight cutoff of about 60 kDa;^{25, 28-29, 32-33, 38-41} however, the exact chemistry of commercial TFC membrane supports and coating films are proprietary.

Interfacial polymerization of TFC membranes is accomplished as follows^{28-29, 32, 42}. The microporous support membrane is immersed in an aqueous solution containing the first reactant (*e.g.*, a diamine monomer). The substrate is placed in contact with an organic solution containing the second reactant (*e.g.*, a triacyl halide). The organic solution is chosen to be immiscible with the aqueous solution so that the reaction proceeds at the interface of the two solutions. A dense but very thin polymer layer forms over the support membrane surface, which inhibits further polyamide formation and stops the reaction. The selective layer formed is very thin, which provides high water permeability, but densely cross-linked, which provides high salt rejection. The most common TFC coating film chemistry explored in the open literature is based on the amine monomer 1,3-diaminobenzene or *m*-phenylenediamine (MPD) polymerized with 1,3,5-tricarbonyl chloride or trimesoyl chloride (TMC), other di/tri-acid chlorides, or combinations thereof. The standard NF membrane derives from piperazine or polypiperazine derivatives polymerized with TMC, other di/tri-acid chlorides, or combinations thereof. It is suspected that most differences in commercial TFC NF/RO membranes result from the use of different support membranes, interfacial polymerization additives, and physical/chemical post-treatments³⁹⁻⁵⁰.

One common goal of post-treatments is to reduce a TFC membrane's propensity for surface fouling. This can be achieved through surface modifications via graft polymerization induced by methods such as plasma exposure⁵¹⁻⁵², UV-photoinitiation⁵³, or redox initiation⁴².

Recently, Kim et al. produced nanostructured RO membranes through plasma induced graft polymerization, in which a PSf supported PA RO membrane is exposed to plasma at atmospheric pressure to prime the surface and then free-radical graft polymerization of a small, hydrophilic, water soluble monomer, poly(methacrylic acid) (PMAA), is applied ⁵². The nanostructured surface roughness of the PMAA film (5.2-7.1 nm thickness) is nearly three times that of the unmodified TFC membrane. Membrane permeability doubled, with negligible changes in salt rejection. The modified membranes appeared to resist gypsum scaling 2-5 times longer than a low-fouling commercial RO membrane. This appears to be the first appearance in the open literature of a plasma-induced graft polymerization process at atmospheric conditions, which makes it potentially compatible with conventional membrane manufacturing infrastructure.

3. NANOTECHNOLOGY-BASED MEMBRANE MATERIALS

3.1. Nanostructured Ceramic Membranes

3.1.1. Zeolite-Coated Ceramic Membranes

A current thrust in ceramic membrane development is to form membranes with water permeability on the range of UF membranes, but solute selectivity like that of NF or RO membranes ¹¹. In 2001, molecular dynamics simulations showed that zeolite membranes—previously applied solely for gas separations—may be applicable for aqueous osmotic separations ⁵⁴. Since then, thin zeolite membranes have been studied for RO desalination of brackish water as well as a variety of wastewaters ⁵⁵⁻⁶¹. For RO applications, ceramic alternatives offer the clear advantage of mechanical stability under high pressures and chemical stability to withstand disinfectants. In many wastewater treatment applications, ceramic membranes are more fouling-resistant and chemically stable than current polymeric membranes.

Zeolites are naturally occurring aluminosilicate minerals with highly uniform sub-nanometer and nanometer scale crystalline structures. Typical zeolite membranes are amorphous silicate, aluminosilicate or aluminophosphate crystalline structures formed via hydrothermal synthesis^{10,62}. Other synthesis methods include *in situ* layer-by-layer crystallization and dry gel conversion in the presence of a template-water vapor⁶³. Aluminosilicate crystals are intrinsically inert, imbuing these membranes with extreme thermal and chemical stability⁶¹. Zeolite crystals consist of a three-dimensional cross-linked (Si/Al)O₄ tetrahedral framework, in which each Al or Si atom occupies the vertex of a network connecting four oxygen atoms. The framework structure contains cavities that allow for the movement and containment of ions and water molecules⁶⁴. The containment of molecules in a given zeolite framework is a function of temperature, water content, ion type, and the ratio of Si to Al atoms in the matrix⁶⁵. Cronstedt, a Swedish mineralogist, first characterized these structures in 1756, terming them zeolites, a term with Greek roots meaning ‘boiling stones’, because of their inherent ability to give up water upon heating⁶⁵. Many natural zeolites can be produced synthetically, while additional structures, with no natural occurrence, have been synthesized and are characterized as zeolites based on their structures, such as zeolite-A produced by Linde Corporation⁶⁵.

A few common zeolite materials employed in membranes include MFI-type, sodalite (SOD), and Linde Type A (LTA). Zeolite ZSM-5 (MFI)—the most commonly applied zeolite in membranes—is composed of a unit cell with the chemical formula Na_nAl_nSi_{96-n}O_{192~16H₂O}(*n*~3)⁶⁵. The MFI structure contains straight channels in one direction and perpendicular sinusoidal channels that are not interconnected⁶¹. The drawback of employing MFI-type zeolites in porous membranes is that the crystals must be oriented with respect to the permeation direction. The hydrated form of SOD, referred to as hydroxyl sodalite⁶⁵, has also

been applied in membrane materials ¹⁰. This mineral has the chemical formula $\text{Na}_6\text{Al}_6\text{Si}_6\text{O}_{24}\cdot 8\text{H}_2\text{O}$ ⁶⁵. Sodalites are not mineralogically defined as zeolites, but feldspathoids because in nature salt molecules are contained in their frameworks. The SOD cage, often referred to as the β -cage, is quite common to zeolite structures and when crystalline networks are created with this cage structure zeolitic properties are exhibited. One common example is the zeolite-A (LTA) unit cell, defined by the chemical formula $\text{Na}_{12}\text{Al}_{12}\text{Si}_{12}\text{O}_{48}\cdot 27\text{H}_2\text{O}$ ⁶⁵. The LTA structure is composed of SOD cages (β -cages) connected by truncated cubo-octahedron (α -cages), forming an interconnected cage structure. The interconnected inner channel in LTA offers the opportunity for simplified membrane fabrication since crystal alignment is unnecessary.

Pore size and framework density are the primary factors of concern when considering zeolites for water separations; pore size determines ion selectivity and framework density determines water permeability. Atoms other than Si and Al can be substituted into the cage structures of zeolites via ion exchange to imbue alternate charge and structural properties. Since the ability to act as a molecular sieve is due to the channel widths, changing the atoms in the framework, and thus the channel widths, will change the sieve properties ⁶⁶. Additionally, both the ion and water molecule mobility through a zeolite depend upon the relative density of the framework structure; open porous structures will facilitate less hindered transport ⁶⁵. This is indicated by the framework density, defined as the number of Si or Al atoms per 1000 Å. Framework densities (normalized for ideal Si frameworks) are 18.4, 16.7, and 14.2 for MFI, SOD, and LTA, respectively ⁶⁷, implying that LTA would be expected to have the largest water mobility.

The Si:Al ratio of a zeolite cage is the most important factor affecting chemical stability, hydrophilic properties, and occurrence of inter-crystalline defects ⁶⁵ –all primary factors of

concern when engineering selective and robust water treatment membranes. An increase in Si:Al ratio implies a decrease in the overall surface charge on the framework. The MFI-type zeolites are capable of a large range of Si:Al ratios, from approximately 30 in the ZSM-5 form to nearly pure Si for the isomorphous silicate type MFI. Noack et al. find that as the Si:Al ratio decreases in MFI-type zeolites water permeability and selectivity for water increase; however, defects simultaneously increase until a point where selectivity is compromised⁶³.

Separations in zeolitic materials occur primarily through molecular sieving, competitive adsorption or ion exchange¹⁰. Ions with small hydrated radii diffuse more quickly through zeolite pore structures. Cationic adsorption occurs onto the negatively charged surface of zeolite membranes, and may enhance diffusion by establishing a charge gradient. Initially, adsorption occurs onto the pore walls. Inter-crystalline molecular sieving occurs when the electrical double layers of these adsorbed ions overlap and inhibit the passage of charged ions⁵⁵⁻⁵⁶. Hydrophilic zeolite membranes previously applied for gas separations are composed of a loose, thick zeolite film through which separation occurs⁶⁸⁻⁷¹. However, the new RO membranes being developed require an ultra-thin, dense layer and so pains must be taken to form nanoscale zeolite coatings to produce membranes with permeability on par with polymeric RO membranes.

Li et al. apply MFI-type zeolite membranes (thickness $\sim 3 \mu\text{m}$) for RO desalination (with 0.1 M NaCl feed solution at 2.07 MPa)⁵⁵. Water flux is $0.112 \text{ kg}\cdot\text{m}^{-2}\cdot\text{h}^{-1}$ with 76.7% Na^+ rejection. The membrane is also challenged with a complex solution, more reminiscent of real RO feed waters, and the resulting water flux and rejection are lower ($0.058 \text{ kg}\cdot\text{m}^{-2}\cdot\text{h}^{-1}$ with Na^+ rejection of 58.1%). The reduced rejection is attributed to double layer compression within intercrystal pores of the zeolite material due to the high ionic strength of the feed solution. Another study with similar MFI membranes reports higher flux and rejection values (>95% of

Na⁺ ions)⁵⁶. Higher trans-membrane pressure increases water permeation and decreases ion permeation, resulting in better separation performance. Higher operating temperature increases both water and salt permeation, but having a larger impact on salt permeation. This is due to the reduced viscosity of the feed solution and increased diffusivity of water molecules and salt ions⁵⁵. The effect of temperature is consistent with that observed for traditional polymeric RO membranes, absent the effects of polymer swelling at higher temperatures⁷². While these membranes served as a proof of concept, higher water flux and salt rejection are both needed for MFI-based RO membranes to be commercially viable.

Duke et al. prepare MFI-type membranes for seawater desalination via template-free secondary growth⁵⁷. Zeolite films are formed over alumina supports by dip coating in a silicalite suspension and grown under hydrothermal conditions. This method improves control over membrane formation and produces fewer defects by decoupling the deposition and crystal growth steps. Alumina content should influence surface hydrophobicity and charge⁶³; however, in this study surface charge did not vary with Si:Al ratio⁵⁷. In RO mode (with 0.5 wt.% sea salts at 700 kPa) rejection is highest (50%) in an alumina-free silicate membrane due to strong electrostatic shielding of Na⁺ ions by the monopolar surface, which maintains the ideal double layer for this application. Because the Si:Al ratio allows for tuning of the surface properties and the resultant electrostatic double layer such membranes could also be tuned for specific ion-selective applications, but further work is needed to fully understand the connection between zeolite chemistry and membrane performance.

Liu et al. form an α -alumina supported MFI-type zeolite membrane via *in situ* crystallization on the inner surface of tubular ceramic membranes for the removal of organics from produced water⁶¹. In RO (with 0.1 M NaCl solution at 2.76 MPa) the membranes produce

a water flux of $0.35 \text{ kg}\cdot\text{m}^{-2}\cdot\text{h}^{-1}$ with Na^+ rejection of 99.4%. Ion separation occurs via size exclusion of hydrated ions as well as Donnan exclusion at pore entries. When tested for produced water treatment the coated membranes exhibit a water flux of $0.33 \text{ kg}\cdot\text{m}^{-2}\cdot\text{h}^{-1}$ with an organics rejection of 96.5%. With non-electrolyte solutions zeolite membrane selectivity is dominated by molecular sieving and so very different rejections are seen for high and low dynamic molecular size compounds. This work produced high salt rejections, but higher permeability must concurrently be achieved for practical application of these zeolite membranes.

Kumakiri et al. synthesize A-type zeolite membranes via hydrothermal synthesis atop a porous α -alumina substrate⁶². The substrate is seeded with crystals, dipped in an alumina-silica solution, and crystallized at 80°C for 5 hours. This process is repeated multiple times until reasonable separation performance is achieved. The membranes tested for performance in RO (with 10 wt.% ethanol feed solution at 1.47 MPa and 30°C) have pure water flux of $0.14 \text{ kg}\cdot\text{m}^{-2}\cdot\text{h}^{-1}$. The membrane selectivity for the ethanol/water mixture is 44%. Flux varies linearly with applied pressure, while selectivity is not significantly influenced. Most significantly, the membrane is mechanically stable up to pressures as high as $50 \text{ kgf}\cdot\text{cm}^{-2}$ (4.90 MPa). If performance of these membranes can be made competitive, their mechanical strength will make them ideal in high-pressure applications.

Kazemimoghadam formed composite polycrystalline hydroxyl SOD membranes atop high porosity tubular mullite supports¹⁰. The active SOD layer was formed through hydrothermal growth by coating the ceramic support with crystal seeds ($\sim 0.4 \text{ nm}$ diameter), dipping it in a homogeneous aluminate-silicate gel, and treating it at 100°C to allow crystal growth. The zeolitic membrane was tested for performance as an RO membrane for water treatment at variable trans-membrane pressures (100 to 300 kPa), feed temperatures (20 to 60

°C), and feed rates (0.5 to 3 L·min⁻¹). Flux increased with trans-membrane pressure, temperature (due to resulting lower viscosity), and feed rates (due to enhanced turbulence and hydrodynamic effects). High permeability was achieved ($\sim 10^{-12}$ m·Pa⁻¹·s⁻¹), on the order of current polymeric seawater RO membranes; however, no salt rejection data was published. If competitive selectivity can also be achieved, these materials may offer new opportunities for RO membranes in high temperature, pressure, and fouling applications.

Here we normalized zeolite membrane water permeability (from each paper reviewed above) by zeolite film thickness and performed the same calculation for permeabilities typically reported for commercial polymeric RO membranes to produce a Darcy permeability—defined as ‘specific water permeability’ in **Table 2**. While the permeability of the relatively thick (~ 3 -50 μm) zeolite films formed to date do not compare to ultra-thin (~ 50 -250 nm) TFC RO membranes, the specific water permeability compares favorably in some cases. Specifically, the SOD membranes produced by Kazemimoghadam et al.¹⁰ appear to have specific water permeability 3 orders of magnitude lower than commercial seawater RO membranes. If defect free zeolite films could be formed with thickness of 0.2 μm , the resultant membrane would have a water permeability of $\sim 0.5 \times 10^{-10}$, which is equivalent to a tight polymeric UF membrane. Obviously, this could make zeolite-based RO membranes a viable alternative material for high flux RO membranes, but with dramatically enhanced thermal, mechanical, and chemical stability. The challenge remains improving control over crystal nucleation and growth to ensure defect free ultra-thin zeolite films, which may require abandoning or substantially modifying traditional hydrothermal synthesis methods⁶².

Perhaps other fields should be examined for insight into new fabrication approaches. For example, Öztürk and Akata present a method for the oriented assembly of zeolite-A monolayers

for nanoelectronics applications ⁷³. E-beam lithography is combined with direct attachment to form patterned mono and double layers of zeolite-A nanocrystals (~250 nm) atop silicon wafers. A dilute PMMA solution is spun onto silicon wafer surfaces to form resist films (~400 and 850 nm thick). The films are pre-baked and then patterns are defined with e-beam lithography. Direct attachment is achieved by applying a zeolite powder to the silicon wafer, pressing the zeolites, and heating. The direct attachment method results in >90% coverage of the silicon surface, strong binding to the wafer, and strong organization with a cube face of each zeolite oriented parallel to the silicon surface. Coverage is limited by the degree of homogeneity of the synthesized nanocrystals and pattern resolution is limited by the size of the nanocrystal, implying further tunability of the procedure. While this method is likely too expensive for large-scale membrane fabrication, alternative low-cost direct attachment methods could be sought by examining the rich knowledge of inorganic thin films in other fields.

3.1.2. Reactive/Catalytic Ceramic Membranes

Reactive surfaces are applied in water treatment as semiconductor-based (e.g., titania, zinc oxide, ferric oxide) membranes activated by UV or sunlight to engage in redox processes for the degradation of organic compounds ⁷⁴⁻⁷⁷. The application of photocatalysis to water treatment was first discussed by Carey et al. in 1976 when they recognized the ability to degrade polychlorobiphenyls (PCBs) ⁷⁸. Semiconductor electronic properties are defined by having a filled valence band and an empty conduction band. In photocatalysis, semiconductors function by absorbing a photon of energy greater than their own bandgap energy, and creating an electron-hole pair via excitation of electrons from the conduction to the valence band ^{74, 79}. Photocatalysis occurs when a semi-conductor nanoparticle is irradiated with an amount of

energy, $h\nu$, greater than its own bandgap energy, ΔE (**Figure 3**). These electron-hole pairs will either recombine (in a matter of nanoseconds) or react with the surrounding media. The latter is only possible if the electron and/or hole can be trapped in a surface defect or captured by an appropriate scavenger in the bulk media⁸⁰.

In bulk semiconductor materials, only the hole or electron is normally available for interaction; however, in nanoscale materials both are available at the surface allowing for high efficiency interactions. The mechanism by which oxidation of organic molecules in water is initiated at the particle surface is not yet fully understood, but theories include direct oxidation by the electron hole (positron), indirect oxidation via hydroxyl radicals produced on the surface or in the solution, or some combination thereof⁷⁴. Suspended nano-photocatalysts are applied for remediation of contaminants; the suspended state provides maximum surface area and activity⁸¹⁻⁸³. The key drawbacks of suspended processes are nanocatalyst recovery and regeneration (or disposal) of spent material. A clever approach is catalyst coated magnetic iron oxide nanoparticles, which would enable magnetic recovery of nanoparticles⁸⁴⁻⁸⁵.

Catalysts coatings have been formed on polymeric membranes to create reactive surfaces for enhanced separations while eliminating the complexity of catalyst recovery⁸⁶⁻⁹¹. Titania nanoparticles are highly photoactive and exhibit antimicrobial activity under UV light^{79, 92}. Water purification systems based on photolytic disinfection are currently available. Inactivation of pathogens occurs by DNA damage from UV irradiation and through the production of reactive oxygen species, in particular hydroxyl radicals, which damage the cell wall of organisms (inactivation by cell lysis). Molinari et al. altered commercially available porous polymeric membranes with a titania layer, by filtering a nanoparticle suspension through and applying UV/vis irradiation and show elevated (4-Nitrophenol) photodegradation⁸⁶. Madaeni and Ghaemi

form “self-cleaning” RO membranes with the addition of titania nanoparticles; the cleaning, as well as elevated flux, witnessed upon UV application are attributed to two concurrent phenomena: photocatalysis and ultra-hydrophilicity⁸⁸. To curtail the inevitable titania-catalyzed UV degradation of the organic parts of the conventional membranes, Mo et al. prepare PSf-supported self-cleaning PA/titania membranes through interfacial polymerization, which contain a layer of silicon dioxide between layers of cross-linked PA and titania⁸⁷. Flux recovery after 15 h of operation (with water cleansing and UV exposure every 3 h) is greater than 98% for these photocatalytic membranes, significantly higher than standard water treatment membranes.

Titania nanopowders are also applied to ceramic membrane surfaces, such as silica⁹³⁻⁹⁴, alumina⁹⁵, zeolites⁹⁶, and activated carbon⁹⁷, which are more stable than polymers under UV light and in the presence of reactive oxygen species. Choi et al. report on reactive membranes with titania coatings atop alumina supports⁹⁵. Acid and surfactant are employed in the sol-gel process to tailor the resulting membrane morphology and produce high efficiency films and composites. XRD analysis reveals anatase crystals throughout the thin film with crystalline size of 8-10 nm. This size range is known to produce the optimum catalytic activity because it is the point where the blue shift occurs favoring surface recombination of electron-hole pairs and allowing for the maximum number of active sites per mass of catalyst⁹⁸. The structure of these films is highly porous and interconnected, enabling a high surface area for both adsorption and photocatalytic activity on the titania surface. Three dip-coatings are sufficient to create a defect-free skin layer (~0.9 μm thick); while more layers may be desirable to provide more active area, each layer also increases processing time and cost⁹⁵. The resulting membrane has water permeability of 6.71 L·m⁻²·bar⁻¹·h⁻¹ and molecular weight cut-off of ~12 kDa. The overall permeability is high considering that the Al₂O₃ substrate has a relatively low permeability (11.0

$\text{L}\cdot\text{m}^{-2}\cdot\text{bar}^{-1}\cdot\text{h}^{-1}$); even higher permeability may be achieved with more permeable ceramic supports (*e.g.*, mullite).

Catalytic ozonation is used for natural organic matter and organic compound removal in water and wastewater treatment; when combined with a catalytic metal oxide other substances can be degraded such as phenols, aromatic hydrocarbons, and humic substances⁹⁹⁻¹⁰². Karnik et al. exhibit the potential for catalytic membranes in combined ozonation/UF for disinfection byproduct removal¹⁰³. Commercially available ceramic membranes (composed of a mixture of alumina, zirconia, and titania) are coated via the layer-by-layer technique with iron oxide nanoparticles (4-6 nm diameter). The coating layer has negligible resistance, witnessed by unchanged membrane permeability. The membranes serve as catalysts in the ozone degradation of natural organic matter and disinfection by-products. Specifically, total trihalomethanes and halogenic acetic acids, are removed up to 90 and 85%, respectively. The proposed mechanism by which this degradation occurs is the decomposition of ozone on the iron oxide coating surfaces, enhancing hydroxyl radical production and, thus, degradation¹⁰⁴⁻¹⁰⁵.

The major limitation of photocatalysis is the fast recombination of the produced electron-hole pairs. This limits degradation of organics and inactivation of organisms with complex, dense cell wall structures, such as bacterial endospores that require longer exposure times^{79, 106}. When immobilized in membranes or in reactive surfaces, the active area is reduced, further limiting the photoactivity⁸⁵. Research shows that doping the particles with ions increases the photoactivity by separating the photo-induced charges and enhancing surface availability¹⁰⁶⁻¹⁰⁸. For disinfection applications, reactive oxygen species production that ultimately leads to cell wall compromise and cell demise is limited by the ability for the nanoparticle to maintain electron-hole pairs^{79, 109}. Krishna et al. coat multi-walled carbon nanotubes (CNTs) (known to

have large surface area and substantial photon-generated electron trapping capacity) with titania in order to delay recombination⁷⁹. Titania-coated CNTs display two times the inactivation rate of commercially available titania alone when tested on *B. cereus* spores.

Both zeolite and catalyst-coated membranes face similar challenges as have always faced ceramic water treatment membranes, that is, high manufacturing cost and low packing density relative to polymeric membranes. An additional hindrance of photocatalytic water treatment is the energy demand for irradiating the surfaces. To minimize this, solar induced photocatalytic surfaces have been investigated and applied^{91, 110}. Reactive surface-mediated photocatalysis for water treatment shows promise, particularly for the purpose of small-scale production where solar energy can be utilized.

3.2 Inorganic-Organic Membranes

3.2.1. Mixed Matrix Membranes

Mixed matrix membranes seek to take advantage of both the low cost and ease of fabrication of organic polymeric membranes and the mechanical strength and functional properties of inorganic materials. Zimmerman et al. first discussed mixed matrix membranes in the 1990's as a way to push the limitations of polymeric membranes for gas separations¹¹¹. Mixed matrix membranes including inorganic molecular sieves, such as zeolites and silicalite, embedded within a polymer matrix are employed to provide preferential flow paths for the target species to pass through¹¹²⁻¹¹⁵. The formation of continuous pathways of fast diffusion molecular sieves is theorized to occur at a volume fraction of filler material known as the 'percolation threshold'. At this point, target molecules can traverse the entire membrane cross-section through the filler^{111 116-117 118}. Above certain high volume fractions, defects tend to occur at the polymer-

filler interface limiting selectivity¹¹¹. Mixed matrix membranes present an opportunity for tunable water treatment membranes as well, through increased selectivity, targeted functionalities, and improved thermal, chemical and mechanical stability. The interplay between enhanced properties and defect formation must be balanced to derive positive benefits without compromising the integrity of the membrane.

Micron-sized inorganic particles are added to typical porous water treatment membranes to achieve enhanced selectivity, as well as other functional properties¹¹⁹⁻¹²³. Inorganic fillers in porous membranes are shown to inhibit macrovoid formation, increase pore interconnectivity, and improve mechanical strength¹²⁰. Such morphological and mechanical changes are desirable to avoid compaction of membranes during high-pressure separations. One example of this is the Zirfon® UF membrane, composed of an asymmetric PSf membrane with zirconia (ZrO₂) particles^{120, 122}. These membranes exhibit elevated permeability without compromise of particle retention^{120, 122}. The increased permeability is due to grain disturbances that occur when zirconia content is sufficiently high (~40 wt.%) during phase inversion formation of the top layer and increase pore distribution preferentially at the particle-matrix interface^{119, 122}. Aerts et al. report that as zirconia particle (~0.9 μm) content increases, elastic strain in Zirfon® UF membranes decreases, producing a more mechanically robust membrane¹¹⁹. Wara et al. dispersed ceramic alumina particles (~0.34 μm) in CA membranes during phase inversion, observing reduced macrovoids and, thus, increased selectivity¹²¹.

Today, mixed matrix membranes comprising nanoparticle fillers are emerging. These membranes are also referred to as polymer-nanocomposite membranes. Isodimensional nanoparticles are commonly used as nanocomposite fillers as they provide the highest surface area per unit volume. Nanoparticles for membrane applications are most often prepared through

the sol-gel process, which yields high purity samples and allows for control over size, composition, and surface chemistry¹²⁴⁻¹²⁵. Additional formation processes include: inert gas condensation, pulsed laser ablation, spark discharge generation, ion sputtering, spray pyrolysis, laser pyrolysis, photothermal synthesis, thermal plasma synthesis, flame synthesis, low-temperature reactive synthesis, flame spray pyrolysis, mechanical alloying/milling, mechanochemical synthesis, and electrodeposition¹²⁴. The favorable characteristics of nanoparticles can be exploited, similar to micron-scale inorganic particles, by directly including these particles in the casting solution.

Attention to nanoparticles for environmental applications has grown as their ability to preferentially disinfect, adsorb, and degrade pollutants in aqueous solutions is realized^{6, 124, 126-128}. Metal oxide nanoparticles, specifically magnesium oxide (MgO) particles, inactivate Gram-positive bacteria, Gram-negative bacteria, and spore cells¹²⁶. Alumina nanoparticles are useful as an adsorbent for nickel [Ni(II)] in aqueous solutions¹²⁹. Iron oxide, aluminum oxide, and titanium oxide nanoparticles adsorb heavy metals¹²⁴. Zero-valent iron nanoparticles have been applied for the removal of halogenated hydrocarbons, radionuclides, and organic compounds¹³⁰⁻¹³². Such nanoparticles pose an efficient alternative to activated carbon for water and wastewater treatment, with increased surface area and activity due to their nanoscale characteristics¹²⁴. Nanocomposite membranes have been researched for a variety of goals, including targeted degradation, enhanced flux and selectivity, decreased fouling propensity, and increased thermal and mechanical stability¹³³⁻¹⁴², while maintaining the ease of fabrication and low cost of their fully polymeric counterparts.

Targeted degradation can be achieved with addition of nanoparticles to polymeric membranes, particularly for reductive dechlorination processes¹⁴³⁻¹⁴⁵. Bi-metallic nanoparticles

(e.g., Fe/Pd, Fe/Ni, Mg/Pd) are applied for pollutant degradation, wherein the first zero-valent metal, often iron, serves as an electron donor and is actually responsible for degrading the target compound while the second metal serves as a catalyst to promote the reaction through hydrogenation¹⁴⁵⁻¹⁵⁰. Wu et al. employ CA supported palladium-coated iron nanoparticles (~10 nm; 1.9 wt.% Pd) formed through microemulsion to facilitate trichloroethylene decomposition and find that dechlorination is significantly enhanced¹⁴³⁻¹⁴⁴. Smuleac et al. show elevated degradation of 2,2'-dichlorobiphenyl with PVDF membranes containing similar Fe/Pd nanoparticles (~20-30 nm) formed through *in situ* polymerization¹⁴⁵. In the latter case, nanoparticles are formed within the polymeric matrix through an ion exchange with Fe²⁺, followed by reduction to Fe⁰, and deposition of Pd. *In situ* formation of nanoparticles inhibits agglomerate formation, a common issue when nanoparticles are dispersed in membrane casting solutions¹⁵¹. Good dispersion of nanoparticles is required to reap benefits for mixed matrix membranes; in some cases, membranes containing nanoparticle agglomerates perform worse than the unmodified membranes with no fillers at all¹⁵².

Particles that alter the surface properties of membranes can change separation performance and fouling behavior^{23, 134, 153}. Yan et al. add alumina nanoparticles (~10 nm; 19 wt.%) to casting solution during phase inversion of PVDF to form mixed matrix UF membranes¹³⁴. While pore density and size are not altered, hydrophilicity, water permeability, fouling resistance, flux recovery, and mechanical stability increase¹³⁴. Maximous and Nakhla prepare PES UF membranes with alumina nanoparticles (~0.48 nm; 0.01-0.05 wt.%) and find that membrane fouling and flux decline are reduced¹³⁵. Fan et al. add polyaniline (PANI) nanofibers to commercial UF membranes (1-15 wt.%) and find increases in water permeability, selectivity, and surface wettability¹³⁶⁻¹³⁷. Antifouling nature improves and flux recovery increases (to as

high as 90%) with particle additions in the blended membranes¹³⁶. Furthermore, flux recovery could be achieved with a simply water cleanse, implying that adsorption to these improved surfaces is much weaker than to unmodified membranes¹³⁷.

Particles with antimicrobial properties can help reduce biofouling of membranes¹⁵⁴. Silver nanoparticles are excellent bacteriocides^{138, 155-157}. Silver nanoparticle coatings are now widely applied as antibacterial safeguards in many consumer products¹⁵⁷. Morones et al. study the activity of nanoscale silver particles embedded in a carbon matrix towards four types of Gram-negative bacteria and find that all four are inactivated due to interaction with the silver nanoparticles¹³⁸; however, only those particles freed from the carbon matrix are able to interact with the cell membranes, enter the cells, and effectively inactivate them. Biofilm formation is successfully reduced in nano-silver containing membranes due to the successive release of ionic silver over the lifetime of a membrane¹³³.

In order to ensure sustained ion release, silver nanoparticles incorporated in membranes must be fully reduced to the zero-valent state¹⁵⁸. Taurozzi et al. find that when PSf membranes are formed with silver nanoparticles included in the casting solution—both following *ex situ* reduction of the nanoparticles prior to addition to the casting solution and with *in situ* reduction during casting—water permeability increased, with negligible reduction in solute rejection¹³³. Enhanced performance is attributed to macrovoid broadening and increased pore size and pore density due to the presence of nanoparticles. Because nanosilver dissolves rapidly in water, long-term testing is needed to quantify the lifetime of these membranes and to understand the impacts of defect formation due silver dissolution.

Mixed matrix membranes have been formed with the addition of nanotubes^{34, 159-160}. Carbon nanotubes exhibit antimicrobial activity¹⁶¹; thus, presenting an opportunity for improved

disinfection or antifouling membranes. Bundling is often an issue, especially with single-walled CNTs, due to the van der Waals interactions between nanotubes and the fact that they are insoluble in water and organic solvents; this hinders the application for large scale fabrication of membrane materials¹⁶². Lin et al. recommend functionalizing CNTs with polymer groups that are structurally similar to the bulk polymer matrix to aid nanotube dispersion and homogenous membrane properties¹⁶⁰.

Choi et al. cast multi-walled CNT/PSf mixed matrix membranes by nonsolvent induced phase inversion³⁴. Nanotubes are pretreated with acid to aid in dispersion throughout the solvent. Surface hydrophilicity of the membranes increases with the presence of CNTs due to the carboxylic acid groups that form on CNT surfaces during acid pretreatment. Pore size increases with nanotube additions up to 1.5 wt.% and then decreases, becoming smaller than pure PSf at 4 wt.%. Water permeability and rejection, however, increased with nanotube additions as high as 4 wt.%, likely because the improved hydrophilicity and resulting anti-fouling ability plays the dominant role in membrane performance. Brunet et al. formed nanotube/polymer membranes by dispersing multi-walled CNTs (4 wt.%) throughout a PSf/PVP polymer matrix via phase inversion¹⁵⁹. PVP seemed to aid in the dispersion of CNTs throughout the membrane casting solution. Mechanical stability (indicated by the degree of elongation to failure) is enhanced in the mixed matrices with well-dispersed nanotubes; however, the presence of CNT aggregates seems to reduce stability. The blended membranes did not display the desired antimicrobial activity because the contact between organisms and the CNTs stabilized in the polymer matrix is not sufficient to enable inactivation. Future applications may attempt to expose CNTs to solution for antimicrobial applications.

Inorganic fillers additionally enhance the thermal and mechanical stability of polymeric membranes by reducing the impacts of heating and membrane compaction. Compaction occurs during the initial stages of membrane operation, resulting in irrecoverable flux decline¹⁶³. The majority of compaction is known to occur in the bulk macrovoid region of asymmetric membranes¹⁶⁴ and so adding mechanically strong fillers to this region is thought to assist in reduced structural losses. Ebert et al. demonstrate increased stability of poly(vinylidene fluoride) (PVDF) membranes when titania nanoparticles are included as inorganic fillers in the phase inversion casting solution¹⁶⁵. Filled membranes exhibit higher thermal stability (as witnessed by minimal change in pore distribution following heat treatment) and less compaction (as seen by minimal structural changes after pressure application in the filled membranes). Calculations show an 83% decrease in pore volume in pure PVDF membranes, but only a 17% decrease in PVDF/titania membranes following compaction¹⁶⁵. In another study, silica and zeolite nanocomposite-PSf supported RO membranes are shown to experience less compaction than pure PSf supported membranes¹⁶⁶. In general, the nanocomposite-PSf supported membranes have higher initial water permeation and less flux decline during compaction. Electron microscopy images verify that the nanocomposite-PSf supports resist the deleterious impacts of compaction by maintaining open surface pores better than the pure PSf supported RO membrane.

Mixed matrix membranes can also be formed by dispersing polymeric structures within inorganic matrices. Arkas et al. synthesized organo-silicon dendritic networks within a porous ceramic membrane and showed the resultant filter was effective at removing toxic polycyclic aromatic compounds from water¹⁶⁷. Dendrimers are polymers with a high level of branching and symmetric structure of central core, repeating polymer units, and terminal functional groups. While dendritic polymer synthesis is more tedious than conventional polymers, the tunable

functional groups and tendency to form nanocavities make them desirable for functional membrane applications. The filters are capable of reducing polycyclic aromatics in water to a few ppb. The filters are also regenerated by acetonitrile washing thanks to the chemical stability of the ceramic backbone.

Nanoparticle-containing mixed matrix membranes, *a.k.a.*, nanocomposite membranes, have the potential to provide novel functionalities, enhanced performance, and heightened stability while maintaining the ease of membrane fabrication. While nanoparticle mixed matrix membranes are not yet commercially available, the micron-scale predecessors would seem to have paved the way for advances in this technology. As industrial-scale nanoparticle production grows, costs of these materials will come down and many of the research level innovations may make their way into the marketplace.

3.2.2. Thin Film Nanocomposite Membranes

Nanoparticle additions have been made to the thin films of TFC RO membranes in order to take advantage of the properties of the nanomaterials. Addition of nanoparticles to interfacial polymerization processes or surface attachment via self-assembly has introduced the concept of thin film nanocomposite (TFN) membranes, which offer potential benefits of enhanced separation performance, reduced fouling, antimicrobial activity, and other novel functionality¹⁶⁸⁻¹⁷³. As with TFC membranes, TFN membrane performance can be fine-tuned with nanoparticle additions to the support membrane (see mixed matrices, **Section 3.2.1**), the coating film, or both.

Zeolite nanoparticle-based TFN RO membranes attempt to leverage the molecular sieving properties of zeolites^{168, 173}. By casting molecular sieves in the thin film of an RO membrane, where diffusion controls the transport process, the goal is to essentially reach the

percolation threshold in the dense selective layer with an individual particle (**Figure 4**). Jeong et al. cast zeolite-polyamide thin films atop PSf support membranes by dispersing zeolite nanoparticles in the TMC solution prior to interfacial polymerization¹⁶⁸. Water permeability of zeolite TFN membranes increases as much as 80% over identically cast TFC membranes at the highest TFN particle loading (0.4 wt.%), with rejections consistently above 90%. Pure water permeability increases even for pore-filled zeolites, although permeability increases more for pore-opened zeolites supporting the role of molecular sieving. These results appear to imply a combination of effects contribute to the permeability enhancement born out of zeolite fillers.

Lind et al. similarly cast TFN membranes also containing LTA nanoparticles (0.2 wt.%) in the thin film through interfacial polymerization and characterized membrane structure, morphology, and separation characteristics¹⁶⁹. The presence of zeolite nanoparticles results in higher permeability, greater negative surface charge, and thicker membranes regardless of particle size used (97, 212, and 286 nm). Larger nanoparticles produce membranes with highly favorable surface properties, while smaller nanoparticles increased permeability more by increasing the characteristic pore size. All TFN membranes reported are less cross-linked than pure polyamide TFC counterparts, suggesting another potential mechanism by which TFN membrane permeability is enhanced. This work implies that the addition of nanoparticles can be tailored to particular membrane applications with the selection of nanoparticle size and type.

Later, TFN membranes were cast by Lind et al. by including sodium- and silver-exchanged LTA nanoparticles (~140 nm; 0.4 wt.%) in the PA polymerization reaction¹⁷³. Increased pure water permeation is found in both TFNs, with more significant increases, as much as 66%, with silver zeolites; rejection (tested with NaCl and PEG) is not affected. Silver-zeolites not only provided more hydrophilic surfaces, but also actively inhibit biofouling due to the

antimicrobial nature of nanosilver. Lee et al. prepared composite PA thin film NF membranes with titania (~60 nm) nanoparticles in the skin layer through interfacial polymerization¹⁷⁰. As titania concentration increases towards 5 wt.%, water flux increases and decreases salt rejection, suggesting significant defects formed in the nanocomposite coating film.

Carbon nanotubes have attracted attention for novel environmental applications. Brady-Estévez et al. demonstrate the use of CNTs for the removal of viral and bacterial pathogens from water at low pressure inputs¹⁷⁴. A thin coating of bundled single-walled CNTs (maximum gap ~0.3 μm) is overlaid on the surface of a PVDF microporous membrane (5 μm pore size). After passing water through the filter all *E. coli* cells (~2 μm) are removed, likely due to size exclusion. More importantly, a fluorescence-based viability test proves that nearly 80% of the bacteria are inactivated after 20 min contact time (an 8-fold increase over the uncoated microporous membrane). This result is confirmed with a metabolic activity test that finds only 6% of the *E. coli* cells are metabolically active following interaction with the filter. Viral pathogen removal is exhibited by passing a suspension containing a model virus, MS2 bacteriophage (~27 nm), through the filter. Size exclusion is not enough to explain the virus removal seen, even with the presence of the nanoporous coating. Results of viral inactivation by the CNT-coated filter are conclusive, yet vary with CNT layer thickness indicating a lower limit of contact time required for inactivation. Full virus removal (5-7 log removal) is observed with a 6 μm skin layer; 3.2-log removal is seen with a thin 2 μm layer. Such uses of CNTs offer an exciting opportunity for use in disinfection and water filtration.

Enhanced hydrophilicity, and thus, reduced fouling is a goal of many TFN studies. Luo et al. produce PES UF membranes dip-coated with titania nanoparticles and find contact angle reduction from 39.6 to 19.2°¹⁷⁵. The same group cast films with controlled titania contents (5,

10, and 15 wt.%) and find the largest reduction in contact angle at 10 wt.% (from 79.6 to 41.2°); at the higher 15 wt.% contact angle reduction dropped off (to 73.8°) possibly because of nanoparticle agglomeration¹⁷². This beneficial breakpoint points toward the existence of optimum particle loading depending on starting materials. Bae et al. form titania nanocomposite polymer membranes through electrostatic self-assembly and again find reductions in fouling, including reductions in initial sharp flux decline and eventual irreversible fouling¹⁷¹. It is found that pore size and water permeability slightly decrease¹⁷¹, but depending on application the anti-fouling capacity may outweigh this loss.

Here, we predict the performance of nanocomposite thin films using a Maxwell mixing model and the relative permeabilities of the filler nanoparticle and thin film polymer coupled with the fractional content of each. Theoretically, the permeability of TFNs containing impermeable nanoparticles (e.g., titania nanoparticles) decreases, while the permeability of TFNs employing permeable nanoparticles (e.g., SOD-zeolite nanoparticles) increases (**Figure 5**). Any nanoparticle with water permeability higher than that of the polymer matrix can increase the permeability of the resulting nanocomposite membrane by providing preferential flow paths through the cross-section. The filler fraction required for reasonable enhancements will depend upon the intrinsic permeabilities of both phases. Conversely, impermeable nanoparticles can only reduce the water permeability of a membrane because they reduce the area available for permeation through the polymer film. However, impermeable fillers can increase membrane permeability through defect formation, which may also compromise solute rejection. This is a simple analysis, but the concept must be kept in mind as research continues on nanocomposite materials. For certain applications, a loss in permeability may be overcome by the benefits of super-hydrophilic or antimicrobial nanoparticles that significantly reduce membrane fouling, but

in general reduced permeability is not a desirable feature. Cost considerations are also important, while antimicrobial and zeolite nanoparticles are expensive, zeolite TFNs have shown higher flux at extremely low loadings such that the cost increase may be minimal.

3.3. Biologically-Inspired Membranes

3.3.1. Aquaporin Membranes

Aquaporins are the protein channels that control water flux across biological membranes. Agre et al. won a Nobel prize for discovering the first of these proteins, which they named Aquaporin-1 (AQP1), in 1993¹⁷⁶. This first characterized aquaporin is found widely in human tissues with the purpose of rapid, passive transport of water across cell membranes. Such transport channels exist in the cells of species in all three domains of life. A single trans-membrane protein is ~120 kDa in size, with a tetramer structure composed of four channels¹⁷⁷. These channels are responsible for the physiological plumbing of our bodies, including our red blood cells, our brain, and our kidneys. Water movement in aquaporins is mediated by selective, rapid diffusion caused by osmotic gradients¹⁷⁸⁻¹⁷⁹. The hourglass shape of AQP1, with selective extracellular and intracellular vestibules at each end, allows water molecules to pass rapidly in a single-file line, while excluding proteins^{178, 180}.

Zhu et al. produced a fundamental study to simulate water permeation in AQP1¹⁸¹. Two factors involved in water transport are defined: osmotic permeability, p_f , molecular movement due to concentration differences resulting in net mass transfer, and diffusion permeability, p_d , random movement of molecules resulting in no net transfer. In the theory, water molecules transport in single-file through a narrow aquaporin channel; a constant number of molecules are assumed to occupy the channel at all times and the water molecules are assumed to move

together in discrete translocations, or hops (**Figure 6**). In the case of diffusion permeability dominated movement, a “permeation event” involves the movement of two molecules between opposite reservoirs. This requires that a molecule moves all the way through a channel and is different than a hop. The ratio of p_f/p_d is, in fact, the number of effective steps a water molecule must move in order to permeate a channel.

The highly selective water permeability of aquaporin channels is an interesting concept when considering water treatment membranes. Biological lipid bilayers containing aquaporins transport water and maintain selectivity that far surpasses all commercial RO membranes. Single aquaporins transfer water molecules at rates of $2\text{-}8 \times 10^9$ molecules per second¹⁷⁷. Kaufman et al. predict that a membrane with 75% coverage of aquaporins could have a hydraulic permeability in the range of $2.5 \times 10^{-11} \text{ m} \cdot \text{Pa}^{-1} \cdot \text{s}^{-1}$, an order of magnitude higher than commercial seawater RO membranes¹⁷⁷.

Kumar et al. include Aquaporin-Z from *E. coli* bacterial cells in a polymeric membrane¹⁸². This aquaporin is selected based on the ability for high water permeation and high selectivity. In addition, it is easy to purify and multiply using a recombinant *E. coli* strain. A symmetric triblock copolymer with a high hydrophobic to hydrophilic block ratio is selected, reminiscent of a lipid-bilayer membrane. The resulting protein-polymer membrane demonstrates over an order of magnitude increase in water permeability over a purely polymeric membrane, as well as full rejection of glucose, glycerol, salt, and urea. These results demonstrate that aquaporins are functional for synthetic applications.

The transport across biological membranes is driven by an osmotic pressure (or salt concentration) gradient, rather than a mechanical applied pressure gradient as in industrial filtration processes. Kaufman et al. demonstrate supported lipid bilayers formed atop dense water

permeable NF membranes that can be operated under a mechanical driving force as RO membranes (**Figure 7**)¹⁷⁷. NF membranes are chosen as the support because of their high permeability and low surface roughness that allowed for minimal distortion of the lipid bilayer. Aquaporin solutions (of protein PM28, the integral protein of a spinach leaf plasma membrane) are deposited onto commercially available NF membranes (NF-270 and NTR-7450) via vesicle fusion. Electrostatic interactions are tailored to optimize surface coverage with the lipid bilayer; formation on NTR-7450 at pH 2 with a low ionic strength solution and with the NF membrane surface and the protein vesicles having opposite charges produces the best results. Full, defect-free coverage is implied by the decrease in permeability of the composite membrane (from ~ 30 to $\sim 2 \times 10^{-12} \text{ m} \cdot \text{Pa}^{-1} \cdot \text{s}^{-1}$). Further work must be done to further optimize the formation of such structures and their resulting permeability and selectivity; however, this work demonstrates the potential for incorporation of biological aquaporins into pressure-driven RO membranes in the future. At this time, aquaporin-based membranes are not commercially available due to the difficulties of attaining large quantities of proteins and producing large areas of membrane material, but research continues in this area. A synthetic approach to producing and purifying aquaporin samples in large quantities might improve practical implementation. Furthermore, techniques to simplify the fabrication and produce mechanically robust membranes will bring the promise of these materials to reality.

3.3.2. Vertically Aligned Nanotube Membranes

Nanotubes have attracted attention because of their many unique properties¹⁸³⁻¹⁸⁴. Carbon nanotubes exhibit a fast mass transport reminiscent of aquaporin water transport in which water transport is 2-5 times higher than theoretical predictions by the Hagen-Poiseuille equation

¹⁸⁵⁻¹⁸⁶, and gas transport is over an order of magnitude larger than Knudsen diffusion predictions ¹⁸⁶. The striking flow rate has been studied with molecular dynamic simulations and attributed to atomic smoothness and molecular ordering, in which water molecules are passed through CNTs in a one dimensional single-file procession ¹⁸⁷⁻¹⁸⁸. This finding implies significant advantages of aligned CNT membranes over conventional membranes through reduced hydraulic driving pressure, and therefore, lower energy costs; however, this will not be the case in desalination applications where productivity is limited by osmotic pressure via the ‘thermodynamic restriction’¹⁸⁹. Carbon nanotube-based membranes may also have longer lifetimes than conventional membrane materials due to the excellent mechanical properties that CNTs exhibit ¹⁹⁰⁻¹⁹¹.

When CNTs act as the selective layer they can form an array of high flux molecular sieves within a polymer matrix (**Figure 8**) at the surface of a membrane. Kim et al. fabricate aligned CNT/polymer membranes that allow for efficient gas separation processing; CNTs allow for increased selectivity and gas flux due to their intrinsic properties ¹⁹². Highly selective, high flux membranes provide a more efficient, lower energy option ⁷. It is the hope that water treatment analogues to these membranes will be produced with similar materials.

Most uniform, aligned nanotube arrays to date are produced through chemical vapor deposition (CVD) ¹⁹³⁻¹⁹⁸. Fornasiero et al. attempted to model and study biological porin ion transport with sub-2 nm diameter CNTs as surrogates ¹⁹⁸. Aligned CNTs are grown through CVD on a silicon surface and then encapsulated through conformal deposition of silicon nitride to form composite membrane structures. The CNTs are adapted by fixing negatively charged functional groups at the ends in order to mimic porin structure and the selectivity region at the openings, which dictates ion transport. Pressure-driven NF is coupled with capillary

electrophoresis for ion concentration analysis in the filtrate. Ion exclusion is found to be as high as 98%. The results show ion transport is dominated by Donnan type rejection based on electrostatic interactions between membrane surface charge and particle charge rather than steric effect¹⁹⁸.

Gao et al. grow dense arrays of titanium carbide crystal-filled, aligned CNTs (inner diameter 10-100 nm) atop a titanium substrate through CVD with a simultaneous solid state reaction¹⁹³. Choi et al. produce uniform (10 nm diameter) aligned CNTs atop nickel deposited silicon substrates through microwave plasma-enhanced CVD; it is found that the nickel thin film characteristics largely control the growth rate and resulting diameter and density of CNTs¹⁹⁴. Maeron et al. produce aligned CNT films (20-28 nm diameter; 20-35 μm thick) atop silicon chips through CVD with gaseous acetylene and nitrogen¹⁹⁷. Overall perpendicular alignment of multi-wall CNTs on the preformed substrate is seen and attributed to high nanotube density, although the individual nanotubes are curved. Yoshikawa et al. produce thin, narrow, uniform, vertically aligned CNTs (2.5-6.0 nm diameter; 20-90 μm length) atop commercial aluminum foil using catalyst-supported CVD¹⁹⁶.

Holt et al. produce gap-free sub-2 nm diameter aligned double-walled CNT membranes (1.3-2 nm pores determined by size exclusion) through an automated and reproducible microelectromechanical system fabrication, using catalytic CVD¹⁸⁶. Pore densities are as high as 0.25×10^{12} pores per cm^2 ¹⁸⁶, the highest example to date. Water flux through these CNT membranes is found to be at least 3 orders of magnitude higher than theoretical, Hagan-Poiseuille predictions¹⁸⁶. These nanoporous membranes offer opportunities for extreme selectivity, without compromising water permeation. While aligned CNT membranes show

promise, alignment via CVD is expensive, sensitive, and not yet applicable for large-scale fabrication.

Films of aligned CNTs have also been produced through self-assembly approaches^{192, 199-200}. Heer et al. accomplish this by drawing aqueous suspension of CNTs (~10 nm diameter; 1-5 μm length) through a 0.2 μm pore ceramic filter and then transferring the deposit to a Teflon surface¹⁹⁹. After rubbing the surface with Teflon or aluminum foil the tubes reorient perpendicular to the surface. The vertically aligned structure is confirmed by electron microscopy images. A magnetic alignment approach for macroscopic film formation, involving high pressure filtration of suspended single-walled CNTs in a magnetic field, is applied by Casavant et al. to produce (125 cm^2 of 10 μm thick) aligned CNT membranes²⁰⁰. Theoretical calculations are confirmed to show that the magnetic alignment was primarily a function of tube diameter, rather than magnetic field. Kim et al. prepare CNT/polymer composite membranes, having similar gas transport properties to nanotube composites prepared through CVD, by passing a single-walled CNT suspended solution through a PTFE filter in order to align nanotubes; a PSf coating is applied in order to maintain perpendicular orientation and impart mechanical strength¹⁹².

Srivastava et al. exhibit the potential for CNT filters in two important environmental applications: the separation of heavy hydrocarbons from petroleum during crude oil post-distillation and the removal of microbial contaminants from drinking water²⁰¹. Macroscale hollow carbon cylinders are produced with densely packed, radially aligned, micron-length multi-walled CNTs through the continuous spray pyrolysis method. To confirm the bio-adsorption of contaminants, namely *E. coli* (2-5 μm), *Staphylococcus aureus* (~1 μm), and the poliovirus (~25 nm), from drinking water, unfiltered biological suspension and post-treatment

filtrate are incubated in both solid and liquid media and then plated; biological growth is seen in the unfiltered samples, but none is found in the filtrate. These biofilters offer not only an efficient means for treatment, but also an economical means. Due to the strong mechanical and thermal stability, CNT filters can be cleaned (by ultrasonication and autoclaving) and reused, whereas conventional water filtration membranes are typically disposed off at the end of one use due to permanent damage from biofouling and inability to withstand cleaning.

A 2007 molecular dynamics simulation by Corry points out the importance of the type of CNT selected for membrane production²⁰². Results show that narrow CNTs with an “armchair” structure – those classified as (5,5) and (6,6)-type nanotubes – might completely reject ions due to the large energy barrier at the nanotube openings created by stable hydrogen bond formation. Larger (7,7)- and (8,8)-type nanotubes will not select against ions in this way. Water on the other hand, forms no stable hydrogen bonds with any CNT types and permeates rapidly. While extreme permeation enhancements are often predicted (as much as 3 orders of magnitude over current membranes), these predictions have been made assuming maximum coverage of CNTs per unit area, but it is not clear that such high packing densities are practically possible. Using the results of this simulation and assuming the CNT packing density achieved experimentally to date (with double-walled CNTs) by Holt et al.¹⁸⁶, Corry projects flux enhancements of 2-fold and 4-fold over a commercially available seawater RO membrane with (5,5) and (6,6) aligned CNT membranes, respectively,²⁰².

A comparison of the achievable performance of aligned nanotube membranes versus current polymeric seawater RO membranes is presented (**Figure 9**), similar to that shown for TFN membranes above, but here including permeability projections compiled by Corry²⁰² and maximum coverage demonstrated by Holt et al.¹⁸⁶. At a fractional content of 0.03% in an

impermeable matrix, a CNT membrane will exceed the commercially available SWRO standard. This limit is within the previously achieved range, but thus far no large-scale aligned CNT membranes have been fabricated. Carbon nanotubes promise mimicry of biological aquaporin channels, with a material producible in large quantities; however, fabrication of large areas of these materials stands in the way of commercial application. Both aquaporin- and CNT- based membranes are limited by their cost and lack of scalability; however, this was also the case for polymeric membranes 50 years ago, so the scale-up issues may be resolved over time if performance enhancements prove practically achievable.

3.3.3. Isoporous Block Copolymer Membranes

One advance aimed at solving the issue of scale up and manufacturing of membranes with uniform, aligned nanopores involves block copolymer self-assembly²⁰³. In 1994, François and his research team formulated an emulsion method whereby water droplets condense on a rapidly cooled polymer surface in a humid environment to create porous structures²⁰⁴⁻²⁰⁵. Water molecules arrange themselves on the surface and polymer precipitates around them. Finally, evaporation of the water droplets occurs, leaving a honeycomb pore structure. This idea is widely applied²⁰⁶⁻²⁰⁹, yet a full understanding of the molecular level activity has yet to be reached. Self-assembly, defined as the “autonomous organization of components into patterns or structures without human intervention²⁰³,” of block copolymers show promise for translating ‘bottom-up’ synthesis methods into large-scale manufacturing processes, which is needed for practical water treatment membranes.

Block copolymers are macromolecules composed of multiple block polymeric species with the ability to self-assemble into highly ordered structures when placed in a selective solvent

^{208, 210-212}. Block copolymer self-assembly provides the opportunity for narrow pore size distributions and high porosities, as well as sharp molecular weight cut-off. In self-assembly, the characteristic differences between blocks will cause separation into microphases during polymerization. An analogy can be drawn to the hydrophobic effect in which natural amphiphilic molecules, such as phospholipids, become ordered in water with a compact hydrophobic region surrounded by dispersed hydrophilic segments in order to reach a thermodynamically favorable arrangement ²¹². Similarly, when water is added to a system of block copolymers dissolved in an aqueous solution, the blocks will align with the hydrophobic ends precipitating and the hydrophilic ends remaining extended in solution ²⁰⁸. Furthermore, when any selective solvent is added to a solvent-nonsolvent system consisting of macromolecules of two distinct regions – one soluble, the other insoluble – a predictable arrangement will form based on the respective interactions of each polymer with the solvent ²¹².

The geometry of block copolymer nanostructures is determined by the molecular weights of the blocks and the ordering depends upon the concentrations of the blocks and the insoluble to soluble ratio ^{210, 212}. At a certain point, known as the critical aggregation concentration (CAC), the blocks will go from dispersed unimers to self-assembled isotropic structures ²¹². The ratio of the insoluble volume to the total volume occupied by the copolymer can generally determine the resultant structure the macromolecule will attain in solvent. If the insoluble volume is less than 33% of the total volume, spherical micelles (hydrophobic core with a hydrophilic corona) will form (**Figure 10**), between 33 and 50% cylindrical micelles form, and then up to the theoretical point of 100% insoluble fraction a membrane (composed of two monolayers) will form ^{210, 212}. Reverse micelles can also be formed with a hydrophilic inner core when nonsolvent, rather than a solvent, is added to the system ²¹³⁻²¹⁴. Additionally, these same ideas can be expanded beyond

diblock copolymers to multi-block systems²¹². By varying the concentrations and conditions under which self-assembly occurs various structures can be formed, including densely packed cylindrical pores ideal for water separation membranes²¹⁵. Techniques for producing such membranes involve phase inversion (which is successful, but expensive as the block copolymer is used for both the support and the selective layers), shear aligning (which typically produces thicker than desired films), and controlled substrate-polymer interactions (which are effective, but difficult to control in large-scale production)²¹⁶. In theory, aligned cylinders formed through nanostructuring of block copolymers could enable a fully polymeric analog to aquaporin or aligned CNT membranes, providing an opportunity to take advantage of nanopore performance, while maintaining ease and economy of large-scale polymeric membrane fabrication.

Self-assembly for bottom-up structure formation can result in membranes containing defects due to the various factors²¹⁷. One particularly interesting characteristic of copolymers is that they are “soft” meaning that they tolerate a large amount of such imperfections and still assemble relatively homogeneously. While imperfections may be seen as a major limitation in some applications, for aqueous membrane materials where total homogeneity is not a requirement this soft nature poses processing and manufacturing advantages. Dove points out that while micellar assemblies are soft and may be reverted to unimers with a change in conditions, there is the opportunity to cause selective crosslinking²¹⁰, which enhances the mechanical, thermal, and chemical stability of the membranes^{5, 207}. The soft nature also means that minimal external fields – electrical or shear – will impact the arrangement²¹². This could have implications for auto-arranging of materials on demand and an opportunity for self-cleaning membranes.

Peinemann et al. demonstrate the ability to combine block copolymer self-assembly with conventional phase inversion to achieve highly ordered, asymmetric porous membranes composed solely of block copolymer materials²¹¹. This process is very complex involving both thermodynamic and kinetic factors: during fabrication, block copolymers will align in order to obtain a thermodynamically favorable, low energy arrangement. However, perpendicular arrangement is difficult to guarantee throughout the thickness of copolymer membranes. Predictions of arrangement must take into account the factors of solvent composition, selectivity, and concentration^{211, 217}. In their one step process, Peinemann's group achieves a non-ordered porous structure—typical of polymeric membranes—overlaid with a 200-300 nm thick dense layer of aligned nanocylinders, with a pore density of 240×10^{12} and an effective pore diameter of 8 nm²¹¹. Water flux through these membranes is $20 \text{ l} \cdot \text{m}^{-2} \cdot \text{h}^{-1}$ at 0.5 bar with 82% rejection of ~ 7 nm albumin²¹¹. One-step fabrication holds promise for large-scale production. Peinmann holds a patent for the process of block (di- and tri-) copolymer membranes for separation applications, including UF and NF²¹⁸.

Phillip et al. report fabrication of a 100 μm thick, nanoporous block copolymer membrane with tunable selectivity, narrow pore size distribution (~ 14 nm), and a 40% void fraction²¹⁹. Membranes are formed using the “doubly reactive” block polymer²¹⁹ combined with selective etching of a single block²²⁰. The process allows for simplified alignment because the block polymer acts as a structural template during crosslinking²¹⁹. Water permeability was lower than predicted, but did increase linearly with applied pressure. If the membrane thickness is decreased to 0.5 μm , the membrane would become competitive (at $5600 \text{ gal} \cdot \text{ft}^{-2} \cdot \text{day}^{-1}$ with a 200 kPa pressure drop) with typical membranes formed through phase inversion. Flux was found to decrease with pH of permeate by as much as 60% (from pH 2 to 12). The molecular weight

cut-off of the membrane was found to correlate with the molecular weight of the etchable block employed, implying further tuning of such membranes for target separation applications is possible.

Another route for employing block copolymers is to form a thin layer atop a sacrificial substrate and then transfer it to a functional support layer. Using copolymers for upper layer alone provides large cost savings and may pose an advantage for large-scale production²²¹. This is fiscally appealing as block copolymers are more costly than typical polymers used in membrane formation. Yang et al. created a NF membrane, with an 80 nm thick top layer of 15 nm diameter cylindrical pores atop a (250 μm) conventional support, capable of filtering viruses²²². This approach holds benefits of a highly tunable top layer, with pores ranging from 10 to 40 nm, and the reliability of conventional supports. The process is limited in its scalability because of the difficulty of transferring films without damage to the porous structure.

To avoid complications in the transfer step, self-assembly of block copolymers directly atop functional supports has been attempted. Here, separate tailoring of the support and selective layers allow for novel membrane fabrication. Fierro et al. employ block copolymer membranes in direct formation atop a conventional porous support and study the impact of polymer selection on physical characteristics²⁰⁶. To predict the assembly outcome the affinity of the substrate for each block employed must be considered, as the substrate tends to be selective towards one of the block units. Orientation of the self-assembly is strongly impacted by the surface composition and roughness on which assembly is initiated^{206, 223}. Phillip et al. fabricate membranes with a 4 μm thin film of monodisperse, 24 nm diameter vertically aligned, hexagonally-packed cylinders directly atop a commercially available microporous support membrane in a single step of controlled evaporation. Ultraviolet light (254 nm) is applied to ensure full adhesion between the

copolymer film and commercial support layer. UV also promotes crosslinking between micelles. A single block is selectively etched to form the open pores. Water permeability in UF testing is lower than expected likely because the pores were not aligned or etched through the full length of the thin film. Membrane rejection of 100 kDa polyethylene oxide is over 93%. This evaporative self-assembly method provides an opportunity for economical scalability by using a simple fabrication process and selecting a commercially available, mechanically robust support layer. In addition, the dual material membrane means that characteristics of support structure and thin film selectivity can be independently fine-tuned with respect to applications.

Li et al. employ a homopolymer (i.e., polyacrylic acid) to guide self-assembly of their diblock copolymer system. Ordered nanoporous films are formed directly atop various polymeric and ceramic porous supports via spin coating followed by solvent evaporation²²⁴. The addition of the homopolymer allowed for the desired pore structure to be achieved under various casting conditions (humidity, substrate, solvent, film thickness) with no need for thermal or solvent treatments. The homopolymer is then selectively removed. In NF tests, liquid permeability ranges from 1.2-1.6 L·m⁻²·bar⁻¹·h⁻¹, increasing with homopolymer content. Molecular weight cut-off of the membranes is determined to be 400-500 Da (defined for 90% rejection of polyethylene glycol). Interestingly, while the homopolymer is necessary to attain self-assembly of cylindrical pores, it can be removed with a simple water soak without changing the pore structure implying that it is not chemically stable in the self-assembled structure. The use of such homopolymer additives presents an opportunity for simple and scalable fabrication of membranes with highly tunable performance characteristics.

Multiblock or star copolymers enable more predictable alignment atop commercial substrates by compensating for the discrepancy in substrate affinity between blocks with a

symmetric arrangement. It is predicted that more complex structures result in a reduced thermodynamic loss due to conformational entropy and provide an opportunity for more specific nanoscale tuning of structures^{204, 206, 225}. Stratford et al. simulate a method for producing what they termed Bijels (bicontinuous interfacially jammed emulsion gels), which are self-assembled three dimensional structures formed through liquid-liquid interfacial sequestering of particles to form a matrix²²⁵. Stratford's predicted kinetic path is applied, using the emulsion technique first presented by François' group²⁰⁴, by Chen's group to prepare tunable porous structures with self-assembling ABA triblock amphiphilic copolymers into a highly ordered honeycomb film²²⁶. With honeycomb structures it is consistently found that the hydrophobic-hydrophilic ratio of the blocks determines the ordering and size of pores; namely, the regularity of pores decreases with increasing hydrophilic block content and pore diameter increased with increasing hydrophobic block length^{205, 208, 226}. The ability to tune pore size with hydrophobic block selection and water content²⁰⁸ is intuitive based on the proposed formation path in the emulsion technique²⁰⁴. Beattie et al. form similar matrices through reversible addition-fragmentation chain transfer^{205, 227}. Kabuto et al. experiment with honeycomb formation using a commercially available polymer and create an asymmetric membrane with a top layer of ordered 3 nm pores²⁰⁷. Upon cross-linking the honeycomb surface inverts from hydrophobic to hydrophilic, allowing for filtration through the pores²⁰⁷. As a further understanding of the mechanisms at play in formation is reached, this highly ordered and predictable membrane formation process will gain exposure in the membrane field.

Membranes with aligned nanopores formed by self-assembly of block copolymers during phase inversion offer a significant promise as fully polymeric analogs to aquaporin and aligned CNT membranes. In principle, these structures could be fine-tuned for water filtration

applications, but may also serve as more ideal support substrates for high-flux, high-selectivity forward and reverse osmosis membranes for desalination and osmotic power production.

4. DISCUSSION

The aims of nanotechnology-enabled water treatment membranes encompass many different goals and performance enhancements. Chemically stable ceramic membranes have been modified for high selectivity NF and potentially RO membranes with zeolite thin film coatings. Self-cleaning and catalytic membranes have been formed with antimicrobial and photocatalytic nanoparticle coatings. Mixed matrix membranes offer enhanced separation performance, fouling resistance, and mechanical stability for filtration applications and as support membranes for TFC or TFN membranes. Thin film nanocomposites seek to produce compaction resistant membranes with silica, fouling-resistant membranes with nanosilver, self-cleaning photocatalytic membranes with titania nanoparticles, or highly permeable and selective membranes with molecular sieve zeolites. Biologically inspired membranes—aquaporins, aligned CNTs, and block copolymers—seek to simultaneously improve selectivity and permeability. Each of these innovative materials concepts promises unique performance enhancements and each has unique hurdles to overcome before it is commercially viable.

Here, we ranked the aforementioned membrane nanotechnologies based on two categories: (1) performance enhancement and (2) state of commercial readiness and three sub-categories within each category. Performance sub-categories considered potential enhancements in membrane (a) permeability, (b) selectivity, and (c) robustness over the current state-of-the-art. Robustness encompasses chemical, mechanical, and thermal stability as well as fouling resistance and enhanced cleanability. Commercial readiness sub-categories included (1)

anticipated material costs, (2) manufacturing scalability, and (3) apparent time to commercialization. Those membrane nanotechnologies that promise significant performance improvements over current industry standard membranes were ranked positive, those that offer lower performance were ranked negative, and those that did not change the performance (or if no information was available) were given a neutral score. Membrane nanotechnologies close to commercial reality, cheaper than the state-of-the-art, and capable of being produced using existing membrane manufacturing infrastructure were ranked positive, those judged oppositely were ranked negative, and those not promising change in the specific metric (or if no information was available) were given a neutral score. The scores given to each membrane nanotechnology reviewed above are shown in **Table 3**.

Reactive/catalytic and zeolite coated ceramic membranes promise improved performance with marginal changes in current inorganic membrane fabrication methods (i.e., low cost impact). However, these innovations are not out of the laboratory yet and will most likely be limited by the same factors that have always limited ceramic membranes—high capital cost and low membrane area density relative to polymeric membrane equivalents. Ceramic membranes with reactive surfaces have been proven effective in laboratory studies, but more research needs to be done to produce commercially viable systems. While negligible improvement to productivity for such membranes has been shown, selectivity can be increased with catalyzed degradation of target compounds. Additionally, reactive surfaces have been shown to be biofouling resistant and so an enhancement in robustness is promised. For these reasons, the ratings of 0 (no improvement) to productivity and +1 (slight improvement) to both selectivity and robustness are assigned. These membranes show no major changes in commercial viability when compared to current ceramic membranes and so neutral ratings are applied in all categories

of time to commercialization. The materials and production cost roughly the same amount as current ceramics and the materials discussed here are between laboratory and pilot-scale testing, but none are known to be commercially available as of yet.

Zeolitic coatings promise the ability to tune the molecular selectivity of ceramic membranes. Thanks to the extreme stability of inorganic materials, these membranes may have a future in desalination and purification of challenging wastewaters (needs currently met primarily by polymeric membranes); however, the synthesis of zeolite films must be improved to obtain thinner layers and achieve competitive water permeability without sacrificing selectivity. In terms of potential performance enhancements, zeolitic coatings are given a –1 rating for productivity because currently these achieve lower flux than commercially available materials. These were rated neutral in terms of selectivity since rejections comparable to current membranes have been shown. These materials were given a +1 rating for robustness, however, because they pose a more chemically and thermally stable alternative to current membranes typically applied for high pressure and complex water separations. Similar to reactive/catalytic surfaces, zeolitic coatings are given neutral scores for commercial viability, with the exception of cost effectiveness. The materials to produce fully zeolitic coatings made presumably cost more than typical polymer membrane materials and ceramic materials and so a –1 rating is assigned.

Mixed matrix membranes and TFNs offer significant performance enhancements with minimal changes to current manufacturing processes. All inorganic-organic materials evaluated offer a significant productivity enhancement when tested against current ‘state of the art’ membranes. Mixed matrices and zeolite TFNs show no significant change to membrane selectivity; however, nanoparticle TFNs do show some decrease in selectivity due to defect formation and so these are given a –1 rating for selectivity. All inorganic-organic materials also

show an enhancement in robustness, through either compaction resistance or hydrophilic, anti-fouling surfaces due to the presence of filler materials, earning them a +1 rating for robustness. Mixed matrix membranes and nanoparticle TFNs both receive ratings of -1 for cost effectiveness due to the added cost of filler materials. Thin film nanocomposites containing zeolites, however, have been shown in the literature to improve on all aspects of performance using only small amounts of relatively inexpensive filler materials and so were rated neutral for cost effectiveness. All materials in this category are given a +1 rating for scalability since all can be produced through current polymeric membrane processes by simply adding nanoparticles to the casting or coating solutions. While mixed matrices have been seen at the laboratory scale only, earning them a neutral score for time to commercialization, early stages of TFN membranes are now commercially available, earning them a +1 score.

Biologically-inspired membranes all promise extremely high performance enhancements, but are currently far from commercial reality. Aquaporin-based membranes promise to revolutionize membranes with at least an order of magnitude increase in flux over the current membranes available, earning them a rating of +3 for productivity. Aligned nanotubes and isoporous block copolymer membranes have also been predicted and shown to reach extreme flux enhancements, earning them a +2 rating for productivity. All biologically-inspired membranes promise to alter the bounds of membrane selectivity with extremely narrow pore distributions. The regular morphology of these membrane materials earns them a +2 for selectivity. Both aquaporin and nanotube-based membranes show no significant changes in membrane robustness if cast within or atop polymeric matrices; however, at this stage pure block copolymer membranes tested are less mechanically stable than current polymeric membranes available. Both aquaporins and nanotubes are expensive to purify and have not yet been formed

in large membrane areas and so both receive a -1 rating for cost effectiveness and scalability. Aquaporins are difficult to attain in large quantities and few studies have shown the ability to form uniform coatings of protein membranes for industrial applications. Aligned CNT films have been produced uniformly, but only over small surfaces. At this point, both materials are in the laboratory production phase and so earn neutral scores for time to commercialization. Block copolymer materials are not significantly more costly than current polymeric membranes, particularly since research is moving towards using the specialized polymers for the selective layers only and so these receive a neutral score for cost. Because self-assembled block copolymer membranes can be formed through typical membrane fabrication processes with current infrastructure they earn a $+1$ for scalability. Aligned block copolymer membranes are in stages of early development and ideal polymer systems must still be found to achieve the outcomes promised, earning them a -1 for time to commercialization. However, if the polymerization conditions can be mastered so that fabrication of these structures can occur reliably and at large scales with minor changes to infrastructure, they will pose a promising, low-cost, fully polymeric counterpart to high performance aquaporin and CNT membranes. Biologically-inspired membranes promise the greatest separation performance enhancements; however, their cost and robustness are unproven and they appear most challenging to produce for large commercial applications. However, this was also the case for polymeric membranes 40-50 years ago and these scale-up issues can be resolved if the performance enhancements promised by these exiting materials prove practically achievable.

While each technology clearly has its own merits, an overall ranking is proposed here by summing the three scores from each category and plotting the total scores for performance enhancement against commercial viability (**Figure 11**). The ideal technology offers both

revolutionary performance enhancements and is already commercially available (upper right quadrant). Biologically-inspired membranes promise the greatest potential performance enhancements and are farthest from commercial reality, while zeolite TFN membranes offer moderate performance enhancement and appear nearest to commercial viability. The other materials offer noteworthy performance enhancement while remaining far from commercial reality. None of the membrane nanotechnologies fell in the optimal (upper right) quadrant of the chart, but this could change over time as biologically inspired membrane technology matures.

Readers should note that we propose this ranking methodology as a means to provoke critical thought rather than as an endorsement or indictment of any specific membrane nanotechnology. We realize limitations are inherent to any such ranking system. The most obvious limitation is that our assessment represents a ‘snapshot in time’ of the technology landscape, which is ever changing. While our intent is to provide an objective evaluation of the technologies, we realize that our ranking may be somewhat subjective. Regardless of the current ranking, each membrane nanotechnology concept described has the potential to revolutionize water treatment to varying degrees, but each material must be developed, matched to the ideal application, and fine-tuned to produce commercially available membranes.

ACKNOWLEDGMENTS

This publication is based on work supported in part by Award No. KUS-C1-018-02, made by King Abdullah University of Science and Technology (KAUST), in addition to the NSF Graduate Research Fellowship, UCLA Cota Robles Fellowship, and the UCLA Faculty Women’s Club Russell and Sallie O’Neill Memorial Scholarship.

REFERENCES

1. *Human Development Report 2006. Chapter 4*, United Nations Development Programme (UNDP), 2006.
2. *Coping with water scarcity. Challenge of the twenty-first century*, United Nations (UN) Water. Food and Agricultural Association (FAO), 2007.
3. *Urban Urgency, Water Caucus Summary*, World Water Council (WWC), Marseille, France, 2007.
4. *Progress on Sanitation and Drinking-Water*, World Health Organization(WHO)/United Nations International Children's Fund (UNICEF) Joint Monitoring Programme for Water Supply and Sanitation, 2010.
5. M. Mulder, *Basic Principles of Membrane Technology*, Kluwer Academic Publishers, London, 1996.
6. M. Ulbricht, Advanced functional polymer membranes, *Polymer*, 2006, **47**, 2217-2262.
7. P. Bernardo, E. Drioli and G. Golemme, Membrane gas separation: A review/state of the art, *Ind. Eng. Chem. Res.*, 2009, **48**, 4638-4663.
8. R. E. Kesting, The 4 Tiers of Structure in integrally skinned phase inversion membranes and their relevance to various separation regimes, *J. Appl. Polym. Sci.*, 1990, **41**, 2739-2752.
9. R. R. Bhave, *Inorganic Membranes: Synthesis, Characteristics, and Applications*, Van Nostrand Reinhold, New York, NY, 1991.
10. M. Kazemimoghadam, New nanopore zeolite membranes for water treatment, *Desalination*, 2010, **251**, 176-180.
11. E. Hoek and A. Jawor, Nano-filtration separations, in *Dekker Encyclopedia of Nanoscience and Nanotechnology*, 2002.
12. J. Benito, M. Sanchez, P. Pena and M. Rodríguez, Development of a new high porosity ceramic membrane for the treatment of bilge water, *Desalination*, 2007, **214**, 91-101.
13. M. H. Hassan, J. D. Way, P. M. Thoen and A. C. Dillon, Single-component and mixed-gas transport in a silica hollow-fiber membrane, *J. Membrane Sci.*, 1995, **104**, 27-42.
14. R. Faibish and Y. Cohen, Fouling-resistant ceramic-supported polymer membranes for ultrafiltration of oil-in-water microemulsions, *J. Membrane Sci.*, 2001, **185**, 129-143.
15. R. Faibish and Y. Cohen, Fouling and rejection behavior of ceramic and polymer-modified ceramic membranes for ultrafiltration of oil-in-water emulsions and microemulsions, *Colloid Surface A*, 2001, **191**, 27-40.
16. S. Loeb and S. Sourirajan, *High flow semipermeable membrane for separation of water from saline solution*, US Patent, US3133132 (1964).
17. R. Kesting, *Synthetic Polymeric Membranes*, McGraw-Hill, New York, NY, 1971.
18. T-H. Young and L-W. Chen, Pore formation mechanism of membranes from phase inversion process, *Desalination*, 1995, **103**, 233-247.
19. G. Guillen, Y. Pan, M. Li and E. M. V. Hoek, A review of nonsolvent induced phase separation membrane formation and characterization, *Desalination*, 2010, *submitted/in review*.
20. I. C. Kim, H. G. Yun and K. H. Lee, Preparation of asymmetric polyacrylonitrile membrane with small pore size by phase inversion and post-treatment process, *J. Membrane Sci.*, 2002, **199**, 75-84.

21. A. K. Ghosh, B. H. Jeong, X. F. Huang and E. M. V. Hoek, Impacts of reaction and curing conditions on polyamide composite reverse osmosis membrane properties, *J. Membrane Sci.*, 2008, **311**, 34-45.
22. M. Sivakumar, D. R. Mohan and R. Rangarajan, Studies on cellulose acetate-polysulfone ultrafiltration membranes II. Effect of additive concentration, *J. Membrane Sci.*, 2005, **268**, 208-219.
23. M. Kabsch-Korbutowicz, K. Majewska-Nowak and T. Winnicki, Analysis of membrane fouling in the treatment of water solutions containing humic acids and mineral salts, *Desalination*, 1999, **126**, 179-185.
24. M. Elimelech, X. Zhu, A. Childress and S. Hong, Role of membrane surface morphology in colloidal fouling of cellulose acetate and composite aromatic polyamide reverse osmosis membranes, *J. Membrane Sci.*, 1997, **127**, 101-109.
25. M. Cheryan, *Ultrafiltration and Microfiltration Handbook*, Technomic Publishing Co., Inc., Lancaster, UK, 1998.
26. J. E. Cadotte, R. J. Petersen, R. E. Larson and E. E. Erickson, New thin-film composite seawater reverse-osmosis membrane, *Desalination*, 1980, **32**, 25-31.
27. A. P. Rao, N. V. Desai and R. Rangarajan, Interfacially synthesized thin film composite RO membranes for seawater desalination, *J. Membrane Sci.*, 1997, **124**, 263-272.
28. H. Hachisuka and K. Ikeda, *Reverse osmosis composite membrane and reverse osmosis treatment method for water using the same*, US Patent, US6413425 (2002).
29. W. E. Mickols, *Composite membrane and method for making the same*. US Patent, US6562266 (2003).
30. R. J. Petersen, Composite reverse-osmosis and nanofiltration membranes, *J. Membrane Sci.*, 1993, **83**, 81-150.
31. A. I. Schafer, A. G. Fane and T. D. Waite, *Nanofiltration Principles and Applications*, Elsevier Advanced Technology, New York, NY, 2005.
32. W. Zhang, G. H. He, P. Gao and G. H. Chen, Development and characterization of composite nanofiltration membranes and their application in concentration of antibiotics, *Separ. Purif. Technol.*, 2003, **30**, 27-35.
33. C. Linder, M. Nemas, M. Perry and R. Ketraro, *Coated membranes*, US Patent, US5028337 (1991).
34. J. H. Choi, J. Jegal and W. N. Kim, Fabrication and characterization of multi-walled carbon nanotubes/polymer blend membranes, *J. Membrane Sci.*, 2006, **284**, 406-415.
35. A. L. Ahmad, M. Sarif and S. Ismail, Development of an integrally skinned ultrafiltration membrane for wastewater treatment: effect of different formulations of PSf/NMP/PVP on flux and rejection, *Desalination*, 2005, **179**, 257-263.
36. M. J. Han and S. T. Nam, Thermodynamic and rheological variation in polysulfone solution by PVP and its effect in the preparation of phase inversion membrane, *J. Membrane Sci.*, 2002, **202**, 55-61.
37. K. W. Lee, B. K. Seo, S. T. Nam and M. J. Han, Trade-off between thermodynamic enhancement and kinetic hindrance during phase inversion in the preparation of polysulfone membranes, *Desalination*, 2003, **159**, 289-296.
38. E. M. V. Hoek, *Colloidal fouling mechanisms in reverse osmosis and nanofiltration*, Ph.D. Dissertation, Yale University, New Haven, CT, 2002.

39. A. P. Rao, S. V. Joshi, J. J. Trivedi, C. V. Devmurari and V. J. Shah, Structure-performance correlation of polyamide thin film composite membranes: Effect of coating conditions on film formation, *J. Membrane Sci.*, 2003, **211**, 13-24.
40. I. C. Kim and K. H. Lee, Preparation of interfacially synthesized and silicone-coated composite polyamide nanofiltration membranes with high performance, *Ind. Eng. Chem. Res.*, 2002, **41**, 5523-5528.
41. S. Y. Kwak, S. H. Kim and S. S. Kim, Hybrid organic/inorganic reverse osmosis (RO) membrane for bactericidal anti-fouling. 1. Preparation and characterization of TiO₂ nanoparticle self-assembled aromatic polyamide thin-film-composite (TFC) membrane, *Environ. Sci. Technol.*, 2001, **35**, 2388-2394.
42. V. Freger, Nanoscale heterogeneity of polyamide membranes formed by interfacial polymerization, *Langmuir*, 2003, **19**, 4791-4797.
43. M. Hirose, H. Ito and Y. Kamiyama, Effect of skin layer surface structures on the flux behaviour of RO membranes, *J. Membrane Sci.*, 1996, **121**, 209-215.
44. C. K. Kim, J. H. Kim, I. J. Roh and J. J. Kim, The changes of membrane performance with polyamide molecular structure in the reverse osmosis process, *J. Membrane Sci.*, 2000, **165**, 189-199.
45. V. Freger, J. Gilron and S. Belfer, TFC polyamide membranes modified by grafting of hydrophilic polymers: an FT-IR/AFM/TEM study, *J. Membrane Sci.*, 2002, **209**, 283-292.
46. M. Kurihara, Y. Fusaoka, T. Sasaki, R. Bairinji and T. Uemura, Development of cross-linked fully aromatic polyamide ultra-thin composite membranes for seawater desalination, *Desalination*, 1994, **96**, 133-143.
47. S. Y. Kwak and D. W. Ihm, Use of atomic force microscopy and solid-state NMR spectroscopy to characterize structure-property-performance correlation in high-flux reverse osmosis (RO) membranes, *J. Membrane Sci.*, 1999, **158**, 143-153.
48. S. Y. Kwak, Relationship of relaxation property to reverse osmosis permeability in aromatic polyamide thin-film-composite membranes, *Polymer*, 1999, **40**, 6361-6368.
49. S. Y. Kwak, S. G. Jung, Y. S. Yoon and D. W. Ihm, Details of surface features in aromatic polyamide reverse osmosis membranes characterized by scanning electron and atomic force microscopy, *J. Polym. Sci. B*, 1999, **37**, 1429-1440.
50. I. J. Roh, S. Y. Park, J. J. Kim and C. K. Kim, Effects of the polyamide molecular structure on the performance of reverse osmosis membranes, *J. Polym. Sci. B*, 1998, **36**, 1821-1830.
51. Y. Yang, L. Wan and Z. Xu, Surface hydrophilization for polypropylene microporous membranes: A facile interfacial crosslinking approach, *J. Membrane Sci.*, 2009, **326**, 372-381.
52. M. Kim, N. Lin, G. Lewis and Y. Cohen, Surface nano-structuring of reverse osmosis membranes via atmospheric pressure plasma-induced graft polymerization for reduction of mineral scaling propensity, *J. Membrane Sci.*, 2010, **354**, 142-149.
53. G. Kang, Y. Cao, H. Zhao and Q. Yuan, Preparation and characterization of crosslinked poly(ethylene glycol) diacrylate membranes with excellent antifouling and solvent-resistant properties, *J. Membrane Sci.*, 2008, **318**, 227-232.
54. J. Lin and S. Murad, A computer simulation study of the separation of aqueous solutions using thin zeolite membranes, *Mol. Phys.*, 2001, **99**, 1175-1181.

55. L. Li, J. Dong, T. Nenoff and R. Lee, Desalination by reverse osmosis using MFI zeolite membranes, *J. Membrane Sci.*, 2004, **243**, 401-404.
56. L. Li, J. Dong and T. Nenoff, Transport of water and alkali metal ions through MFI zeolite membranes during reverse osmosis, *Separ. Purif. Technol.*, 2007, **53**, 42-48.
57. M. Duke, J. O'Brien-Abraham, N. Milne, B. Zhu, J. Lin and J. Diniz da Costa, Seawater desalination performance of MFI type membranes made by secondary growth, *Separ. Purif. Technol.*, 2009, **68**, 343-350.
58. J. Lu, N. Liu, L. Li and R. Lee, Organic fouling and regeneration of zeolite membrane in wastewater treatment, *Separ. Purif. Technol.*, 2010, **72**, 203-207.
59. L. Li and R. Lee, Purification of produced water by ceramic membranes: Material screening, process design and economics, *Separ. Purif. Technol.*, 2009, **44**, 3455-3484.
60. L. Li, N. Liu, B. McPherson and R. Lee, Enhanced water permeation of reverse osmosis through MFI-type zeolite membranes with high aluminum contents, *Ind. Eng. Chem. Res.*, 2007, **46**, 1584-1589.
61. N. Liu, L. Li, B. McPherson and R. Lee, Removal of organics from produced water by reverse osmosis using MFI-type zeolite membranes, *J. Membrane Sci.*, 2008, **325**, 357-361.
62. I. Kumakiri, T. Yamaguchi and S. Nakao, Application of a Zeolite A membrane to reverse osmosis process, *J. Chem. Eng. Jpn.*, 2000, **33**, 333-336.
63. M. Noack, P. Kölsch, V. Seefeld, P. Toussaint, G. Georgi and J. Caro, Influence of the Si/Al-ratio on the permeation properties of MFI-membranes, *Micropor. Mesopor. Mat.*, 2005, **79**, 329-337.
64. R. F. Lobo, *Handbook of Zeolite Science and Technology*, Marcel Dekker, Inc., New York, NY, 2003.
65. A. Dyer, *An Introduction to Zeolite Molecular Sieves*, John Wiley & Sons Ltd., Chichester, UK, 1988.
66. Y. Li, T. Chung and S. Kulprathipanja, Novel Ag⁺-zeolite/polymer mixed matrix membranes with a high CO₂/CH₄ selectivity, *AIChE J.*, 2007, **53**, 610-616.
67. C. Baerlocher and L. B. McCusker, *Database of Zeolite Structures*, <http://www.iza-structure.org/databases/>.
68. W. Yuan, Y. Lin and W. Yang, Molecular sieving MFI-Type zeolite membranes for pervaporation separation of xylene isomers, *J. Am. Chem. Soc.*, 2004, **126**, 4776-4777.
69. Y. Li, H. Chen, J. Liu and W. Yang, Microwave synthesis of LTA zeolite membranes without seeding, *J. Membrane Sci.*, 2006, **277**, 230-239.
70. M. Lovallo, A. Gouzinis and M. Tsapatsis, Synthesis and characterization of oriented MFI membranes prepared by secondary growth, *AIChE J.*, 2004, **44**, 1903-1913.
71. M. Kondo, M. Komori, H. Kita and K. Okamoto, Tubular-type pervaporation module with Zeolite NaA membrane, *J. Membrane Sci.*, 1997, **133**, 133-141.
72. V. Freger, Swelling and morphology of the skin layer of polyamide composite membranes: An atomic force microscopy study, *Environ. Sci. Technol.*, 2004, **38**, 3168-3175.
73. S. Ozturk and B. Akata, Oriented assembly and nanofabrication of Zeolite A monolayers, *Micropor. Mesopor. Mat.*, 2009, **126**, 228-233.
74. D. Bahnemann, Photocatalytic water treatment: Solar energy applications, *Sol. Energy*, 2004, **77**, 445-459.

75. E. Pramauro, A. Prevot, M. Vincenti and R. Gamberini, Photocatalytic degradation of naphthalene in aqueous TiO₂ dispersions: Effect of nonionic surfactants, *Chemosphere*, 1998, **36**, 1523-1542.
76. B. Prevot, Analytical monitoring of photocatalytic treatments. Degradation of 2, 3, 6-trichlorobenzoic acid in aqueous TiO₂ dispersions, *Talanta*, 1999, **48**, 847-857.
77. M. Hoffmann, S. Martin, W. Choi and D. Bahnemann, Environmental applications of semiconductor photocatalysis, *Chem. Rev.*, 1995, **95**, 69-96.
78. J. Carey, J. Lawrence and H. Tosine, Photodechlorination of PCB's in the presence of titanium dioxide in aqueous suspensions, *B. Environ. Contam. Tox.*, 1976, **16**, 697-701.
79. V. Krishna, S. Pumprueg, S. H. Lee, J. Zhao, W. Sigmund, B. Koopman and B. M. Moudgil, Photocatalytic disinfection with titanium dioxide coated multi-wall carbon nanotubes, *Process Saf. Environ.*, 2005, **83**, 393-397.
80. G. Rothenberger, J. Moser, M. Graetzel, N. Serpone and D. Sharma, Charge carrier trapping and recombination dynamics in small semiconductor particles, *J. Am. Chem. Soc.*, 1985, **107**, 8054-8059.
81. A. Modestov and O. Lev, Photocatalytic oxidation of 2, 4-dichlorophenoxyacetic acid with titania photocatalyst. Comparison of supported and suspended TiO₂, *J. Photoch. Photobio. A*, 1998, **112**, 261-270.
82. S. Horikoshi, H. Hidaka and N. Serpone, Environmental remediation by an integrated microwave/UV-illumination method. 1. Microwave-assisted degradation of Rhodamine-B dye in aqueous TiO₂ dispersions, *Environ. Sci. Technol*, 2002, **36**, 1357-1366.
83. A. Prevot, C. Baiocchi, M. Brussino, E. Pramauro, P. Savarino, V. Augugliaro, G. Marci and L. Palmisano, Photocatalytic degradation of acid blue 80 in aqueous solutions containing TiO₂ suspensions, *Environ. Sci. Technol*, 2001, **35**, 971-976.
84. W. Fu, H. Yang, M. Li, L. Chang, Q. Yu, J. Xu and G. Zou, Preparation and photocatalytic characteristics of core-shell structure TiO₂/BaFe₁₂O₁₉ nanoparticles, *Mater. Lett.*, 2006, **60**, 2723-2727.
85. Y. Ao, J. Xu, D. Fu, L. Ba and C. Yuan, Deposition of anatase titania onto carbon encapsulated magnetite nanoparticles, *Nanotechnology*, 2008, **19**, 405604.
86. R. Molinari, M. Mungari, E. Drioli, A. Di Paola, V. Loddo, L. Palmisano and M. Schiavello, Study on a photocatalytic membrane reactor for water purification, *Catal. Today*, 2000, **55**, 71-78.
87. J. Mo, S. H. Son, J. Jegal, J. Kim and Y. H. Lee, Preparation and characterization of polyamide nanofiltration composite membranes with TiO₂ layers chemically connected to the membrane surface, *J. Appl. Polym. Sci.*, 2007, **105**, 1267-1274.
88. S. S. Madaeni and N. Ghaemi, Characterization of self-cleaning RO membranes coated with TiO₂ particles under UV irradiation, *J. Membrane Sci.*, 2007, **303**, 221-233.
89. A. Rahimpour, S. S. Madaeni, A. H. Taheri and Y. Mansourpanah, Coupling TiO₂ nanoparticles with UV irradiation for modification of polyethersulfone ultrafiltration membranes, *J. Membrane Sci.*, 2008, **313**, 158-169.
90. Y. Mansourpanah, S. S. Madaeni, A. Rahimpour, A. Farhadian and A. H. Taheri, Formation of appropriate sites on nanofiltration membrane surface for binding TiO₂ photo-catalyst: Performance, characterization and fouling-resistant capability, *J. Membrane Sci.*, 2009, **330**, 297-306.
91. M. Moosemiller, C. Hill and M. Anderson, Physicochemical properties of supported-Al₂O₃ and TiO₂ ceramic membranes, *Separ. Sci. Technol.*, 1989, **24**, 641-657.

92. C. Burda, Y. Lou, X. Chen, A. Samia, J. Stout and J. Gole, Enhanced nitrogen doping in TiO₂ nanoparticles, *Nano Lett.*, 2003, **3**, 1049-1051.
93. I. Ilisz, A. Dombi, K. Mogyorósi and I. Dékány, Photocatalytic water treatment with different TiO₂ nanoparticles and hydrophilic/hydrophobic layer silicate adsorbents, *Colloid Surface A*, 2003, **230**, 89-97.
94. W. Dong, C. Lee, X. Lu, Y. Sun, W. Hua, G. Zhuang, S. Zhang, J. Chen, H. Hou and D. Zhao, Synchronous role of coupled adsorption and photocatalytic oxidation on ordered mesoporous anatase TiO₂-SiO₂ nanocomposites generating excellent degradation activity of RhB dye, *Appl. Catal. B-Environ.*, 2009.
95. H. Choi, E. Stathatos and D. Dionysiou, Sol-gel preparation of mesoporous photocatalytic TiO₂ films and TiO₂/Al₂O₃ composite membranes for environmental applications, *Appl. Catal. B-Environ.*, 2006, **63**, 60-67.
96. S. Fukahori, H. Ichiura, T. Kitaoka and H. Tanaka, Capturing of bisphenol A photodecomposition intermediates by composite TiO₂-zeolite sheets, *Appl. Catal. B-Environ.*, 2003, **46**, 453-462.
97. J. Matos, J. Laine and J. Herrmann, Effect of the type of activated carbons on the photocatalytic degradation of aqueous organic pollutants by UV-irradiated titania, *J. Catal.*, 2001, **200**, 10-20.
98. Z. Zhang, C. Wang, R. Zakaria and J. Ying, Role of particle size in nanocrystalline TiO₂-based photocatalysts, *J. Phys. Chem. B*, 1998, **102**, 10871-10878.
99. F. Beltran, F. Rivas and R. Montero-de-Espinosa, Ozone-enhanced oxidation of oxalic acid in water with cobalt catalysts. 1. Homogeneous catalytic ozonation, *Ind. Eng. Chem. Res.*, 2003, **42**, 3210-3217.
100. B. Legube and K. Leitner, Catalytic ozonation: A promising advanced oxidation technology for water treatment, *Catal. Today*, 1999, **53**, 61-72.
101. L. Liotta, M. Gruttadauria, G. Di Carlo, G. Perrini and V. Librando, Heterogeneous catalytic degradation of phenolic substrates: Catalysts activity, *J. Haz. Mater.*, 2009, **162**, 588-606.
102. R. Gracia, J. Aragües and J. Ovelleiro, Study of the catalytic ozonation of humic substances in water and their ozonation byproducts, *Ozone-Sci. Eng.*, 1996, **18**, 195-208.
103. B. Karnik, S. Davies, M. Baumann and S. Masten, Fabrication of catalytic membranes for the treatment of drinking water using combined ozonation and ultrafiltration, *Environ. Sci. Technol.*, 2005, **39**, 7656-7661.
104. J. Ma and N. Graham, Degradation of atrazine by manganese-catalysed ozonation: Influence of humic substances, *Water Res.*, 1999, **33**, 785-793.
105. J. Ma and N. Graham, Degradation of atrazine by manganese-catalysed ozonation: Influence of radical scavengers, *Water Res.*, 2000, **34**, 3822-3828.
106. G. Liu, X. Zhang, Y. Xu, X. Niu, L. Zheng and X. Ding, Effect of ZnFe₂O₄ doping on the photocatalytic activity of TiO₂, *Chemosphere*, 2004, **55**, 1287-1291.
107. X. Qiu and C. Burda, Chemically synthesized nitrogen-doped metal oxide nanoparticles, *Chem. Phys.*, 2007, **339**, 1-10.
108. Y. Bessekhoud, D. Robert, J. Weber and N. Chaoui, Effect of alkaline-doped TiO₂ on photocatalytic efficiency, *J. Photoch. Photobio. A*, 2004, **167**, 49-57.
109. L. Brunet, D. Y. Lyon, E. M. Hotze, P. J. J. Alvarez and M. R. Wiesner, Comparative photoactivity and antibacterial properties of C-60 fullerenes and titanium dioxide nanoparticles, *Environ. Sci. Technol.*, 2009, **43**, 4355-4360.

110. V. Augugliaro, C. Baiocchi, A. Bianco Prevot, E. García-López, V. Loddo, S. Malato, G. Marci, L. Palmisano, M. Pazzi and E. Pramauro, Azo-dyes photocatalytic degradation in aqueous suspension of TiO₂ under solar irradiation, *Chemosphere*, 2002, **49**, 1223-1230.
111. C. Zimmerman, A. Singh and W. Koros, Tailoring mixed matrix composite membranes for gas separations, *J. Membrane Sci.*, 1997, **137**, 145-154.
112. R. Mahajan, R. Burns, M. Schaeffer and W. J. Koros, Challenges in forming successful mixed matrix membranes with rigid polymeric materials, *J. Appl. Polym. Sci.*, 2002, **86**, 881-890.
113. R. Mahajan, D. Q. Vu and W. J. Koros, Mixed matrix membrane materials: An answer to the challenges faced by membrane based gas separations today? *J. Chin. Inst. Chem. Eng.*, 2002, **33**, 77-86.
114. M. D. Jia, K. V. Peinemann and R. D. Behling, Molecular-sieving effect of the zeolite-filled silicone-rubber membranes in gas permeation, *J. Membrane Sci.*, 1991, **57**, 289-296.
115. L. Y. Jiang, T. S. Chung and S. Kulprathipanja, Fabrication of mixed matrix hollow fibers with intimate polymer-zeolite interface for gas separation, *AIChE J.*, 2006, **52**, 2898-2908.
116. S. Kirkpatrick, Percolation and conduction, *Rev. Mod. Phys.*, 1973, **45**, 574-588.
117. H. Frisch and J. Hammersley, Percolation processes and related topics, *J. Ind. Appl. Math.*, 1963, **11**, 894-918.
118. J. Ottino and N. Shah, Analysis of transient sorption and permeation of small molecules in multiphase polymer systems, *Polym. Eng. Sci.*, 2004, **24**, 153-162.
119. P. Aerts, A. R. Greenberg, R. Leysen, W. B. Krantz, V. E. Reinsch and P. A. Jacobs, The influence of filler concentration on the compaction and filtration properties of Zirfon®-composite ultrafiltration membranes, *Separ. Purif. Technol.*, 2001, **22-3**, 663-669.
120. P. Aerts, S. Kuypers, I. Genne, R. Leysen, J. Mewis, I. F. J. Vankelecom and P. A. Jacobs, Polysulfone-ZrO₂ surface interactions. The influence on formation, morphology and properties of zirfon-membranes, *J. Phys. Chem. B*, 2006, **110**, 7425-7430.
121. N. M. Wara, L. F. Francis and B. V. Velamakanni, Addition of alumina to cellulose-acetate membranes. *J. Membrane Sci.*, 1995, **104**, 43-49.
122. I. Genne, S. Kuypers and R. Leysen, Effect of the addition of ZrO₂ to polysulfone based UF membranes, *J. Membrane Sci.*, 1996, **113**, 343-350.
123. A. Bottino, G. Capannelli and A. Comite, Preparation and characterization of novel porous PVDF-ZrO₂ composite membranes, *Desalination*, 2002, **146**, 35-40.
124. Y. C. Sharma, V. Srivastava, V. K. Singh, S. N. Kaul and C. H. Weng, Nano-adsorbents for the removal of metallic pollutants from water and wastewater, *Environ. Technol.*, 2009, **30**, 583-609.
125. D. M. Fernandes, R. Silva, A. A. W. Hechenleitner, E. Radovanovic, M. A. C. Melo and E. A. G. Pineda, Synthesis and characterization of ZnO, CuO and a mixed Zn and Cu oxide, *Mater. Chem. and Phys.*, 2009, **115**, 110-115.
126. P. K. Stoimenov, R. L. Klinger, G. L. Marchin and K. J. Klabunde, Metal oxide nanoparticles as bactericidal agents, *Langmuir*, 2002, **18**, 6679-6686.
127. N. Savage and M. S. Diallo, Nanomaterials and water purification: Opportunities and challenges, *J. Nanopart. Res.*, 2005, **7**, 331-342.
128. Z. R. Yue and J. Economy, Nanoparticle and nanoporous carbon adsorbents for removal of trace organic contaminants from water, *J. Nanopart. Res.*, 2005, **7**, 477-487.

129. Y. C. Sharma, V. Srivastava, S. N. Upadhyay and C. H. Weng, Alumina nanoparticles for the removal of Ni(II) from aqueous solutions. *Ind. Eng. Chem. Res.*, 2008, **47**, 8095-8100.
130. J. G. Darab, A. B. Amonette, D. S. D. Burke, R. D. Orr, S. M. Ponder, B. Schrick, T. E. Mallouk, W. W. Lukens, D. L. Caulder and D. K. Shuh, Removal of pertechnetate from simulated nuclear waste streams using supported zerovalent iron, *Chem. Mater.*, 2007, **19**, 5703-5713.
131. S. M. Ponder, J. G. Darab and T. E. Mallouk, Remediation of Cr(VI) and Pb(II) aqueous solutions using supported, nanoscale zero-valent iron, *Environ. Sci. Technol.*, 2000, **34**, 2564-2569.
132. S. M. Ponder, J. G. Darab, J. Bucher, D. Caulder, I. Craig, L. Davis, N. Edelstein, W. Lukens, H. Nitsche, L. F. Rao, D. K. Shuh and T. E. Mallouk, Surface chemistry and electrochemistry of supported zerovalent iron nanoparticles in the remediation of aqueous metal contaminants, *Chem. Mater.*, 2001, **13**, 479-486.
133. J. S. Taurozzi, H. Arul, V. Z. Bosak, A. F. Burban, T. C. Voice, M. L. Bruening and V. V. Tarabara, Effect of filler incorporation route on the properties of polysulfone-silver nanocomposite membranes of different porosities, *J. Membrane Sci.*, 2008, **325**, 58-68.
134. L. Yan, Y. S. Li and C. B. Xiang, Preparation of poly(vinylidene fluoride)(PVDF) ultrafiltration membrane modified by nano-sized alumina (Al_2O_3) and its antifouling research, *Polymer*, 2005, **46**, 7701-7706.
135. N. Maximous, G. Nakhla, W. Wan and K. Wong, Preparation, characterization and performance of Al_2O_3 /PES membrane for wastewater filtration, *J. Membrane Sci.*, 2009, **341**, 67-75.
136. Z. F. Fan, Z. Wang, M. R. Duan, J. X. Wang and S. C. Wang, Preparation and characterization of polyaniline/polysulfone nanocomposite ultrafiltration membrane, *J. Membrane Sci.*, 2008, **310**, 402-408.
137. Z. F. Fan, Z. Wang, N. Sun, J. X. Wang and S. C. Wang, Performance improvement of polysulfone ultrafiltration membrane by blending with polyaniline nanofibers, *J. Membrane Sci.*, 2008, **320**, 363-371.
138. J. R. Morones, J. L. Elechiguerra, A. Camacho, K. Holt, J. B. Kouri, J. T. Ramirez and M. J. Yacaman, The bactericidal effect of silver nanoparticles, *Nanotechnology*, 2005, **16**, 2346-2353.
139. T. H. Bae and T. M. Tak, Effect of TiO_2 nanoparticles on fouling mitigation of ultrafiltration membranes for activated sludge filtration, *J. Membrane Sci.*, 2005, **249**, 1-8.
140. X. C. Cao, J. Ma, X. H. Shi and Z. J. Ren, Effect of TiO_2 nanoparticle size on the performance of PVDF membrane, *Appl. Surf. Sci.*, 2006, **253**, 2003-2010.
141. J. F. Li, Z. L. Xu, H. Yang, L. Y. Yu and M. Liu, Effect of TiO_2 nanoparticles on the surface morphology and performance of microporous PES membrane, *Appl. Surf. Sci.*, 2009, **255**, 4725-4732.
142. S. S. Hosseini, Y. Li, T. S. Chung and Y. Liu, Enhanced gas separation performance of nanocomposite membranes using MgO nanoparticles, *J. Membrane Sci.*, 2007, **302**, 207-217.
143. L. Wu, M. Shamsuzzoha and S. M. C. Ritchie, Preparation of cellulose acetate supported zero-valent iron nanoparticles for the dechlorination of trichloroethylene in water, *J. Nanoparticle Res.*, 2005, **7**, 469-476.

144. L. F. Wu and S. M. C. Ritchie, Enhanced dechlorination of trichloroethylene by membrane-supported Pd-coated iron nanoparticles, *Environ. Prog.*, 2008, **27**, 218-224.
145. V. Smuleac, L. Bachas and D. Bhattacharyya, Aqueous-phase synthesis of PAA in PVDF membrane pores for nanoparticle synthesis and dichlorobiphenyl degradation, *J. Membrane Sci.*, 2009, **346**, 310-317.
146. Y. Shih, Y. Chen, M. Chen, Y. Tai and C. Tso, Dechlorination of hexachlorobenzene by using nanoscale Fe and nanoscale Pd/Fe bimetallic particles, *Colloid Surface A*, 2009, **332**, 84-89.
147. Y. Han, W. Li, M. Zhang and K. Tao, Catalytic dechlorination of monochlorobenzene with a new type of nanoscale Ni (b)/Fe (b) bimetallic catalytic reductant, *Chemosphere*, 2008, **72**, 53-58.
148. D. Meyer and D. Bhattacharyya, Impact of membrane immobilization on particle formation and trichloroethylene dechlorination for bimetallic Fe/Ni nanoparticles in cellulose acetate membranes, *J. Phys. Chem. B*, 2007, **111**, 7142-7154.
149. B. Zhu and T. Lim, Catalytic reduction of chlorobenzenes with Pd/Fe nanoparticles: Reactive sites, catalyst stability, particle aging, and regeneration., *Environ. Sci. Technol.*, 2007, **41**, 7523-7529.
150. E. Hadnagy, L. Rauch and K. Gardner, Dechlorination of polychlorinated biphenyls, naphthalenes and dibenzo-p-dioxins by magnesium/palladium bimetallic particles, *J. Environ. Sci. Heal. A*, 2007, **42**, 685-695.
151. J. S. Baker and L. Y. Dudley, Biofouling in membrane systems—A review, *Desalination*, 1998, **118**, 81-89.
152. M. Z. Rong, M. Q. Zhang, Y. X. Zheng, H. M. Zeng, R. Walter and K. Friedrich, Structure-property relationships of irradiation grafted nano-inorganic particle filled polypropylene composites, *Polymer*, 2001, **42**, 167-183.
153. N. A. Ochoa, M. Masuelli and J. Marchese, Effect of hydrophilicity on fouling of an emulsified oil wastewater with PVDF/PMMA membranes, *J. Membrane Sci.*, 2003, **226**, 203-211.
154. D. Lee, R. E. Cohen and M. F. Rubner, Antibacterial properties of Ag nanoparticle loaded multilayers and formation of magnetically directed antibacterial microparticles, *Langmuir*, 2005, **21**, 9651-9659.
155. I. Sondi and B. Salopek-Sondi, Silver nanoparticles as antimicrobial agent: A case study on E-coli as a model for Gram-negative bacteria, *J. Colloid Interf. Sci.*, 2004, **275**, 177-182.
156. J. Fabrega, S. R. Fawcett, J. C. Renshaw and J. R. Lead, Silver nanoparticle impact on bacterial growth: Effect of pH, concentration, and organic matter. *Environ. Sci. Technol.*, 2009, **43**, 7285-7290.
157. C. Marambio-Jones and E. M. V. Hoek, A review of the antibacterial effects of silver nanomaterials and potential implications for human health and the environment, *J. Nanoparticle Res.*, 2010, **12**, 1-21.
158. V. V. Tarabara, in *Nanotechnology Applications for Clean Water*, eds. N. Savage, M. Diallo, J. Duncan, A. Street and R. Sustich, William Andrew Inc., Norwich, NY, 2009, pp. 59-75.
159. L. Brunet, D. Y. Lyon, K. Zodrow, J. C. Rouch, B. Caussat, P. Serp, J. C. Remigy, M. R. Wiesner and P. J. J. Alvarez, Properties of membranes containing semi-dispersed carbon nanotubes, *Environ. Eng. Sci.*, 2008, **25**, 565-575.

160. Y. Lin, M. Meziani and Y. Sun, Functionalized carbon nanotubes for polymeric nanocomposites, *J. Mater. Chem.*, 2007, **17**, 1143-1148.
161. S. Kang, M. Pinault, L. D. Pfefferle and M. Elimelech, Single-walled carbon nanotubes exhibit strong antimicrobial activity, *Langmuir*, 2007, **23**, 8670-8673.
162. P. Ajayan, Nanotubes from carbon, *Chem. Rev.*, 1999, **99**, 1787-1800.
163. K. M. Persson, V. Gekas and G. Tragardh, Study of membrane compaction and its influence on ultrafiltration water permeability, *J. Membrane Sci.*, 1995, **100**, 155-162.
164. G. Jonsson, Methods for determining the selectivity of reverse osmosis membranes, *Desalination*, 1978, **24**, 19-37.
165. K. Ebert, D. Fritsch, J. Koll and C. Tjahjawiguna, Influence of inorganic fillers on the compaction behaviour of porous polymer based membranes, *J. Membrane Sci.*, 2004, **233**, 71-78.
166. M. M. Pendergast, J. M. Nygaard, A. K. Ghosh, E. M. V. Hoek, Using nanocomposite membrane materials to understand and control reverse osmosis membrane compaction, *Desalination*, 2010, **261**, 255-263.
167. M. Arkas, D. Tsiourvas and C. M. Paleos, Organosilicon dendritic networks in porous ceramics for water purification, *Chem. Mater.*, 2005, **17**, 3439-3444.
168. B. H. Jeong, E. M. V. Hoek, Y. S. Yan, A. Subramani, X. F. Huang, G. Hurwitz, A. K. Ghosh and A. Jawor, Interfacial polymerization of thin film nanocomposites: A new concept for reverse osmosis membranes, *J. Membrane Sci.*, 2007, **294**, 1-7.
169. M. Lind, A. Ghosh, A. Jawor, X. Huang, W. Hou, Y. Yang and E. Hoek, Influence of Zeolite Crystal Size on Zeolite-Polyamide Thin Film Nanocomposite Membranes, *Langmuir*, 2009, **25**, 10139-10145.
170. H. S. Lee, S. J. Im, J. H. Kim, H. J. Kim, J. P. Kim and B. R. Min, Polyamide thin-film nanofiltration membranes containing TiO₂ nanoparticles, *Desalination*, 2008, **219**, 48-56.
171. T. H. Bae, I. C. Kim and T. M. Tak, Preparation and characterization of fouling-resistant TiO₂ self-assembled nanocomposite membranes, *J. Membrane Sci.*, 2006, **275**, 1-5.
172. M. L. Luo, W. Tang, J. Q. Zhao and C. S. Pu, Hydrophilic modification of poly(ether sulfone) used TiO₂ nanoparticles by a sol-gel process, *J. Mater. Process. Tech.*, 2006, **172**, 431-436.
173. M. L. Lind, B. H. Jeong, A. Subramani, X. F. Huang and E. M. V. Hoek, Effect of mobile cation on zeolite-polyamide thin film nanocomposite membranes, *J. Mater. Res.*, 2009, **24**, 1624-1631.
174. A. S. Brady-Estevéz, S. Kang and M. Elimelech, A single-walled-carbon-nanotube filter for removal of viral and bacterial pathogens, *Small*, 2008, **4**, 481-484.
175. M. L. Luo, J. Q. Zhao, W. Tang and C. S. Pu, Hydrophilic modification of poly(ether sulfone) ultrafiltration membrane surface by self-assembly of TiO₂ nanoparticles, *Appl. Surf. Sci.*, 2005, **249**, 76-84.
176. P. Agre, S. Sasaki and M. J. Chrispeels, Aquaporins: A family of water channel proteins, *Am. J. Physiol-Renal*, 1993, **265**, F461.
177. Y. Kaufman, A. Berman and V. Freger, Supported lipid bilayer membranes for water purification by reverse osmosis, *Langmuir*, 2010, **26**, 7388-7395.
178. P. Agre, *Aquaporin Water Channels*, Nobel Lecture, Stockholm, SE, 2003.
179. A. Meinild, D. Klaerke and T. Zeuthen, Bidirectional water fluxes and specificity for small hydrophilic molecules in Aquaporins 0-5, *J. Biol. Chem.*, 1998, **273**, 32446.

180. P. Agre, G. M. Preston, B. L. Smith, J. S. Jung, S. Raina, C. Moon, W. B. Guggino and S. Nielsen, Aquaporin CHIP: The archetypal molecular water channel, *Am. J. Physiol-Renal*, 1993, **265**, F463-476.
181. F. Q. Zhu, E. Tajkhorshid and K. Schulten, Theory and simulation of water permeation in Aquaporin-1, *Biophysical Journal*, 2004, **86**, 50-57.
182. M. Kumar, M. Grzelakowski, J. Zilles, M. Clark and W. Meier, Highly permeable polymeric membranes based on the incorporation of the functional water channel protein Aquaporin Z, *P. Natl. Acad. Sci. USA*, 2007, **104**, 20719-20724.
183. T. W. Ebbesen, Carbon nanotubes, *Annu. Rev. Mater. Sci.*, 1994, **24**, 235-264.
184. T. W. Ebbesen, Nanotubes, nanoparticles, and aspects of fullerene related carbons, *J. Phys. Chem. Solids*, 1997, **58**, 1979-1982.
185. S. Ahadian and Y. Kawazoe, An artificial intelligence approach for modeling and prediction of water diffusion inside a carbon nanotube. *Nanoscale Res. Lett.*, 2009, **4**, 1054-1058.
186. J. K. Holt, H. G. Park, Y. M. Wang, M. Stadermann, A. B. Artyukhin, C. P. Grigoropoulos, A. Noy and O. Bakajin, Fast mass transport through sub-2-nanometer carbon nanotubes, *Science*, 2006, **312**, 1034-1037.
187. G. Hummer, J. C. Rasaiah and J. P. Noworyta, Water conduction through the hydrophobic channel of a carbon nanotube, *Nature*, 2001, **414**, 188-190.
188. A. Kalra, S. Garde and G. Hummer, Osmotic water transport through carbon nanotube membranes, *P. Natl. Acad. Sci. USA*, 2003, **100**, 10175-10180.
189. L. Song, J. Y. Hu, S. L. Ong, W. J. Ng, M. Elimelech and M. Wilf, Emergence of thermodynamic restriction and its implications for full-scale reverse osmosis processes, *Desalination*, 2003, **155**, 213-228.
190. J. P. Salvetat, G. A. D. Briggs, J. M. Bonard, R. R. Bacsá, A. J. Kulik, T. Stockli, N. A. Burnham and L. Forro, Elastic and shear moduli of single-walled carbon nanotube ropes, *Phys. Rev. Lett.*, 1999, **82**, 944-947.
191. J. P. Salvetat, A. J. Kulik, J. M. Bonard, G. A. D. Briggs, T. Stockli, K. Metenier, S. Bonnamy, F. Beguin, N. A. Burnham and L. Forro, Elastic modulus of ordered and disordered multiwalled carbon nanotubes, *Adv. Mater.*, 1999, **11**, 161-165.
192. S. Kim, J. R. Jinschek, H. Chen, D. S. Sholl and E. Marand, Scalable fabrication of carbon nanotube/polymer nanocomposite membranes for high flux gas transport, *Nano Lett.*, 2007, **7**, 2806-2811.
193. Y. Gao, J. Liu, M. Shi, S. H. Elder and J. W. Virden, Dense arrays of well-aligned carbon nanotubes completely filled with single crystalline titanium carbide wires on titanium substrates, *Appl. Phys. Lett.*, 1999, **74**, 3642-3644.
194. Y. C. Choi, Y. M. Shin, Y. H. Lee, B. S. Lee, G. S. Park, W. B. Choi, N. S. Lee and J. M. Kim, Controlling the diameter, growth rate, and density of vertically aligned carbon nanotubes synthesized by microwave plasma-enhanced chemical vapor deposition, *Appl. Phys. Lett.*, 2000, **76**, 2367-2369.
195. A. Huczko, Synthesis of aligned carbon nanotubes, *Appl. Phys. A-Mater.*, 2002, **74**, 617-638.
196. N. Yoshikawa, T. Asari, N. Kishi, S. Hayashi, T. Sugai and H. Shinohara, An efficient fabrication of vertically aligned carbon nanotubes on flexible aluminum foils by catalyst-supported chemical vapor deposition, *Nanotechnology*, 2008, **19**, 245607.

197. P. Mauron, C. Emmenegger, A. Zuttel, C. Nutzenadel, P. Sudan and L. Schlapbach, Synthesis of oriented nanotube films by chemical vapor deposition, *Carbon*, 2002, **40**, 1339-1344.
198. F. Fornasiero, H. G. Park, J. K. Holt, M. Stadermann, C. P. Grigoropoulos, A. Noy and O. Bakajin, Ion exclusion by sub-2-nm carbon nanotube pores, *P. Natl. Acad. Sci. USA*, 2008, **105**, 17250-17255.
199. W. A. deHeer, W. S. Basca, C. T. Gerfin, R. Humphrey-Baker, L. Forro and D. Ugarte, Aligned carbon nanotube films: Production and optical and electronic properties, *Science*, 1995, **268**, 845-847.
200. M. J. Casavant, D. A. Walters, J. J. Schmidt and R. E. Smalley, Neat macroscopic membranes of aligned carbon nanotubes, *J. Appl. Phys.*, 2003, **93**, 2153-2156.
201. A. Srivastava, O. N. Srivastava, S. Talapatra, R. Vajtai and P. M. Ajayan, Carbon nanotube filters, *Nat. Mater.*, 2004, **3**, 610-614.
202. B. Corry, Designing carbon nanotube membranes for efficient water desalination, *J. Phys. Chem. B*, 2008, **112**, 1427-1434.
203. G. M. Whitesides and B. Grzybowski, Self-assembly at all scales, *Science*, 2002, **295**, 2418-2421.
204. G. Widawski, M. Rawiso and B. Francois, Self-organized honeycomb morphology of star-polymer polystyrene films, *Nature*, 1994, **369**, 387-389.
205. D. Beattie, K. H. Wong, C. Williams, L. A. Poole-Warren, T. P. Davis, C. Barner-Kowollik and M. H. Stenzel, Honeycomb-structured porous films from polypyrrole-containing block copolymers prepared via RAFT polymerization as a scaffold for cell growth, *Biomacromolecules*, 2006, **7**, 1072-1082.
206. D. Fierro, K. Buhr, C. Abetz, A. Boschetti-de-Fierro and V. Abetz, New insights into the control of self-assembly of block copolymer membranes, *Aust. J. Chem.* 2009, **62**, 885-890.
207. T. Kabuto, Y. Hashimoto and O. Karthaus, Thermally stable and solvent resistant mesoporous honeycomb films from a crosslinkable polymer, *Adv. Funct. Mater.*, 2007, **17**, 3569-3573.
208. C. Rodriguez-Abreu and M. Lazzari, Emulsions with structured continuous phases, *Curr. Opin. Colloid In.*, 2008, **13**, 198-205.
209. H. Yabu, Y. Hirai and M. Shimomura, Electroless plating of honeycomb and pincushion polymer films prepared by self-organization, *Langmuir*, 2006, **22**, 9760-9764.
210. A. Dove, Controlled ring-opening polymerisation of cyclic esters: polymer blocks in self-assembled nanostructures, *Chem. Commun.*, 2008, **2008**, 6446-6470.
211. K. V. Peinemann, V. Abetz and P. F. W. Simon, Asymmetric superstructure formed in a block copolymer via phase separation, *Nat. Mater.*, 2007, **6**, 992-996.
212. T. Smart, H. Lomas, M. Massignani, M. V. Flores-Merino, L. R. Perez and G. Battaglia, Block copolymer nanostructures, *Nano Today*, 2008, **3**, 38-46.
213. R. O'Reilly, C. Hawker and K. Wooley, Cross-linked block copolymer micelles: functional nanostructures of great potential and versatility, *Chem. Soc. Rev.*, 2006, **35**, 1068-1083.
214. H. Jung, K. Price and D. McQuade, Synthesis and characterization of cross-linked reverse micelles, *Polymer*, 1993, **34**, 4969.
215. W. Phillip, M. Hillmyer and E. Cussler, Cylinder orientation mechanism in block copolymer thin films upon solvent evaporation, *Macromolecules*, 2010, **43**, 7763-7770.

216. W. Phillip, B. O'Neill, M. Rodwogin, M. Hillmyer, E. Cussler, Self-assembled block copolymer thin films as water filtration membranes, *ACS Appl. Mater. Interface*, 2010, **2**, 847-853.
217. J. Y. Cheng, A. M. Mayes and C. A. Ross, Nanostructure engineering by templated self-assembly of block copolymers, *Nat. Mater.*, 2004, **3**, 823-828.
218. K. V. Peinemann, P. F. Abetz, W. Simon, G. Johannsen, G., *Isoporous membrane and method of production thereof*, US Patent, US0173694 (2009).
219. W. A. Phillip, M. Amendt, B. O'Neill, L. Chen, M. A. Hillmyer and E. L. Cussler, Diffusion and flow across nanoporous polydicyclopentadiene-based membranes. *ACS Appl. Mater. Interface*, 2009, **1**, 472-480.
220. L. Chen, W. A. Phillip, E. L. Cussler and M. A. Hillmyer, Robust nanoporous membranes templated by a doubly reactive block copolymer, *J. Am. Chem. Soc.*, 2007, **129**, 13786-13787.
221. M. J. Fasolka and A. M. Mayes, Block copolymer thin films: Physics and applications, *Annu. Rev. Mater. Res.*, 2001, **31**, 323-355.
222. S. Y. Yang, I. Ryu, H. Y. Kim, J. K. Kim, S. K. Jang and T. P. Russell, Nanoporous membranes with ultrahigh selectivity and flux for the filtration of viruses, *Adv. Mater.*, 2006, **18**, 709-712.
223. K. Fukunaga, T. Hashimoto, H. Elbs and G. Krausch, Self-assembly of a lamellar ABC triblock terpolymer thin film. Effect of substrates, *Macromolecules*, 2003, **36**, 2852-2861.
224. X. Li, C. Fustin, N. Lefèvre, J. Gohy, S. De Feyter, J. De Baerdemaeker, W. Egger and I. Vankelecom, Ordered nanoporous membranes based on diblock copolymers with high chemical stability and tunable separation properties, *J. Mater. Chem*, 2010, **20**, 4333-4339.
225. K. Stratford, R. Adhikari, I. Pagonabarraga, J. C. Desplat and M. E. Cates, Colloidal jamming at interfaces: A route to fluid-bicontinuous gels, *Science*, 2005, **309**, 2198-2201.
226. X. Yao, H. W. Yao, Y. T. Li and G. Chen, Preparation of honeycomb scaffold with hierarchical porous structures by core-crosslinked core-corona nanoparticles, *J. Colloid Interf. Sci.*, 2009, **332**, 165-172.
227. J. S. Wang and K. Matyjaszewski, Controlled living radical polymerization-atom-transfer radical polymerization in the presence of transition-metal complexes. *J. Am. Chem. Soc.*, 1995, **117**, 5614-5615.
228. G. Guillen and E. M. V. Hoek, Modeling the impacts of feed spacer geometry on reverse osmosis and nanofiltration processes, *Chem. Eng. J.*, 2009, **149**, 221-231.

TABLES

Table 1. Membrane characterizations by pore type and target species

Pore Type (size range, nm)	Membrane Type (pore size, nm)	Species^c	Dimensions^c (nm)
Macropores (> 50)	Microfiltration^a (50 - 500)	yeasts & fungi	1 000 - 10 000
		bacteria	300 - 10 000
		oil emulsions	100 - 10 000
Mesopores (2 - 50)	Ultrafiltration^a (2 - 50)	colloidal solids	100 - 1 000
		viruses	30 - 300
		proteins/polysaccharides	3 - 10
		humics/nucleic acids	< 3
Micropores (0.2 - 2)	Nanofiltration^a (≤ 2) Reverse Osmosis^b (0.3-0.6) Forward Osmosis^b (0.3-0.6)	common antibiotics	0.6 - 1.2
		organic antibiotics	0.3 - 0.8
		inorganic ions	0.2 - 0.4
		water	0.2

^a See reference ⁶.

^b See reference ⁸.

^c See reference ⁵.

Table 2. Performance comparison of organic and inorganic membranes

Membrane Type	Test Temp (°C)	Film Thickness (μm)	Water Permeability (m·Pa ⁻¹ ·s ⁻¹)	Specific Water Permeability (m ² ·Pa ⁻¹ ·s ⁻¹)	Solute Type (concentration)	Solute Rejection (%)	Solute Permeability (m·s ⁻¹)	Reference
SWRO *	20	~0.2	~3×10 ⁻¹²	~0.6×10 ⁻¹⁸	NaCl (32 g/l)	> 99.5	~2×10 ⁻⁸	228
BWRO	20	~0.1	~10×10 ⁻¹²	~1×10 ⁻¹⁸	NaCl (2 g/l)	99.0	~7×10 ⁻⁸	228
HFRO	20	~0.1	~20×10 ⁻¹²	~2×10 ⁻¹⁸	NaCl (0.5-1.5 g/l)	98.5	~1×10 ⁻⁷	228
NF	20	~0.05	~40×10 ⁻¹²	~2×10 ⁻¹⁸	MgSO4 (0.5 g/l)	95.0	~10×10 ⁻⁷	228
MFI	20	~3	~0.01×10 ⁻¹²	~0.04×10 ⁻¹⁸	NaCl (0.1 M)	76.7	7×10 ⁻⁷	55
MFI	30	~3	~0.03×10 ⁻¹²	~0.1×10 ⁻¹⁸	NaCl (0.1 M)	98.0	2×10 ⁻⁷	56
MFI	20	~1.2	~0.03×10 ⁻¹²	~0.04×10 ⁻¹⁸	NaCl (0.1 M)	99.4	0.6×10 ⁻⁷	61
SOD	20	~50	~2×10 ⁻¹²	~100×10 ⁻¹⁸	none tested	-	-	10
LTA	30	~5	~0.03×10 ⁻¹²	~0.1×10 ⁻¹⁸	none tested	-	-	62

*Commercial polymeric seawater RO (SWRO), brackish water RO (BWRO), high-flux RO (HFRO)

228

55

56

61

10

62

Table 3. Comparison of nanotechnology-enabled technologies

Nanotechnology-Enabled Membrane Concept		Potential Performance Enhancement			Potential Commercial Viability		
		Productivity	Selectivity	Robustness	Cost Effectiveness	Scalability	Time to Commercialization
Nanostructured Ceramic Membranes	Reactive/Catalytic Surfaces	0	+	+	0	0	0
	Zeolitic Coatings	-	0	+	-	0	0
Inorganic-Organic Membranes	Mixed Matrices	+	0	+	-	+	0
	Nanoparticle TFNs	+	-	+	-	+	+
	Zeolite TFNs	+	0	+	0	+	+
Biologically-Inspired Membranes	Aquaporins	+++	++	0	-	-	0
	Aligned Nanotubes	++	++	0	-	-	0
	Block Copolymers	++	++	-	0	+	-

LIST OF FIGURES

Figure 1. Conceptual depiction of the asymmetric structure of an inorganic membrane.

Figure 2. Conceptual cross-section of an asymmetric, integrally skinned membrane.

Figure 3. Schematic of nanoparticle mediated photocatalysis. Adapted from ⁷⁴.

Figure 4. Conceptual cross-section of a membrane containing molecular sieves throughout the polymeric thin film, providing preferential flow paths for water as indicated by arrows. Adapted from ¹⁶⁸.

Figure 5. Theoretical projection of the possibilities for thin films containing nanoparticles (permeable and impermeable) compared to current polymeric seawater RO membranes.

Figure 6. Molecular ordering of water molecules being transported through nanoscale channels (aquaporins and carbon nanotubes) as predicted by molecular dynamics simulations. Adapted from ¹⁸⁷.

Figure 7. Conceptual cross-sectional image of a semi-permeable lipid bi-layer membrane cast atop a nanofiltration-type support membrane. Adapted from ¹⁷⁷.

Figure 8. Conceptual image of an array of aligned nanotubes embedded in a nonporous polymeric matrix.

Figure 9. Theoretical projection of the possibilities for aligned carbon nanotube membranes compared to current polymeric seawater RO membranes.

Figure 10. Di-block copolymer micelle formation upon reaching the critical micelle concentration. Adapted from ²²⁶.

Figure 11. Comparison of the potential performance and commercial viability of nanotechnology-enabled membrane advances based on review of current literature. Performance enhancement relates to permeability, selectivity, and robustness, while commercial viability relates to material cost, scalability, and compatibility with existing manufacturing infrastructure.

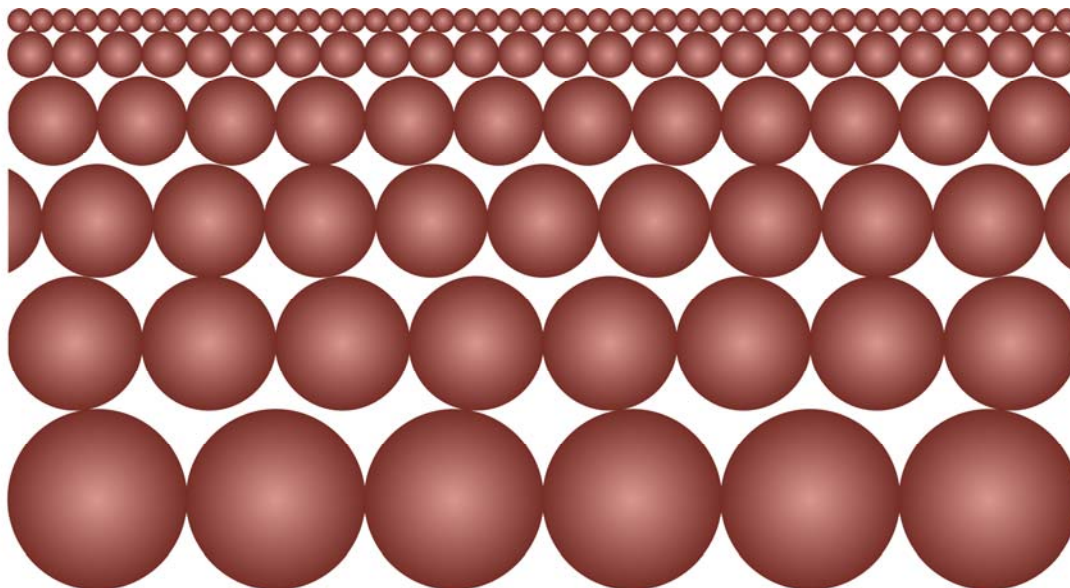
FIGURES

Figure 1. Conceptual depiction of the asymmetric structure of an inorganic membrane.

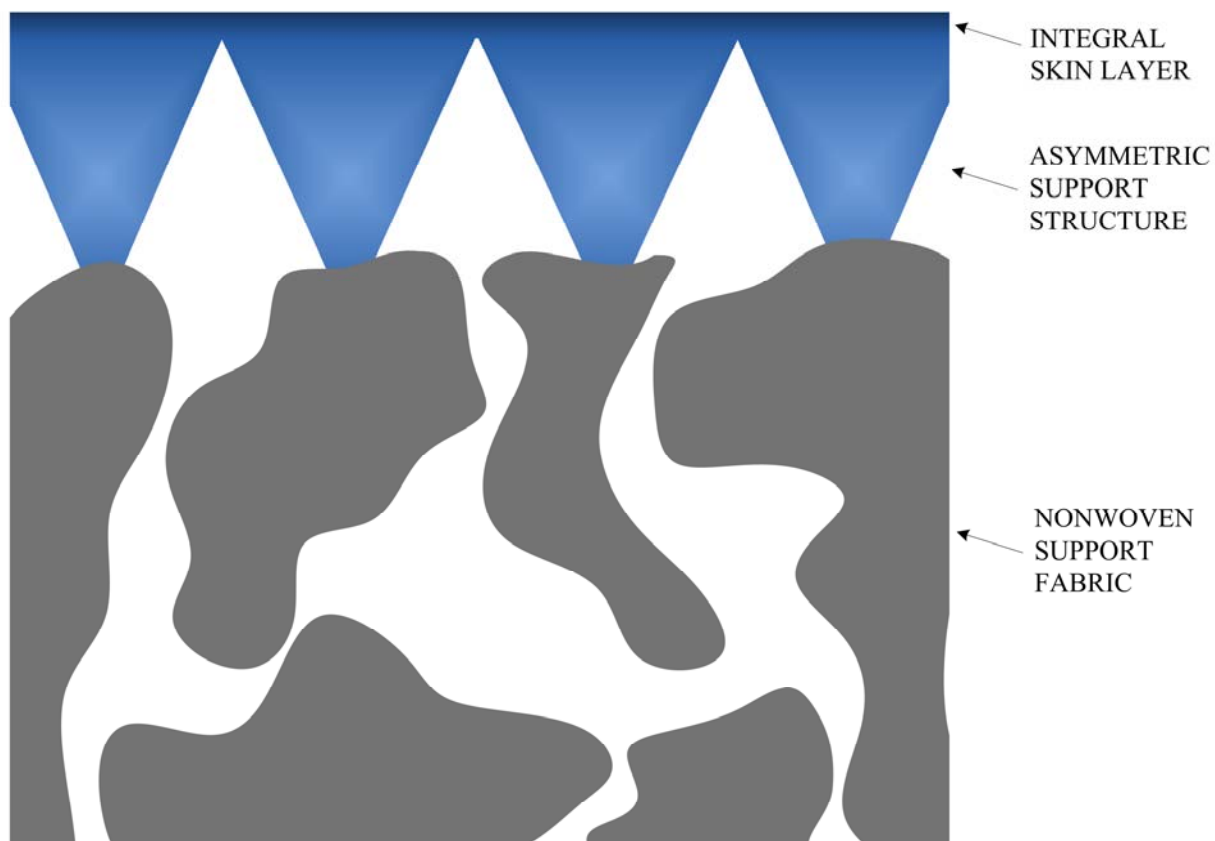


Figure 2. Conceptual cross-section of an asymmetric, integrally skinned membrane.

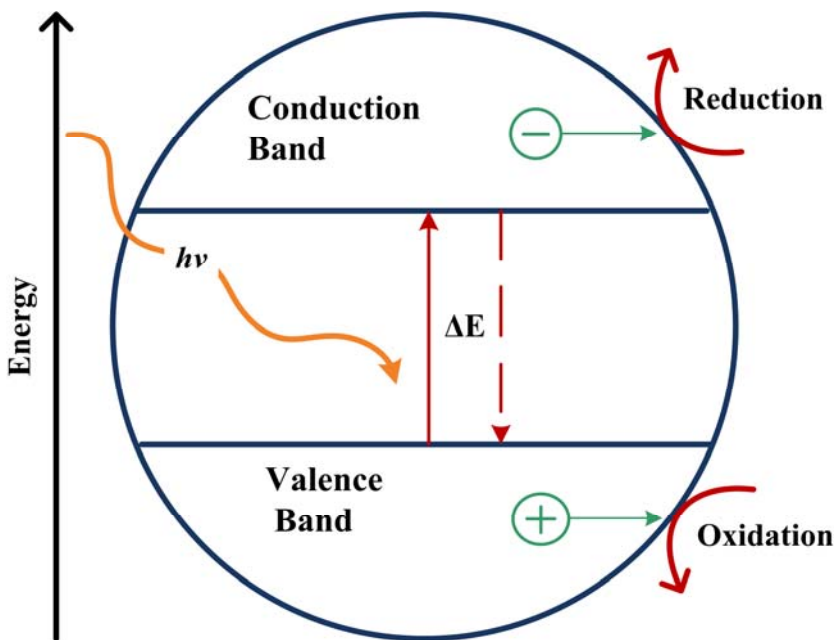


Figure 3. Schematic of nanoparticle mediated photocatalysis. Adapted from ⁷⁴.

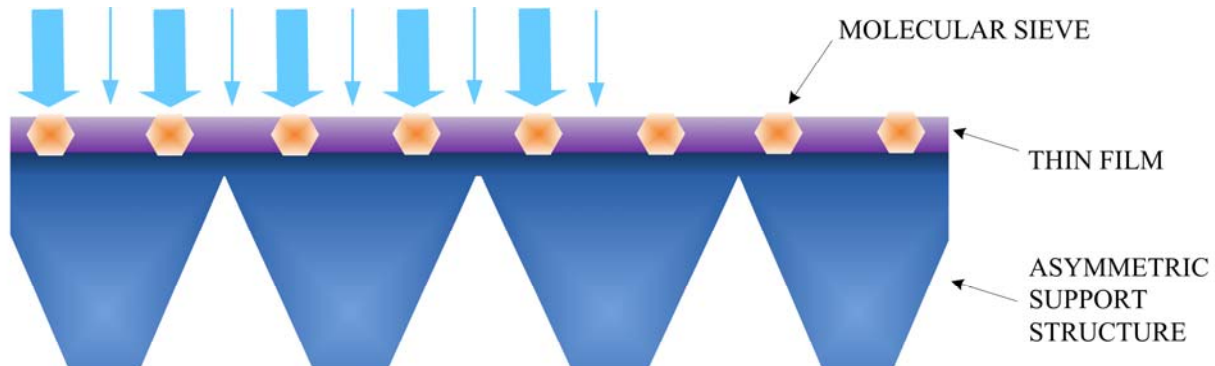


Figure 4. Conceptual cross-section of a membrane containing molecular sieves throughout the polymeric thin film, providing preferential flow paths for water as indicated by arrows. Adapted from ¹⁶⁸.

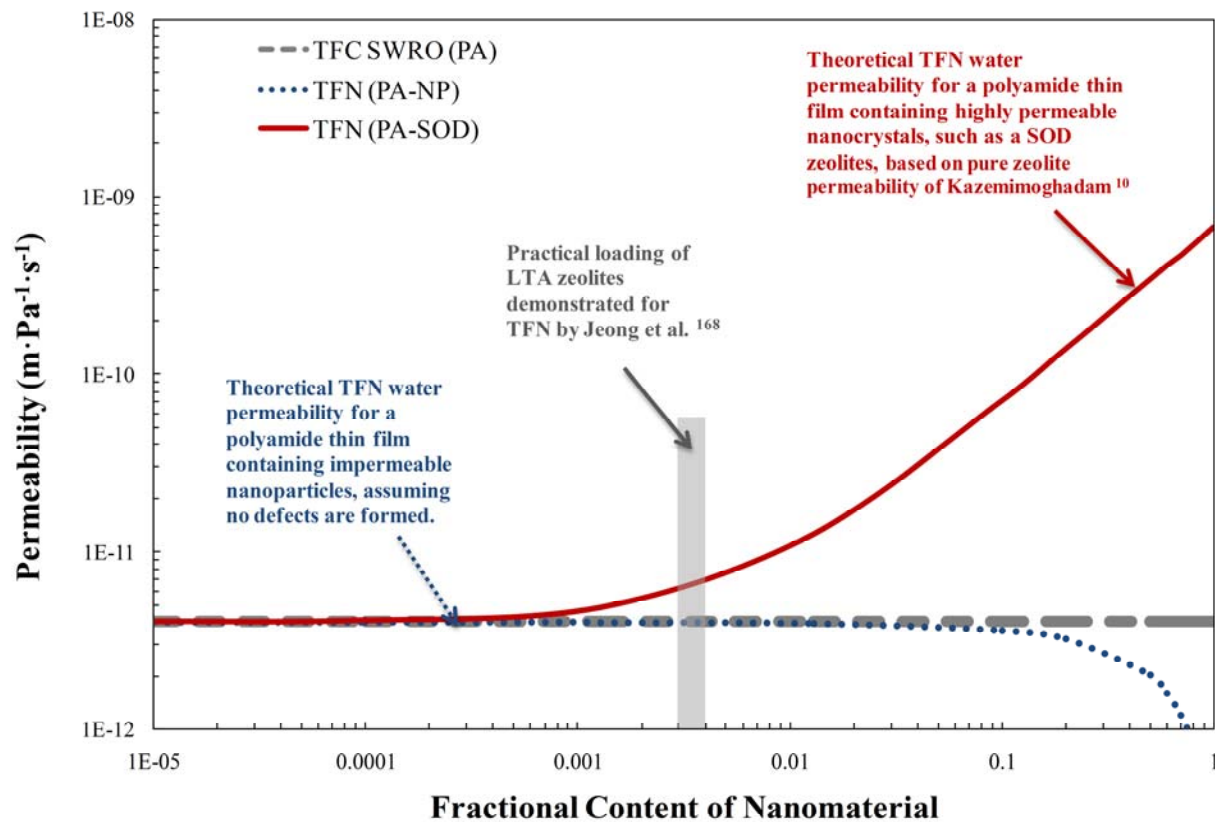


Figure 5. Theoretical projection of the possibilities for thin films containing nanoparticles (permeable and impermeable) compared to current polymeric seawater reverse osmosis membranes.

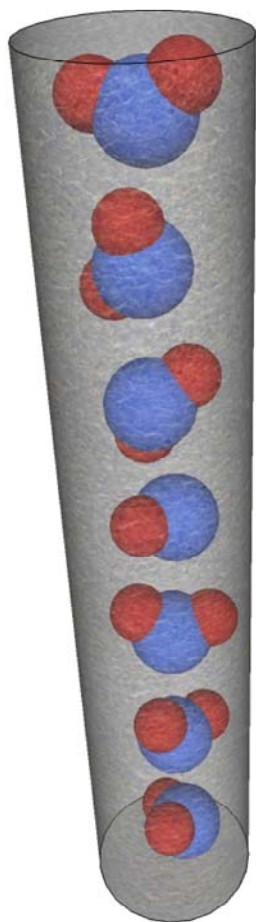


Figure 6. Molecular ordering of water molecules being transported through nanoscale channels (aquaporins and carbon nanotubes) as predicted by molecular dynamics simulations. Adapted from ¹⁸⁷.

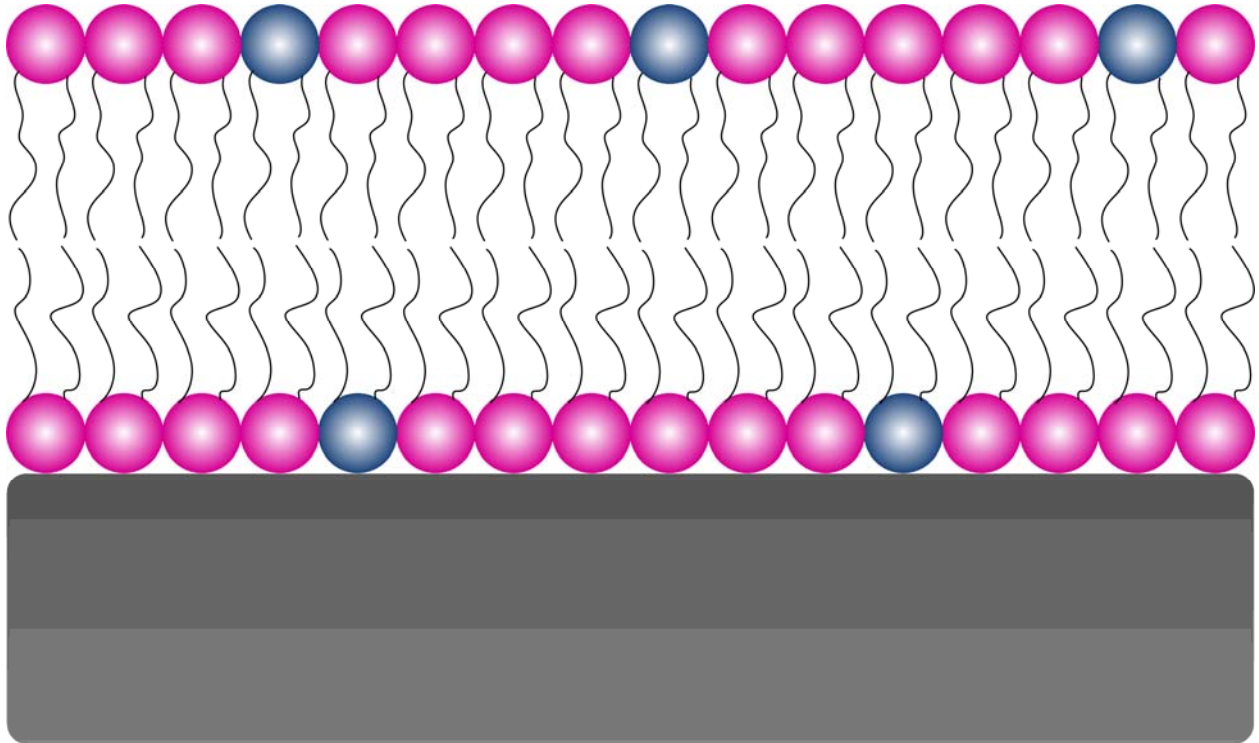


Figure 7. Conceptual cross-sectional image of a semi-permeable lipid bi-layer membrane cast atop a nanofiltration-type support membrane. Adapted from ¹⁷⁷.

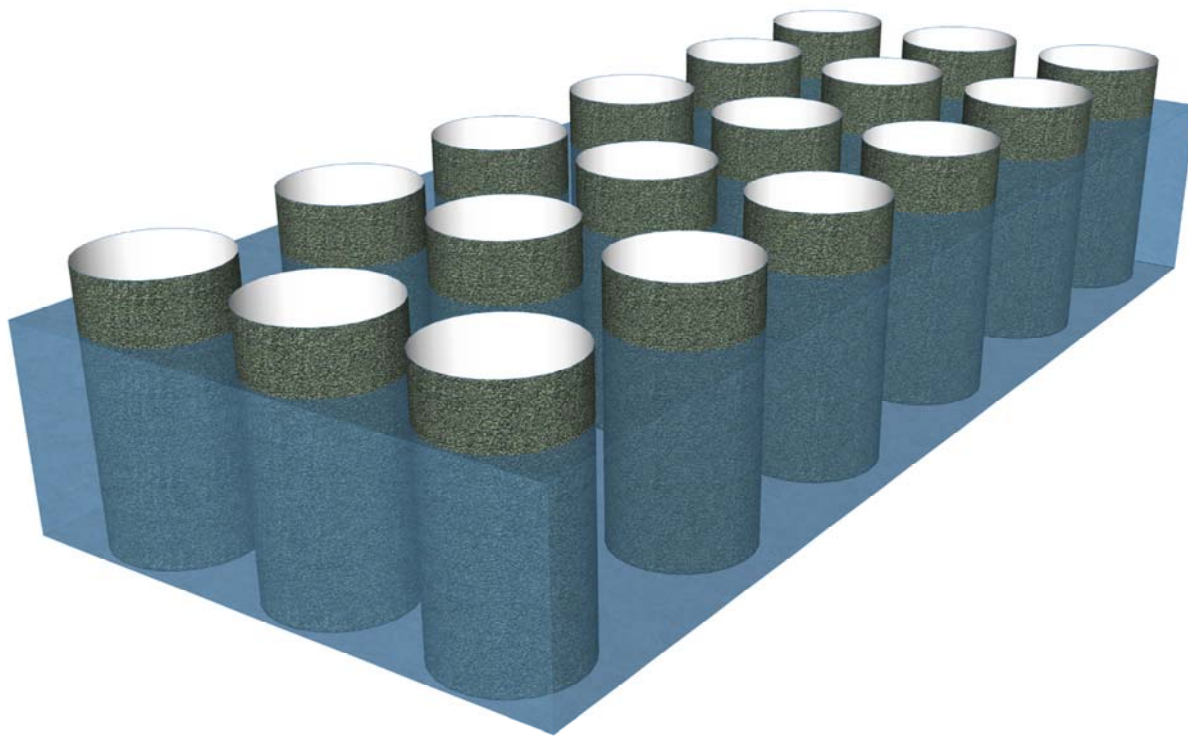


Figure 8. Conceptual image of an array of aligned nanotubes embedded in a nonporous polymeric matrix.

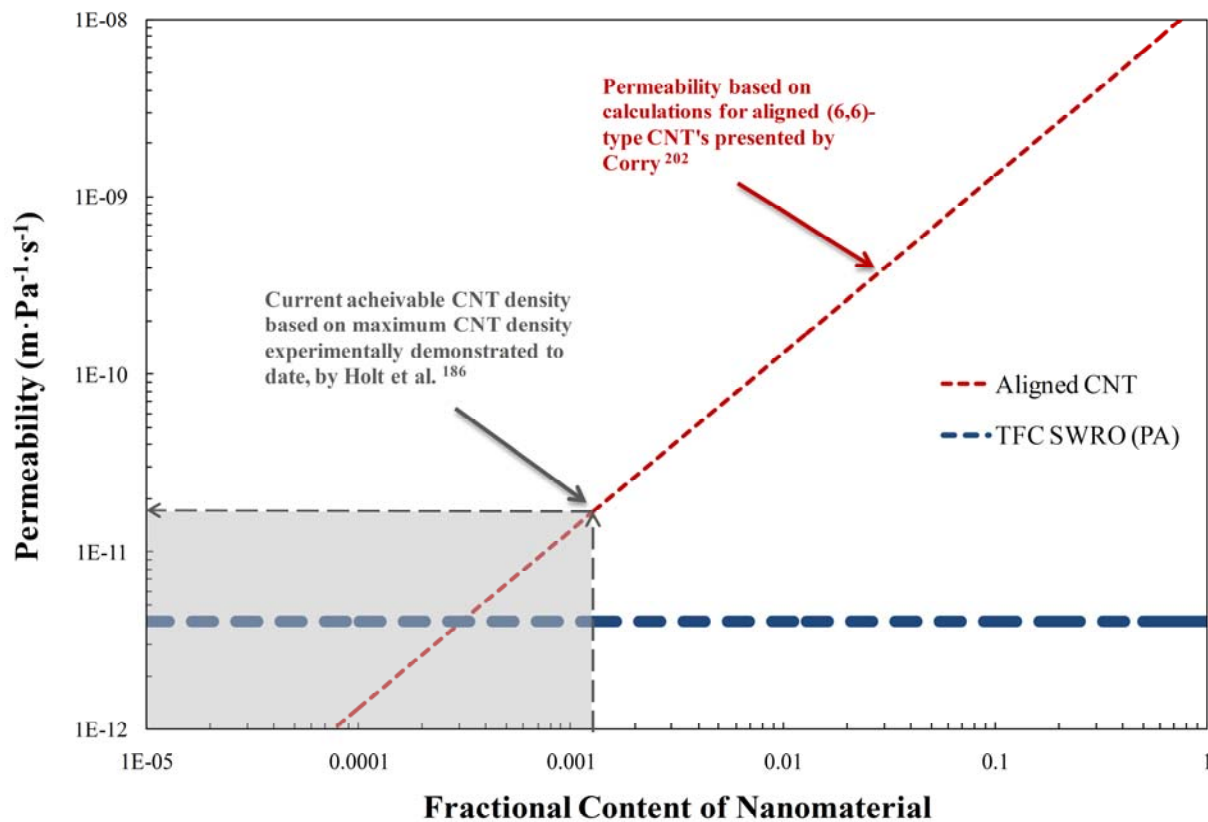


Figure 9. Theoretical projection of the possibilities for aligned carbon nanotube membranes compared to current polymeric seawater reverse osmosis membranes.

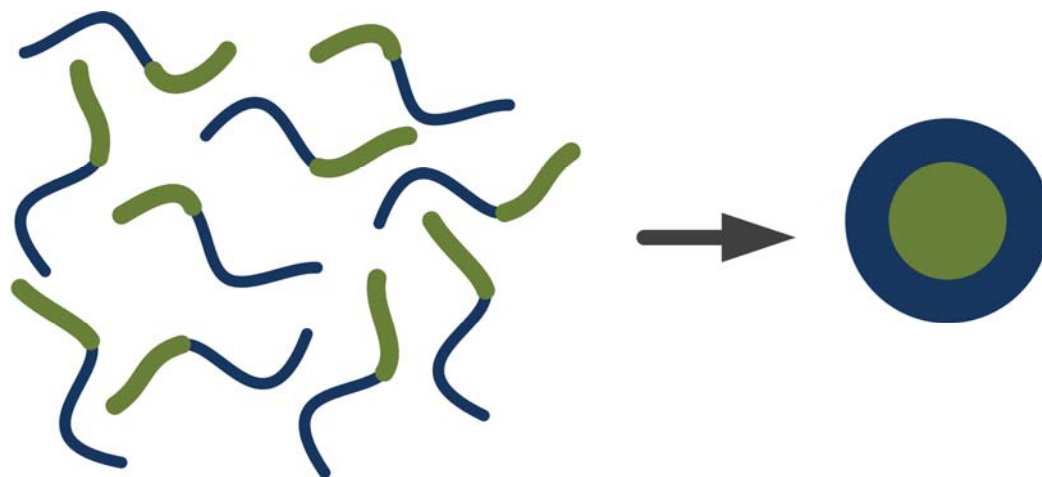


Figure 10. Di-block copolymer micelle formation upon reaching the critical micelle concentration. Adapted from ²²⁶.

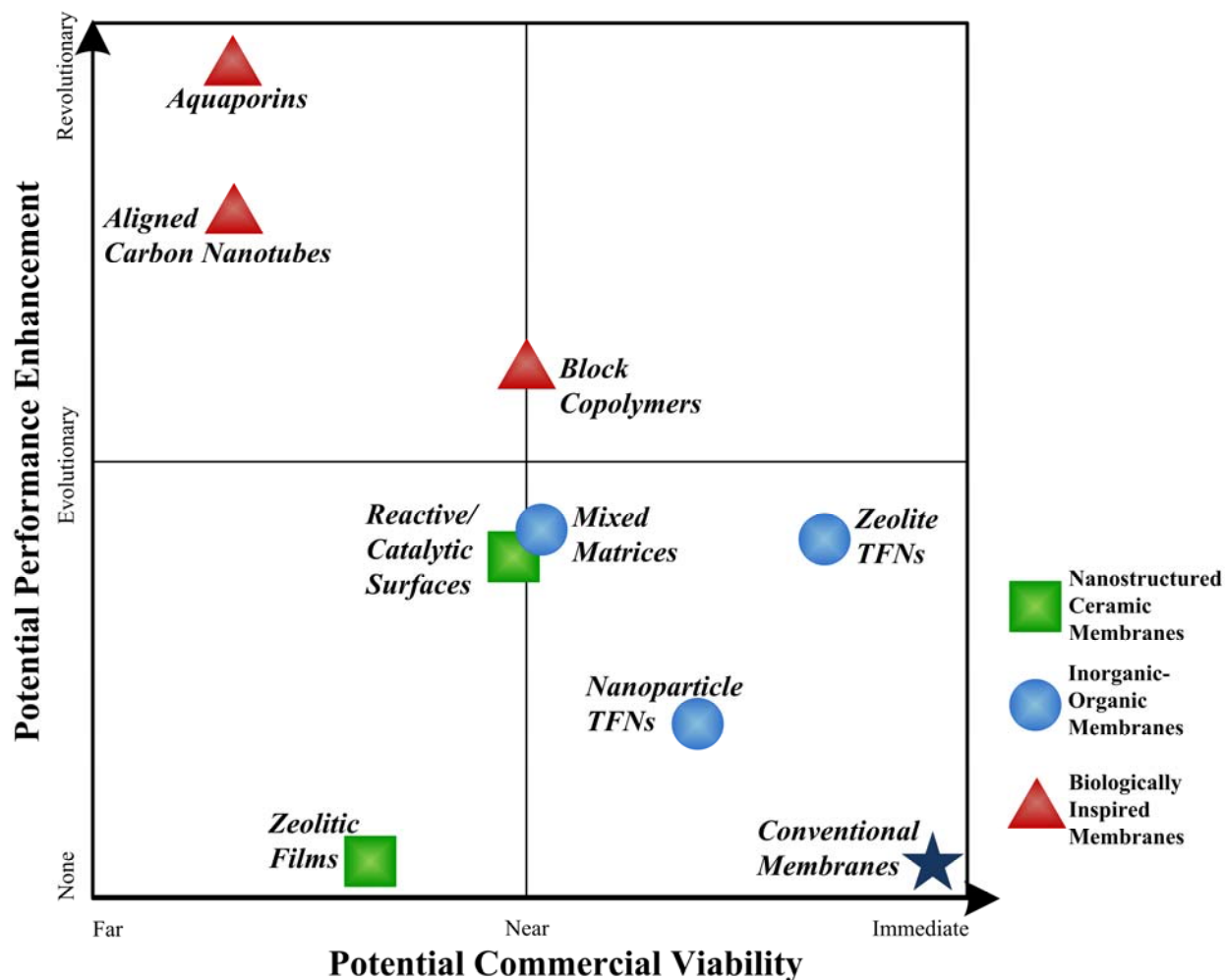
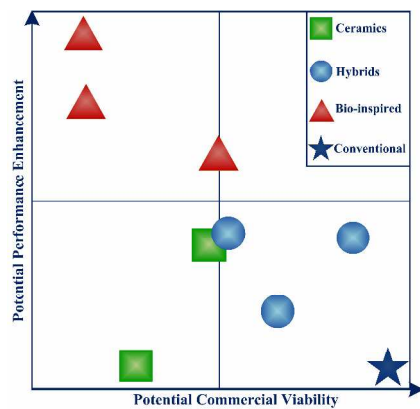


Figure 11. Comparison of the potential performance and commercial viability of nanotechnology-enabled membrane advances based on review of current literature. Performance enhancement relates to permeability, selectivity, and robustness, while commercial viability relates to material cost, scalability, and compatibility with existing manufacturing infrastructure.

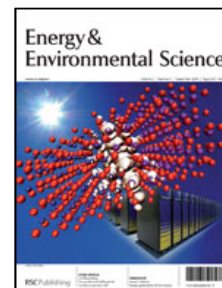
Our world currently faces a global water challenge. More than ever, existing fresh water resources need protection and new water resources must be developed in order to meet the world's growing demand for clean water. This will require better water treatment technology. Nanotechnology is being used to enhance conventional ceramic and polymeric water treatment membrane materials through various avenues. Among the numerous concepts proposed, the most promising to date include zeolitic and catalytic nanoparticle coated ceramic membranes, hybrid inorganic-organic nanocomposite membranes, and bio-inspired membranes such as hybrid protein-polymer biomimetic membranes, aligned nanotube membranes, and isoporous block copolymer membranes. The current state of nanotechnologies is evaluated and a framework for comparison is laid out. As we move forward, continued research efforts and materials development are required to ensure that we protect our environmental resources and produce clean water in an energy efficient manner for the future of our world.



Nanotechnology-enabled water treatment membrane materials look to revolutionize clean water through zeolitic and catalytic ceramics, hybrid composites, and bio-inspired membranes.

Energy & Environmental Science

Guidelines to Referees



Energy & Environmental Science (EES) — www.rsc.org/ees

EES is a new, community-spanning journal that bridges the various disciplines involved with energy and the environment.

The journal publishes insightful, high-impact science (original research and topical reviews) of the highest quality.

June 2010 - the first official EES Impact Factor is announced as 8.50

The journal's scope is intentionally broad, covering all aspects of energy conversion and storage (and their environmental impact), as well as aspects of global atmospheric science, climate change and environmental catalysis.

It is the policy of the Editorial Board to stress a very high standard for acceptance in EES

Accepted papers must report insightful, high quality science in the journal's scope that will be of significant general interest to the journal's wide readership.

We ask referees to examine manuscripts very carefully, and recommend rejection of articles which do not meet our high novelty and impact expectations.

Please state if a paper would be better suited to a more specialised journal. **Routine**, fragmented or incremental work, however competently researched and reported, should not be recommended for publication. If you rate the article as 'routine' yet recommend acceptance, please give specific reasons for this in your report.

EES has enjoyed a great start as a journal, attracting much attention and publishing many great articles from world-leading research groups.

Thank you very much for your assistance in evaluating this manuscript. Your help and guidance as a referee is greatly appreciated.

With our best wishes,

Professor Nathan Lewis
Editor-in-Chief

Philip Earis (ees@rsc.org)
Managing Editor

General Guidance (For further details, see the RSC's [Refereeing Procedure and Policy](#))

Referees have the responsibility to treat the manuscript as confidential. Please be aware of our [Ethical Guidelines](#) which contain full information on the responsibilities of referees and authors.

When preparing your report, please:

- Comment on the originality, importance, impact and scientific reliability of the work;
- State clearly whether you would like to see the paper accepted or rejected and give detailed comments (with references, as appropriate) that will both help the Editor to make a decision on the paper and the authors to improve it;

Please inform the Editor if:

- There is a conflict of interest;
- There is a significant part of the work which you are not able to referee with confidence;
- If the work, or a significant part of the work, has previously been published, including online publication, or if the work represents part of an unduly fragmented investigation.

When submitting your report, please:

- Provide your report rapidly and within the specified deadline, or inform the Editor immediately if you cannot do so. We welcome suggestions of alternative referees.

If you have any questions about reviewing this manuscript, please contact the Editorial Office at ees@rsc.org